Entwicklung Stammzell-basierter Konstrukte für den Kreuzband- und Sehnenersatz

Dissertation zur Erlangung des
naturwissenschaftlichen Doktorgrades
an der Bayerischen Julius-Maximilians-Universität Würzburg

vorgelegt von
Meike Haddad-Weber
aus Wimbern/Wickede (Ruhr)

Würzburg, 2010

Eingereicht am ……..……

Mitglieder der Promotionskommission

Vorsitzender: ……

Gutachter: PD Dr. Ulrich Nöth

Gutachter: Prof. Dr. Georg Krohne

Tag des Promotionskolloquiums: ……

Doktorurkunde ausgehändigt am: ……..……..

Hiermit erkläre ich ehrenwörtlich, dass ich die vorliegende Dissertation selbstständig angefertigt und keine anderen als die von mir angegebenen Hilfsmittel und Quellen verwendet habe. Des Weiteren erkläre ich, dass diese Arbeit weder in gleicher noch in ähnlicher Form in einem Prüfungsverfahren vorgelegen hat und ich noch keinen Promotionsversuch unternommen habe.

Würzburg, 18.10.2010

Meike Haddad-Weber

For my parents, my brother Lars,
and particularly my husband Dani & my little son Cedric

The thesis is based on the following manuscripts:

Haddad-Weber M, Haddad D, Stehle J, Krohne G, Steinert AF, Nöth U. Collagen fiber-based ACL constructs. German patent application DPMA 102009059901.0: "Kollagenfaser-Konstrukte für den Kreuzbandersatz", Haddad-Weber M, Haddad D and Nöth U (The publication of this manuscript has to be postponed until a envisioned second patent application has been filed).

Haddad-Weber M, Haddad D, Wilms A, Rackwitz L, Steinert AF, Lotz C, Hiller KH, Gohlke F, Rolf O, Nöth U. Intratendinous injection of mesenchymal stem cells after rotator cuff repair - an experimental study in rabbits (submitted).

Haddad-Weber M, Prager P, Kunz M, Seefried L, Jakob F, Murray MM, Evans CH, Nöth U, Steinert AF. BMP12 and BMP13 gene transfer induce ligamentogenic differentiation in mesenchymal progenitor and anterior cruciate ligament cells. Cytotherapy 12:505-13; 2010.

Steinert AF, Weber M, Kunz M, Palmer GD, Nöth U, Evans CH, Murray MM. In situ IGF-1 gene delivery to cells emerging from the injured anterior cruciate ligament. Biomaterials 29:904-916, 2008.

The signatures of all co-authors confirming M. Haddad-Weber’s proportion to the above mentioned publications and manuscripts have been submitted to the deanery of the department of biology, University of Würzburg.

Table of content

Chapter 1

Introduction

In the US, patients suffer from more than 32 million traumatic or repetitive motion injuries to ligaments, tendons, and the joint capsule per year (Butler et al., 2007). There are numerous areas throughout the body where ligaments and tendons experience such injuries. Particularly the anterior cruciate ligament (ACL), the posterior cruciate ligament (PCL), the medial collateral ligament (MCL), and the patellar, the Achilles tendon , the digital flexor tendons, the ulnar collateral ligament, and the rotator cuff tendons at the shoulder are among the most often severed ligaments and tendons (Cooper et al., 2006; Doroski et al., 2007; Woo et al., 2006b).

Rotator cuff injuries are the most frequent of traumatic tears with 4.4 million physician visits in 2003 in the US (Butler et al., 2007). Over 300,000 patients require direct repair (Rotini et al., 2008). For the ACL, more than 200,000 reconstructions are performed in the US per year (Albright et al., 1999). Both, the ACL and the rotator cuff tendon are examples for poor intrinsic healing potential and limited vascularization (Lu et al., 2005). Therefore, surgical treatment is necessary in these cases to avoid further damage.

The untreated ruptures of the ACL are associated with long-term complications such as pain, joint swelling, and knee instability that can result in degenerative changes such as osteoarthritis (Caruso and Dunn, 2004; Woods and Gratzer, 2005). Traditionally, ACL ruptures have been treated with autografts and allografts. Usually autografts, such as hamstring tendons and bone-patellar tendon-bone grafts have been the most popular and successful replacements for the ruptured ACL. These methods for ACL reconstruction induce tissue defects that may lead to donor site morbidity and minimize functional ability (Butler et al., 2007; Laurencin and Freeman, 2005). Also, allografts could transmit diseases, cause immunogenic responses, and possess only a reduced tensile strength (Laurencin and Freeman, 2005).

Rotator cuff tears are also related with pain and functional restricted movement of the shoulder. Furthermore, they frequently lead to fatty degeneration of the rotator cuff muscles (Gerber et al., 2004; Hashimoto et al., 2003; Koike et al., 2005; Nakagaki et al., 1996; Tytherleigh-Strong et al., 2001). Depending on the grade of the tear different therapies are currently available. Reattachment of the tendon to the bone and reconstruction of the rotator cuff with different muscle flaps in bigger defects are

examples for surgical repair (Boehm et al., 2004; Goutallier et al., 2003b). In 40 to 50% of the tears, rotator cuff repair fails due to excessive muscle contraction and neurovascular damage (Butler et al., 2007; Dines et al., 2007; Miniaci and MacLeod, 1999; Zingg et al., 2007).

Given the frequency and increasing costs of these injuries and the sometimes poor result after of surgical intervention, it is not unexpected that new therapeutical strategies such as tissue engineering approaches have become of major interest in current clinical research. Tissue engineering is an interdisciplinary field, which bridges the gap of biological, chemical, and engineering principles toward the development of substitutes for the repair of tissue function (Coats et al., 2005). The classical tissue engineering triad uses three-dimensional cell carries (scaffolds), together with differentiated or undifferentiated cells that have been expanded *in vitro* and the use of stimuli e.g. growth factors (Laurencin and Freeman, 2005).

With regard to the current situation, tissue engineering approaches may play an important role in the reconstruction of injured ACLs and rotator cuffs in the future. Therefore, the overall aim of this thesis was to develop and validate different basic strategies for the replacement of ligaments and tendons. The first strategy makes use of collagen scaffolds. The second strategy was to develop MSC based therapies and the third one implied BMP transduced MSCs in a collagen hydrogel. All three strategies represent different promising tissue engineering approaches for the treatment of ligament and tendon ruptures. Next to inducing and controlling ligamentogenic and tendogenic differentiation of MSCs and fibroblasts, the biomechanical stability of the scaffolds had to be optimized, because sufficient biomechanical stability is mandatory for successful musculoskeletal therapies.. The overall aim of this work was to pioneer for a tissue engineering or cell based product for ACL or rotator cuff repair.

1. Anatomy

1.1 Anterior cruciate ligament

The anterior cruciate ligament (ACL) is the major intra-articular ligament of the knee. It arises from the anterior part of the intercondylar eminentia of the tibia and spreads to the posterolateral aspect of the intercondylar fossa of the femur. The ACL is covered by a synovial layer and consists of an anteromedial and a posterolateral bundle (Woo et al., 2006a). These two bundles are important as a constriction to anterior-posterior translation and rotational moments about the knee (Woo et al., 2006a). The length of an ACL is about 25 to 41 mm and the diameter about 10 to 20 mm (Arnoczky, 1983). The main function is to control the motion by connecting the femur to the tibia and to stabilize the knee joint. This means that the ACL supports and strengthens the knee preventing extreme anterior translation of the femur that could cause a dislocation or fracture of bones in the knee joint (Laurencin and Freeman, 2005). The tensile forces are ranging from 67 N for ascending stairs to 630 N for jogging and during activities of daily living. The maximum tensile load is about 1730 N (Ge et al., 2006).

The ACL is the most injures ligament in the knee with more than 200,000 ruptures every year in USA (Freeman et al., 2007). Untreated ACL ruptures result in joint dysfunctions, which consequently can lead to damage of meniscus tissue and the development of degenerative joint disease (Ge et al., 2006). Because of the poor healing potential, surgical replacement is recommended in the young adult after ACL ruptures. Autografts are taken from the patellar, hamstring, or quadriceps tendon of the patients. The patellar tendon graft is removed with bone from the patellar and the insertion of the tibia (so called bone-patellar-bone graft). After transplantation the success of the grafts is dependent on the revascularization and the ligamentization of the graft which is progressively surrounded by the synovial membrane (Amiel et al., 1986b). Additionally, autografts possess good mechanical strength (Freeman et al., 2007). However, autografts exhibit disadvantages such as dysfunctions and donor site morbidity (Cooper et al., 2006). Furthermore, there is an insufficient supply of tissue for a second donation if the graft has failed.

Allografts are taken from cadavers preventing donor site morbidity, postoperative pain and reduce surgical time (Ge et al., 2006). Nevertheless, allografts have the risk of disease transmission such as HIV and hepatitis and immune response to the

foreign tissue. Furthermore, allografts cannot be sterilized without altering the mechanical properties of the tissue (Ge et al., 2006).

Alternatively, a variety of non-degradable synthetic materials were used clinically for ACL repair (Freeman et al., 2007; Vunjak-Novakovic et al., 2004). These include carbon fibers, polyethylene terephthalate (Leeds-Keio ligament), polyester (Dacron®), polypropylene (Kennedy Ligament Augmentation Device), and polytetrafluoroethylene (Gore-Tex®) (Freeman et al., 2007; Vunjak-Novakovic et al., 2004). After replacement, problems such as fragmentation, stress shielding of new tissue, fatigue, creep, and wear debris were observed frequently leading to synovitis and arthritis (Freeman et al., 2007).

1.1.1 Ligaments and tendons

Ligaments and tendons are classified as dense and regularly arranged connective tissue. Ligaments and tendons are essential components of the musculoskeletal system and connect bone to bone respectively muscles. Both are important structures that govern motion and share load in diarthrodial joints. The form of ligaments and tendons can diversify according to anatomic requirements.

Ligaments connect bone to bone in order to control the relative motion. In contrast, tendons attach muscle to bone and transfer the contraction of the muscle to a movement in the skeletal construction.

1.1.1.1 Structure and composition of the extracellular matrix

The structure and composition of ligaments and tendons is very similar. Both tissues are composed of fibroblasts surrounded by an extracellular matrix (ECM) formed by two components: a solid, highly ordered arrangement of macromolecules (mainly collagen type I) and water (65-70% of the total weight). In addition to collagen type I, the ECM consists of collagen types III, IV, V and VI, elastin, proteoglycans, glycoproteins, and small amounts of other proteins (Doroski et al., 2007; Hoffmann and Gross, 2007; Scott, 2003) (Figure 1).

The specialized mechanical properties of ligaments and tendons depend on the composition, organization, and interaction of the matrix components. Collagen is the predominant component and has a percentage of 70-80% dry weight (Woo et al., 2006b). Collagen type I is integrated into bundles of slackly reticular collagen type III

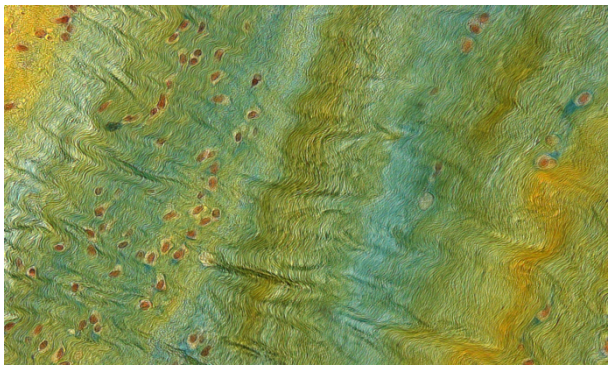

Figure 1: Fibroblasts embedded in a dense collagen matrix and connective tissue of a human ACL. Movat's pentachrom staining showing collagen fibers (yellow), proteoglycans (blue), and cell nuclei (red) of fibroblasts. Original magnification: 200x.

(12% dry weight) and V (8% dry weight). Fibrillar collagen type I give ligaments and tendons the high tensile strength and is directly related to the structure of the molecule. The tropocollagen subunit is a rod about 300 nm in length and 1.5 nm in diameter, made up of a triple helix with two alpha-1 chains and one alpha-2 chain (Scott, 2003). Tropocollagen subunits spontaneously self-assemble after secretion and cross-link into microfibrils. In this way, collagen molecules combine to form structured units of microfibrils (five collagen molecules), subfibrils in ligament (subfascicles in tendon), and fibrils. The fibrils are arranged in densely packed, highly ordered parallel bundles (Hoffmann and Gross, 2007). The bundles are oriented in a distinct longitudinal pattern, with proteoglycans and glycoproteins in connection with water, binding the fibrils together to form fascicles (Figure 2).

Proteoglycans are the second largest component of ligaments and tendons. They have an important role in organizing the ECM and interacting with the tissue fluid (Dodds and Arnoczky, 1994). Proteoglycans consist of a core protein with one or more covalently attached glycosaminoglycan chains (Jonsson et al., 2003; Yoon and Halper, 2005) and can be distinguished into two groups.

The small leucin-rich repeat proteoglycans include decorin, biglycan, fibromodulin and lumican as well as the modular organized proteoglycans like versican, aggrecan, brevican and testican (Silver et al., 2003; Yoon and Halper, 2005; Zhang et al., 2005). Because of the negative charge, proteoglycans have a large capacity to bind water and are mostly entrapped within and between collagen fibrils and fibers (Yoon and Halper, 2005).

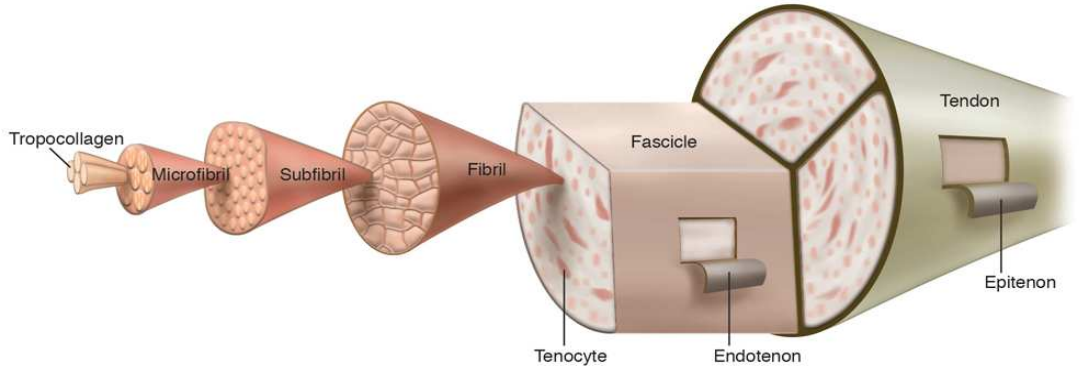

Figure 2: Structure of ligaments and tendons. Ligaments and tendons are non-mineralized, dense connective tissue. The main component is collagen type I, synthesized from ligamentocytes and ligamentoblasts and respectively, from tenocytes and tenoblasts, cross-linked, and organized in fascicles (from Towler and Gelbermann, 2006).

The most abundant proteoglycan is decorin which binds to almost all collagen types. However, decorin is representing a key regulator of matrix assembly because it limits collagen fibril formation and thus regulates tendon remodeling due to tensile force. The affinity of biglycan binding to collagen type I is equivalent to decorin and the interaction. In contrast, aggrecan is found richly in area where the tissue is subject to compression forces (Silver et al., 2003; Yoon and Halper, 2005).

Additionally, glycoproteins are found in ligaments and tendons and facilitate interactions between the fibroblasts and the surrounding matrix (Dodds and Arnoczky, 1994). Glycoproteins are macromolecules that contain oligosaccharide chains (glycans) covalently attached to their polypeptide (Kannus, 2000). Following glycoproteins have been identified in ligaments and tendons: fibronectin, tenascin-C, tenomodulin, thrombospondin, and undulin (Docheva et al., 2005; Miller and McDevitt, 1991; Shukunami et al., 2006).

Fibronectin is a dimeric glycoprotein that is present during the early tendon development. *In vitro* studies showed specific functions of fibronectin in terms of interactions with collagen. Binding of collagen fibrils by fibronectin regulates fibrillogenesis (Kuo et al., 2008).

Tenomodulin is a transmembrane glycoprotein that is only expressed in dense connective tissue like ligament, tendon, skeletal muscle, cornea, and the sclera (Shukunami et al., 2006). This transmembrane glycoprotein is regulated by scleraxis and is necessary for the proliferation and maturation of the fibroblasts (Docheva et al., 2005).

Another extracellular matrix glycoprotein is tenascin. Particularly, tenascin-C is found in the developing ligament and tendon. It interacts with integrins, collagens, proteoglycans, and fibronectin.

Elastin is a protein in connective tissue that is elastic and allows tissues to resume their shape after stretching or contracting. Elastin is a coiled 68 kDa protein with a high content of hydrophobic amino acids (e.g. glycine, valine alanine, and proline), that is made by linking many tropoelastin protein molecules, in a reaction catalyzed by lysyl oxidase to make a massive insoluble, durable cross-linked array. Elastin elongates and straightens under tension, exposing hydrophobic surfaces to the aqueous environment and losing entropy from the coiled configuration. Elastin and collagen fibrils work in tandem (Scott, 2003). While elastin provides elasticity, collagen provides inflexibility to connective tissue.

1.1.1.2 Blood supply and innervation of the ACL

The major blood supply to the ACL arises from the ligamentous branches of the middle genicular artery, as well as some terminal branches of the Aa. genus inferiors medialis and lateralis (Dodds and Arnoczky, 1994). A group of vessels that supplies the infrapatellar fat pad contributes branches to the synovial envelope of the cruciates. The synovial vessels arborize to form a network of periligamentous vessels which enwrap the ligament to its complete length (Dodds and Arnoczky, 1994). The synovial membrane around the ACL has many capillaries. These vessels anastomose with the network of intraligamentous vessels, which are oriented in a longitudinal direction and lie parallel to the collagen bundles of the ligament.

The ACL is crossed with vasomotor nerve fibers of the Nervus tibialis and various mechanoreceptors (Arnoczky, 1983). At the insertion area of the femur, the tibia, and the subsynovial connective tissue, Pacini corpuscles, Ruffini corpuscles and free nerve endings are found (Halata et al., 1999; Haus and Halata, 1990). Approximately 1% of the volume of the ACL is occupied by specialized nerve receptors and free nerve endings (Dodds and Arnoczky, 1994). This observation shows the important role of the ACL as an active stabilizer of the knee joint. The proprioceptors of the ACL act as sensors for the joint position and influence the activity of joint stabilized musculature.

1.2 Rotator cuff

The rotator cuff is the largest tendinous structure in the body and plays an important role in providing movement and stability at the shoulder joint (Tytherleigh-Strong et al., 2001). It is a composite tendon formed from four muscles that take their origin from the blade of the scapula and pass over the glenohumeral joint to insert circumferentially around the humeral head (Tytherleigh-Strong et al., 2001). The M. supraspinatus (SSP), M. infraspinatus (ISP), M. teres minor, and M. subscapularis (SSC) are forming the rotator cuff (Favard et al., 2007). However, the SSP, ISP, and teres minor are participated in shoulder abduction and external rotation. In contrast, the SSC internally rotates the shoulder (Bencardino et al., 2003).

Rotator cuff injuries are the most frequent traumatic and attritional tears, with about 4.4 million physician visits in 2003 only in US (Butler et al., 2007). Rotator cuff tears show an increase with advanced age and are often caused by abrasion arise from high stresses and strains. Particularly, overhead activities (e.g. athletes and craftsmen) with equal pattern of movement overstrain the rotator cuff (Brockmeier et al., 2008; Liem et al., 2008). Rotator cuff tears influence activity of daily living and are related with substantial pain and disability. For this reason, each year more than 300,000 surgeries are performed for the reconstruction of the rotator cuff in the US (Rotini et al., 2008). The treatment of rotator cuff tears diversifies according to the degree of the lesions (acute, partial, or chronic). Nonoperative treatments contain pain and anti-inflammatory medications, physical therapy, and subacromial injections of local anesthetic, steroids, or both (Wolf et al., 2007). The standard surgical procedure is the arthoscopic or open reconstruction of the tear along with a subacromial decompression in the form of an acromioplasty (Wolf et al., 2007). In the case of an acute tear, rotator cuff is best reconstructed as soon as possible, optimally within 6 weeks after injury (Matsen, 2008). Chronic massive rotator cuff defects with accompanying osteoarthritis of the humeral head are treated with a shoulder arthroplasty (anatomical or inverse) with a careful preservation of the coracoacromial arch.

More than 30% of the rotator cuff tears are difficult to treat and the failure rate is 13 to 68% after primary repair (Rotini et al., 2008). Chronic rotator cuff tears are related with structural and architectural reorganization of the musculotendinous unit, including tendon retraction, fatty muscle infiltration, interstitial connective tissue

proliferation, and atrophy (Gerber et al., 2008; Goutallier et al., 1994; Thomazeau et al., 1997).

The muscles whose tendons are torn change the orientation of their fibers, lose muscle tissue, and undergo fatty infiltration (Goutallier et al., 1994). While muscular atrophy seems to be partially reversible, fatty degeneration of the rotator cuff muscles appears to be irreversible in the shoulder (Gerber et al., 2004; Goutallier et al., 1994). Goutallier et al. have scaled the fatty degeneration of the rotator cuff in different grades (Table 1) (Goutallier et al., 1994). Furthermore, fatty muscular degeneration may increase after repair, even if tendon-to-bone healing is obtained (Gerber et al., 2004).

Table 1: Fatty infiltration grades of rotator cuff muscles on computed tomography (CT) sections (from Goutallier et al. 1994).

Fatty infiltration grade	CT signal
Grade 0	No fat
Grade 1	The muscle contains some fatty streaks
Grade 2	The fatty infiltration is important, but there is still
Grade 3	As much fat as muscle
Grade 4	More fat than muscle

1.2.1 Skeletal muscle

Skeletal muscle is the contractile tissue of the body and is derived from the mesodermal layer of embryonic germ cells. It makes up approximately 40 to 45% of the human body weight (Garrett and Best, 2000; Van Loocke et al., 2004). Skeletal muscle is a composite structure that consists of muscle cells, an organized network of nerves and blood vessels, and an extracellular connective tissue matrix (Figure 3). Muscle includes contractile filaments that move past each other and change the size of the cells. Their function is to make force and cause motion. Contraction of the skeletal muscles is used to move the body and can be lightly controlled. The functional unit of a skeletal muscle consist of the muscle fiber, which is a cylindrical, elongated cell with multiple nuclei, the so-called syncytium (Garrett and Best, 2000). The single fibers range from 10 to 100 µm in width and a few millimeters to 30 cm in

length. The cytoplasm of the fiber is the sarcoplasm, which is encapsulated inside a cell membrane called sarcolemma. Additionally, the endomysium is a fine membrane surrounding each individual fiber.

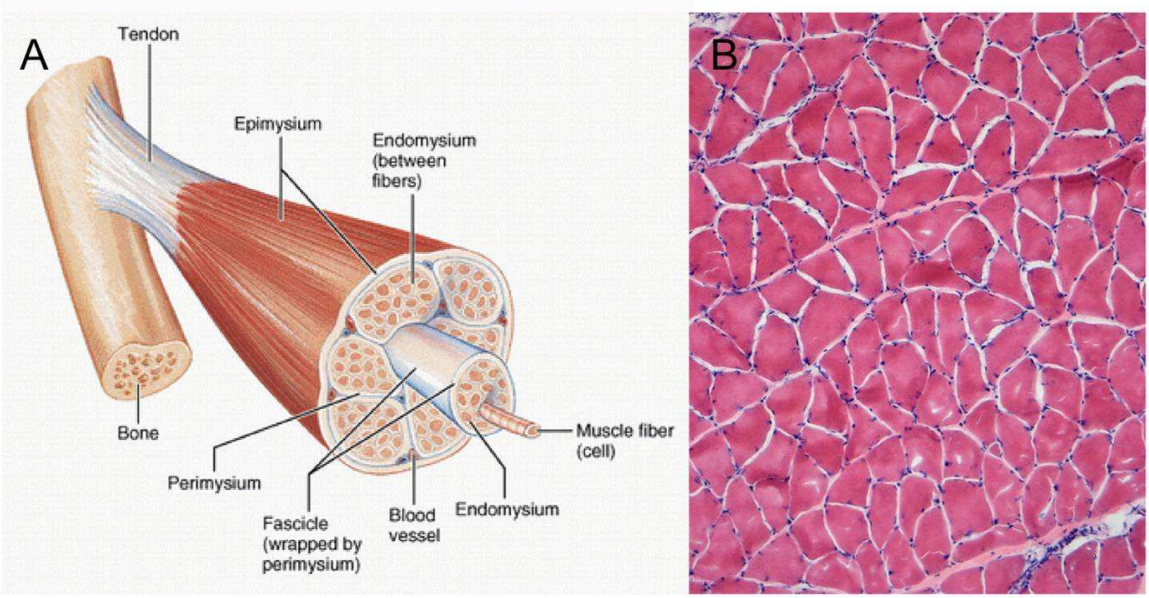

Figure 3: Structure of the skeletal muscle. (A) Graphic of the structure of a skeletal muscle. The muscle consists of skeletal muscle tissue, connective tissue, nerve tissue, and blood or vascular tissue from http://www.medical-look.com/human_anatomy/organs/Skeletal_muscle_fiber.html. (B) Cross section of muscle fibers of the Musculus semitendinosus (SSP). Magnification: 100x.

All fibers are arranged together in bundles covered by the perimysium. These bundles are themselves arranged, and the whole muscle is sheathed in a cover called the epimysium (Figure 3). The epimysium is positioned through the entire length of the muscle, from the tendon origin to the tendon insertion. The complete unit is called the musculotendinous unit (Jarmey and Myers, 2006). The skeletal muscle is a mixture of 2 different muscle fibers: fast twitch glycolytic and slow twitch, oxidative fibers. In contrast to fast twitch fibers, slow twitch fibers (the so called red fibers) contain large amounts of myoglobin and mitochondria (Garrett and Best, 2000). These fibers contract for long periods of time but with little force while fast twitch fibers contract quickly and powerfully but fatigue very rapidly. Though this postural control is generally maintained as a subconscious reflex, the muscles responsible react to conscious control like non-postural muscles.

The cellular structure, the myofibrils are composed of repeating units called sarcomeres (Figure 4). In the sarcomer a dark A-band and a light I-band, alternate

regularly. The central region of the A-band, termed the H-band, is less dense than the rest of the band (Stryer, 1995). The I-band is halved by a very thin dense, narrow Z-line. The underlying molecular plan of a sarcomer is revealed by cross-sections of a myofibril, which show that there are two kinds of interacting protein filaments. The thick filaments have diameters of about 15 nm and the thin filaments of about 9 nm.

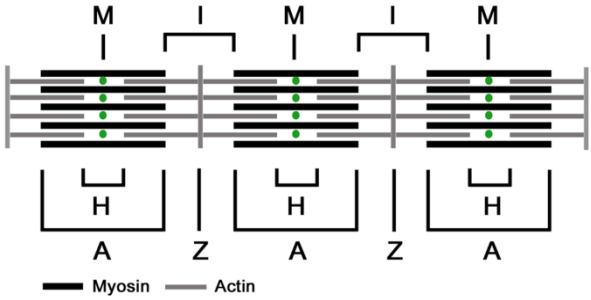

Figure 4: Bands and lines in the contractile apparatus of the skeletal muscle. The I-band is the so called actin-filament and the A-band is the myosin-filament, which overlaps with the actin-filament. The H-band is the central region of the A-band. This band contains only myosin-filaments. The contractile apparatus consists of the Z-line, the zone of apposition of actin filaments belonging to 2 sarcomers, and the M-line, a band of connections between the myosin-filament.

The main protein of the thick filament is myosin, a hexameric molecule with a molecular weight of about 520 kDa. There are further proteins that make up the thick filament. Among those are C-protein, M-protein, and titin, whereas titin is a large protein (10^6 Da) involved in the tiny filamentous connection between the ends of the thick filament and the Z-line. The thin filament consists of actin, tropomyosin, and the troponin complex. The thick and thin filaments interact by cross-bridges, which are domains of myosin molecules. The cross-bridges, using the energy of ATP, pull the actin strands together. Therefore, the dark and light sets of filaments increasingly overlap, resulting in muscle contraction (Jarmey and Myers, 2006). Furthermore, M-protein, myosin, and creatine kinase are associated with thick filaments at the M-line. Creatine kinase catalyzes the phosphorylation of ADP to form ATP and may be important in sustaining the supply of energy molecules to the cross-bridges.

1.2.2 Blood supply and innervation of skeletal muscle

Generally, each muscle is supplied via one artery, which brings nutrients into the muscle and a few veins to remove metabolic waste products surrendered by the

muscle into the blood (Jarmey and Myers, 2006). Theses blood vessels penetrate through the center of the spreads, but the blood vessels can also migrate towards one end. The blood vessels branch into a capillary plexus which enter the endomysium around each muscle fiber. During exercise the capillaries expand, increasing the amount of blood flow in the muscle by up to 800 times. In contrast, the muscle tendon has a distinct lower blood supply, because it is a relatively inactive tissue (Jarmey and Myers, 2006).

The innervation of each skeletal muscle is controlled by the somatic nervous system. Usually the innervations to a muscle penetrate at the same place as the blood supply. The motor unit consists of a motor nerve fiber and all muscle fibers excited by it. Each skeletal muscle fiber is excited to contract by chemical released from a somatic motor neuron. The nerve supply penetrates through the connective tissue into the endomysium of a skeletal muscle in the same way than the blood supply. The nerve penetrating the muscle comprises roughly identical proportions of sensory and motor nerve fibers, while some muscle may receive only sensory branches. A neuromuscular junction is the synapse terminal of a motor neuron with the motor end plate (Jarmey and Myers, 2006).

1.3 Tissue Engineering

Tissue engineering is an interdisciplinary field that applies the principles of engineering and life sciences toward the development of biological substitutes that restore, maintain or improve tissue or organ function (Langer and Vacanti, 1993). Tissue engineering of ligaments and tendons could be a promising method as an alternative therapy to repair of ligament and tendon defects.

The classical triad for the fabrication of a tissue engineered construct is based on 3 columns, scaffolds, cells, and different stimuli (Figure 5), e.g. tissue specific growth factors or biomechanical stimuli (Bell, 2000).

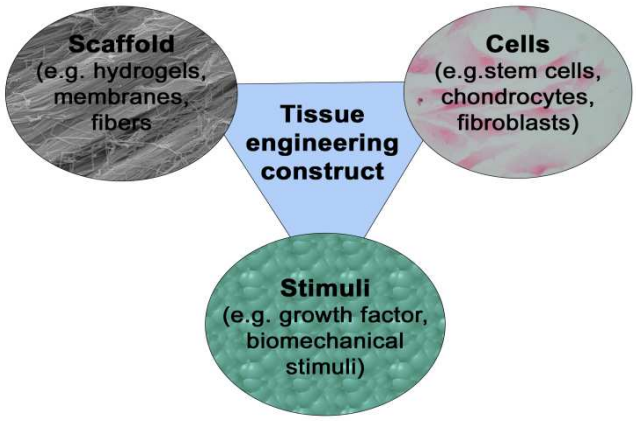

Figure 5: The tissue engineering triad for the fabrication of tissue engineered constructs. The components of a tissue engineered construct are scaffolds, cells, and stimuli.

1.3.1 Scaffolds

The limitations associated with biological and synthetic grafts have initiated a growing interest in tissue engineering constructs for ligament and tendon reconstruction. The optimal way would be to mimic the normal ligament/tendon organization (Ge et al., 2006). For this, a 3D matrix exhibits the advantage of a closely reconstructing of the spatial organization of the native tissue. For ACL replacement the ideal scaffold should be biocompatible, biodegradable, mechanical stable, and able to promote the formation of ligamentogenic tissue (Cooper et al., 2005; Ge et al., 2006). Furthermore, the mechanical behavior should be like the natural ACL. For ligament and tendon reconstruction several biomaterials have been described. Among these

are hydrogels or membranes made from alginate, collagen, silk, fibrin, chitosan, or hyaluronic acid (Altman et al., 2002a; Noth et al., 2005; Weber et al., 2002).

Especially collagen the major component of ligament and tendon tissue is of great interest. Many collagen based constructs have been applied for the ACL reconstruction. The collagen was isolated from bovine submucosa and intestine, bovine skin as well as rat tails (Dunn et al., 1995; Ge et al., 2006; Goulet et al., 1997; Noth et al., 2007a; Noth et al., 2005). A study of Dunn et al. with cell-colonized collagen constructs, showed the proliferation and matrix formation of ACL and patellar tendon fibroblasts on cross-linked collagen fibers while the ingrowth was inconsistent (Dunn et al., 1995). Chen et al. observed the differentiation of MSCs into ligament-forming cells when they were cultured on mechanical stimulated collagen scaffolds (Chen et al., 2006). Expression of ligament-specific markers and formation of ligament-like extracellular matrix was also shown when MSCs in a collagen type I hydrogel were cultured in a bioreactor under cyclic stretching (Noth et al., 2005). The mechanical load of these collagen type I hydrogel scaffolds was not comparable to the native ligament. Composite scaffolds consisting of extruded cross-linked collagen fibers within a collagen hydrogel showed with cells higher elastic modulus and maximum load than without cells (Gentleman et al., 2003). A complex ACL construct was developed from Goulet et al. (Goulet et al., 1997). The ACL construct consisted of ACL fibroblast in a collagen hydrogel whereas cross-linking reagents were used. This study observed that mechanical stimulation changed the structure and induced remodeling (Goulet et al., 1997). Tenocyte-seeded collagen type I/III bioscaffolds for reconstruction of rotator cuff tendon defects showed also a great therapeutic potential of this bioscaffold (Chen et al., 2006).

Silk is an additional biomaterial used for ACL tissue engineering constructs. Silk fiber bundles are wound into strands that are wound into cords and arranged to form the matrix (Laurencin and Freeman, 2005). Silk fibers are arranged as collagen fibers in ligaments and tendons. Nevertheless, two problems were described for the use of silk fibers. First, native silkworm silk fibers were allergenic as a result of the glu-like protein coating, sericin (Vunjak-Novakovic et al., 2004). Second, silk fibers have high linear stiffness but in a parallel geometry the silk fiber fall short of the tensile strength and linear stiffness compared to a native ACL (Vunjak-Novakovic et al., 2004). Altman et al. (2002) showed the biocompatibility and the mechanical stability of sericin-free silk fibers. Twisted silk fibers seeded with MSCs reached a maximum

load of 2337 ± 72 N (Altman et al., 2002a; Altman et al., 2002b). Like collagen, silk has been used as suture material (Petrigliano et al., 2006). Fan et al. showed the great potential of MSC-seeded silk ACL scaffolds in a pig model (Fan et al., 2010).
Small intestinal submucosa (SIS) was found to enhance the stability (Woo et al., 2006c). SIS is an acellular collagen based matrix consisting of more than 90% fibrillar collagen (collagen type I, III, and V) (Fini et al., 2007). Because of good clinical results in bladder augmentation, ureter or urethral repair, dural substitutes, vascular grafts, and skin substitutes, SIS was introduced for the reconstruction of rotator cuff tendon. A comparison of SIS and a human dermal matrix, both coated with tenocytes isolated from the rotator cuff, revealed the proliferation and the extracellular matrix synthesis (Fini et al., 2007). For the human dermal matrix it is reported that the matrix retain the major biological components of the dermis including bFGF and blood vessel channels (Fini et al., 2007). Different *in vivo* and clinical studies showed side effects when SIS was used (Fini et al., 2007; Rotini et al., 2008; Zheng et al., 2005). Zheng et al. observed inflammatory reactions (Zheng et al., 2005). Funakoshi et al. showed that the use of chitin enhance the biological and mechanical regeneration of rotator cuff tendons (Funakoshi et al., 2006).
An alternative for tissue engineering constructs are synthetic materials. They are often thermoplastics that allow different fibers and foams with usual industrial process engineering. These synthetic materials are noted for excellent mechanical strength. However, the hydrophobicity and lack of signaling molecules of the synthetic materials reduce cell adhesion, proliferation, and following functions (Fan et al., 2008). The most important synthetic materials are diverse poly lactic acids (PLA). When MSCs were seeded on PLA fibers, a good cell growth, the expression of ligament-specific markers, and the formation of ligament-like extracellular matrix were detected (Heckmann et al., 2007). Lu et al. investigated the use of biomaterials such as polyglycolic acid (PGA), poly-L-lactic acid (PLLA), and polylactic-co-glycolic acid (PLGA) for the ACL reconstruction (Lu et al., 2005). Fibronectin coated PLA fibers showed an increased cell attachment and a maximum load of 298 ± 59 N was measured (Lu et al., 2005). Cooper et al. used PLLA seeded with ACL fibroblasts and have demonstrated the growth and ligamentogenic differentiation of seeded fibroblasts (Cooper et al., 2006). Laurencin and Freeman have produced a three dimensional braided PLGA scaffold (Laurencin and Freeman, 2005). The *in vivo* results showed an ultimate tensile stress of 298 ± 59 N (ultimate tensile stress of a

rabbit ACL 251 ± 47 N). Also, the design and the composition of the braided PLGA advanced the cell attachment and proliferation (Laurencin and Freeman, 2005).

1.3.2 Cells

1.3.2.1 Fibroblasts

The ideal cell source should provide cells that are readily available for clinical use, reveal robust proliferation, and possess the potential to elaborate ECM in an organized fashion (Petrigliano et al., 2006). In a comparison of intra-articular rabbit ACL fibroblasts and extra-articular tendon fibroblasts Dunn et al. showed attachment, proliferation, and collagen synthesis of fibroblasts on a collagen fiber ligament scaffold (Dunn et al., 1995). Fibroblast proliferation and function was depended on the tissue culture medium and the origin of the fibroblasts whereas patellar tendon fibroblasts proliferate more rapidly than ACL fibroblasts when cultured on collagen fiber scaffold versus tissue culture plastic (Dunn et al., 1995). A comparison of ACL and MCL fibroblasts on a synthetic biodegradable polymer fiber scaffold also revealed rapid proliferation and collagen synthesis (Lin et al., 1999; Yang et al., 1999). While fibroblasts maintain many of the phenotypic qualities necessary for collagen synthesis, they are relatively inactive and have limited potential for further differentiation.

1.3.2.2 Mesenchymal stem cells

Mesenchymal stem cells (MSCs) derived from adult human tissues have offered bright prospects for cell based tissue engineering and have distinct advantages. Adult MSCs can be easily isolated from a variety of adult tissues such as bone marrow, adipose tissue, synovial membrane, and trabecular bone (Tuan et al., 2003). Furthermore, MSCs can be expanded in culture in large numbers and have the potential to differentiate into osteoblasts, chondrocytes, adipocytes, fibroblasts (ligamentogenic and tenogenic), muscle, stroma cells, and other tissues of mesenchymal origin (Pittenger, 2008). Autologous MSCs were already used in clinical case studies for the treatment of segmental bone defects, femoral head necrosis, and articular cartilage reconstruction (Noth et al., 2007b; Quarto et al., 2001; Wakitani et al., 2004).

The induction of MSC differentiation into ligament, tendon, and muscle has only be investigated in animal models (Young *et al.*, 1998; Awad *et al.*, 1999; Fan *et al.*, 2009) (Figure 6). Besides the differentiation of the cells, the mechanical loading is one important issue concerning cell based ligament/tendon tissue engineering (Tuan et al., 2003). Hsieh et al. revealed that the tensile strength and stretch loading are essential for the proper formation and alignment of the ligament/tendon structure (Hsieh et al., 2000). Altman et al. observed cell proliferation, attachment on silk fibers, expression of ligament fibroblasts marker and formation of oriented collagen fibers when MSCs were cultured on silk fibers in a bioreactor with controlled longitudinal and torsional strain (Altman et al., 2002b). In animal models, MSCs isolated from bone marrow, have been used for Achilles tendon repair. In particular, MSCs seeded onto a collagen type I scaffold incorporated into the healing tendons (Young et al., 1998). The MSC-seeded scaffolds showed a better alignment of cells and collagen fibers and were more similar to the native Achilles tendon compared to the unseeded control.

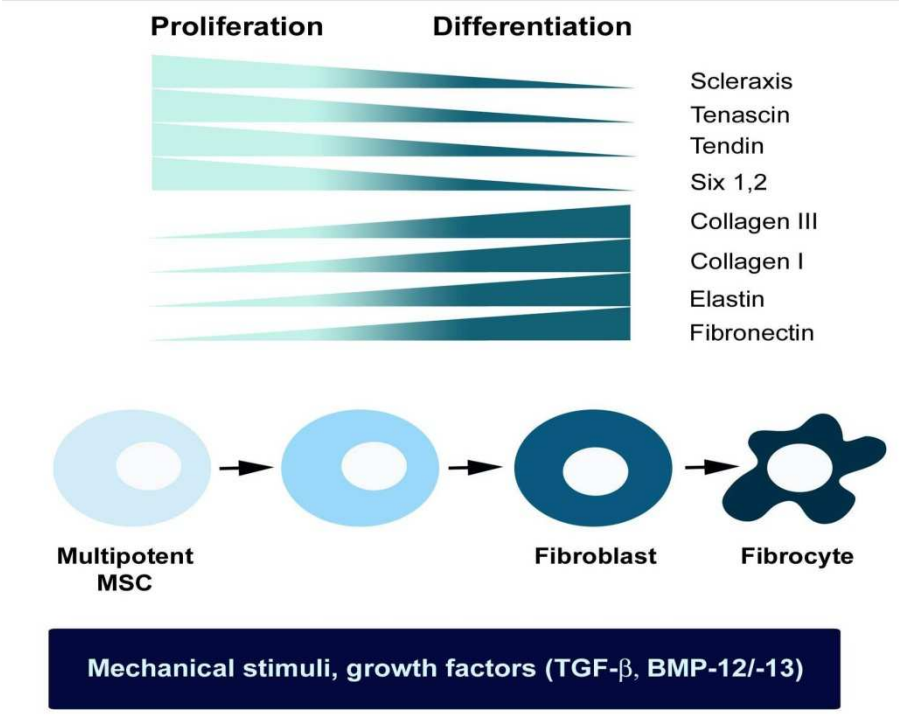

Figure 6: Ligamentogenic differentiation of MSCs. Multipotent MSCs in combination with growth factors (e.g. BMP-12 and -13) or mechanical stimuli differentiate to ligamentogenic fibroblasts. The differentiated cells produce a ligamentogenic ECM, e.g. scleraxis, tenascin, collagen type I and III, and fibronectin.

1.3.3 Stimuli

A number of different growth factors, such as transforming growth factor-β (TGF-β), basic fibroblast growth factor (bFGF), insulin-like growth factor (IGF), epidermal growth factor (EGF), and plated-derived growth factor (PDGF) have been tested for their effects on ligament and tendon healing (see Table 2). These growth factors have been shown to promote ligament and tendon healing, such as cell proliferation, collagen synthesis, matrix synthesis, angiogenesis, and cell outgrowth.

Bone morphogenetic proteins (BMP) form a subgroup of the TGF-β superfamily (Wang et al., 2005; Wolfman et al., 1997; Xiao et al., 2007). The BMP family contains more than 20 proteins (Xiao et al., 2007). BMP-12, a human homolog of murine growth and differentiation factor-7 (GDF-7) induces the formation of ligament and tendon-like tissue, increased the mechanical strength and stiffness, and the re-establishment of the collagen fibers (Fu et al., 2003; Lou et al., 2001; Rodeo et al., 2007). BMP-12 may have the potential to induce the differentiation of MSCs into ligamentocytes and tenocytes (Wang et al., 2005). Also BMP-13, a human homolog of murine GDF-6 induces the formation of ligament and tendon-like tissue and increased the collagen synthesis (Helm et al., 2001; Wolfman et al., 1997).

For ligament and tendon healing the application of these factors allows the therapeutically influence to the regeneration. Important seems to be the interaction of different factors in a specific progression and concentration (Woo et al., 2004). Growth factors require a strict local application to avoid potential adverse effects of a systemic treatment. Otherwise growth factors are subjected to a fast degradation. After intravenous application the half-life of the proteins is only a few minutes whereas the use of the slow-release-system could not enhance this (Deehan and Cawston, 2005).

A possible answer to this problem could be the use of somatic gene therapy (Evans and Robbins, 1999). Both *in vivo* and *ex vivo* strategies have been used to transfer genes to cells in a variety of ligaments e.g. ACL, MCL and patellar tendon. A variety of different vectors including liposomes, adenovirus, and retrovirus have been described, with varying efficiencies (Gerich et al., 1996; Nakamura et al., 2001; Wolfe et al., 2001). After transduction of the cells and expression of the genes, high level of mediator proteins could be directly produced and released in the defect area. However, the employment of gene therapy for ligament and tendon healing is still at its beginnings.

Table 2: Growth factor effects on ligament and tendon healing.

Growth Factor	Study	Tissue	Effect
TGF-β1	Meany Murray et al. 2003 Marui et al., 1997 Gupta et al., 2007	ACL MCL Rotator cuff tendon	↑ Cellular proliferation ↑ Collagen synthesis
PDGF	Nakamura et al., 1998 Hildebrand et al., 1998 Batten et al., 1996 Dines et al., 2007	Patellar ligament MCL Rotator cuff tendon	↑ Collagen synthesis ↑ Angiogenesis ↑ Matrix synthesis
EGF-1	Deie et al., 1997	MCL	↑ Cellular proliferation ↑ Cell migration
FGF-2	Kobayashi et al., 1997	ACL	↑ Cellular proliferation ↑ Angiogenesis ↑ ACL repair
IGF-I	Steinert et al., 2008 Schmidt et al., 1995 Dines et al., 2007	ACL MCL Rotator cuff tendon	↑ Cellular proliferation ↑ Collagen synthesis ↑ Matrix synthesis ↑ Ligament repair
BMP-12	Majewski et al., 2008 Rodeo et al., 2007 Lou et al., 2001	Achilles tendon Tendon Rotator cuff	↑ Mechanical strength ↑ Stiffness ↑ Collagen synthesis ↑ Re-establishment of collagen fibers
BMP-13	Helm et al., 2001 Wolfman et al., 1997	Progenitor cells Ligament, tendon	↑ Differentiation of progenitor cells to ligamentocytes and tenocytes ↑ Collagen synthesis

In addition to growth factors, it is well known that biomechanical stimulation have also influence on ligament and tendon healing. Biomechanical stimuli can induce changes in the cell behavior and collagen architecture (Woo *et al.*, 2006b). Barry et al. showed that the cellular response in terms of alignment and cellular metabolism was highly dependent on the applied strain profile (Barry, 2003). The cyclic tensile strain has influence on a fibroblast-seeded collagen construct. This means, the cellular proliferation was enhanced by the application of cyclic strain and the rate of collagen synthesis and matrix metalloproteinase productions were strain profile dependent. Several theories have been established to explain the effect of biomechanical stimulation on cellular response with regard to cell morphology and matrix production. It is generally believed that mechanotransduction signals are sensed by deformation

of the cytoskeleton that is transmitted from the surrounding matrix via transmembrane cellular adhesion molecules, resulting in reorganization of the cytoskeleton and initiating up-regulation of ECM synthesis (Barry, 2003; Petrigliano *et al.*, 2006). During mechanotransduction, the attachment of integrins to ECM proteins creates a physical link between the ECM and the interior of the cell. Mechanical signaling pathways translate loading of the ECM into cell signaling cascades that change gene expression (Benhardt and Cosgriff-Hernandez, 2009).

Furthermore, Altman et al. reported that undifferentiated human BMSCs subjected to multidimensional mechanical strains showed up-regulated ligament fibroblasts markers and resulted in the formation of oriented collagen fiber characteristic for ligaments (Altman *et al.*, 2002a; Altman *et al.*, 2002b; Vunjak-Novakovic *et al.*, 2004; Lee *et al.*, 2007). Noth et al. revealed an enhanced fibronectin expression in mechanical stimulated human MSCs (Noth *et al.*, 2005). This means, the biomechanical stimulation of cultured ligament fibroblasts upregulated the expression of collagens type I and type III, fibronectin, and tenascin-C (Chiquet-Ehrismann *et al.*, 1994; Chiquet *et al.*, 1996; Toyoda *et al.*, 1998; Trachslin *et al.*, 1999; Kim *et al.*, 2002; Petrigliano *et al.*, 2006).

Altogether the effects of mechanical stimulation on fibroblasts and BMSCs are dependent on the magnitude (Brighton *et al.*, 1991; Weyts *et al.*, 2003; Benhardt and Cosgriff-Hernandez, 2009), duration (Nagatomi *et al.*, 2001; Benhardt and Cosgriff-Hernandez, 2009), and frequency (Nagatomi *et al.*, 2001) of mechanical stress. After cyclic stretching (10%, 0.16 Hz) ACL fibroblasts showed an increased type I and type III collagen mRNA expression (Kim *et al.*, 2002).

Chapter 2

Collagen fiber based constructs for the ACL replacement

Abstract

The anterior cruciate ligament (ACL) is the most injured ligament of the knee. Because of the poor results of the primary repair by the use of tendon implants (e.g. semitendinosus and patellar tendon), the faithful reproduction is the treatment of choice. Due to the fact that collagen type I is the main component of an ACL, the structure, the sterilization and the biomechanical stability of collagen type I fibers, isolated from rat tails, were investigated. Scanning and transmission electron micrographs and biomechanical testing showed no influence of different sterilization methods to collagen type I fibers. These results suggest that collagen type I scaffolds have the ability to reproduce the native ACL structure, particularly in the field of the biomechanical stability.

2.1 Introduction

Because of increased participation in sports, the frequency of anterior cruciate ligament (ACL) ruptures is rapidly increasing. Currently over 100,000 patients rupture their ACL each year. The ACL fails to heal after rupture, and loss of ACL function leads to knee instability, loss of proprioceptive function (Beynnon et al., 1997), and osteoarthritis in over 60% of patients (Pattee et al., 1989). Since primary repair of the ACL has been found to fail in greater than 50% of patients (Kaplan et al., 1990; Sherman et al., 1991), the recommended treatment for the ACL deficient knee with instability is ligament reconstruction with biologic grafts such as autologous patellar tendon or hamstring tendon. However, this operation does not restore the complex architecture and biomechanics of the ACL, and more than 50% of patients will have radiographic changes consistent with osteoarthritis 7 years after surgery (Aglietti et al., 1992b; Anderson et al., 1994b; Shoemaker et al., 1993). Thus, ACL rupture is a clinically important problem, and there remains a need for improved treatments. The cost to society for ACL reconstruction is over one billion dollars per year. Furthermore, as the average age of patients is in the mid-twenties, new strategies to optimize healing of the ligament, restore knee function, and minimize the development of osteoarthritis are necessary.

ACL tissue engineering constructs could be a promising alternative whereas high mechanical and biochemical properties are directed to the ACL construct to restore the function of a native ACL.

The ultimate load of human ACLs can reach up to a value of 2160 N for younger people (Woo et al., 1991). Therefore, the composition of the ligament is directly correlated with the mechanical properties. ACLs are consisted of packed collagen fiber bundles oriented in a parallel fashion to offer for stability of joints in the musculoskeletal system. Collagen type I have a percentage of 70-80% (dry weight) (Woo et al., 2006c). Collagen type III (12% of dry weight) and V (8% of dry weight) are further components. Additionally, elastin fibers are present (2% of dry weight) (Hoffmann and Gross, 2006; Woo et al., 2006c).

Fibrillar collagen type I give ligaments the high tensile strength and is directly related to the structure of the molecule. Tropocollagen subunit is a rod about 300 nm long and 1.5 nm in diameter, made up of a triple helix with two alpha-1 chains and one alpha-2 chain (Scott, 2003). Tropocollagen subunits spontaneously self-assemble

after secretion and cross-linking into microfibrils. In this way, collagen molecules combine to form structured units of microfibrils (five collagen molecules), subfibrils in ligament (subfascicles in tendon), and fibrils. These fibrils are arranged in densely packed, highly ordered parallel bundles (Hoffmann and Gross, 2007). These bundles are oriented in a distinct longitudinal pattern, with proteoglycans and glycoproteins in connection with water incorporated in a matrix, binding the fibrils together to form fascicles.

2.2 Material and Methods

2.2.1 Isolation and sterilization of collagen fibers

In agreement with Vice Dean Prof. T. Dandekar some results are not shown here due to a patent application in preparation. Collagen fibers were isolated from rat tails. Therefore, the dermis was removed with care. Afterwards the collagen fibers were manually isolated. After washing with phosphate buffered saline (PBS), the collagen fibers were sterilized by the use of different sterilization procedures.

2.2.2 Biomechanical testing of collagen fibers

The effect to the stability of different sterilization procedures was biomechanically tested. Cross-sectional area of the collagen fibers was measured using a non-contact laser scanner micrometer (LDM-303H-SP; Takikawa Engineering, Tokyo, Japan).

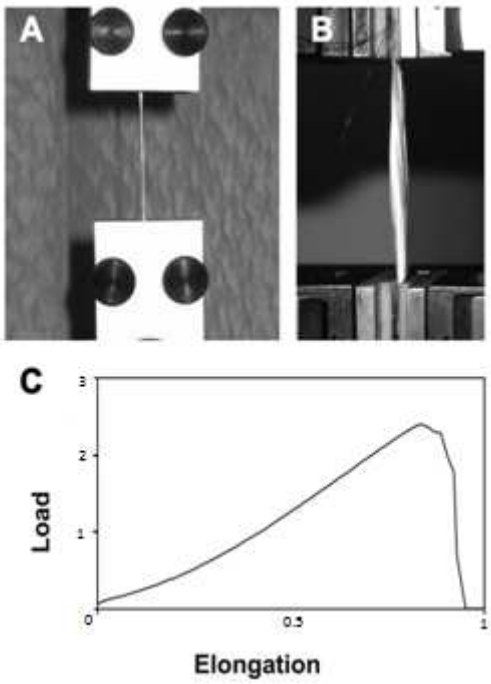

Figure 7: (A) Collagen fiber and (B) collagen scaffold clamped in a material testing machine. (C) Typical load-elongation curve of the tensile strength.

Tensile tests were done using a materials testing machine (Figures 7A and B; Model 1445, Zwick, Ulm, Germany). Load to failure tests were done separately for collagen single fibers (n=20). To prevent slippage of the fibers special clamps were used. Preload was 0.01 N with a displacement of 20 cm/min. During the measurement, the collagen was kept moist.

Load-elongation and stress-stain curves were generated and the ultimative load and the linear stiffness were investigated. For the single fibers additionally the elastic modulus (E-modulus = Young's modulus) was determined.

For each collagen fiber, a stress-strain curve was established. The slope S of the linear region of such a curve is directly related to the elasticity module of the fiber according to the formula E=S/A, where E refers to the E-module and A to the cross-section area of the fiber. S corresponds to $\Delta\sigma/\Delta l$, where $\Delta\sigma$ indicates the change in tension and Δl the change in the length of the fiber (Woo et al., 1999).

2.2.3 Electron microscopy

For scanning electron microscopy (SEM), collagen fibers were fixed for at least 45 min with 2.5% glutaraldehyde (50 mM cacodylate pH 7.2, 50 mM KCl, 2.5 mM $MgCl_2$) at room temperature, then immersed in 2% OsO_4 buffered with 50 mM cacodylate (pH 7.2) for 2 h at 4°C, washed with H_2O and incubated overnight at 4°C with 0.5% uranyl acetate (in H_2O). The fibers were dehydrated in a graded ethanol series, embedded in Epon812 and ultrathin sectioned (Schoft et al., 2003). Sections were analyzed with a Zeiss EM10 (Zeiss/LEO, Oberkochen, Germany).

For transmission electron microscopy (TEM), collagen fibers were fixed in 0.05 M cacodylate buffer containing 2.5% glutaraldehyde (pH 7.2), dehydrated, embedded in Epon and ultrathin sectioned. Sections were analyzed with an EM10 transmission electron microscope (LEO, now Zeiss).

2.3 Results

2.3.1 Electron microcopy

Typical SEM and TEM photographs of the rat tail collagen fibers are shown in Figure 9. SEM of single collagen fibers revealed a predominantly parallel orientation of the fibrils with slightly twisted fibril bundles. Comparing untreated and γ-irradiated collagen fibers, no structural differences were observed.

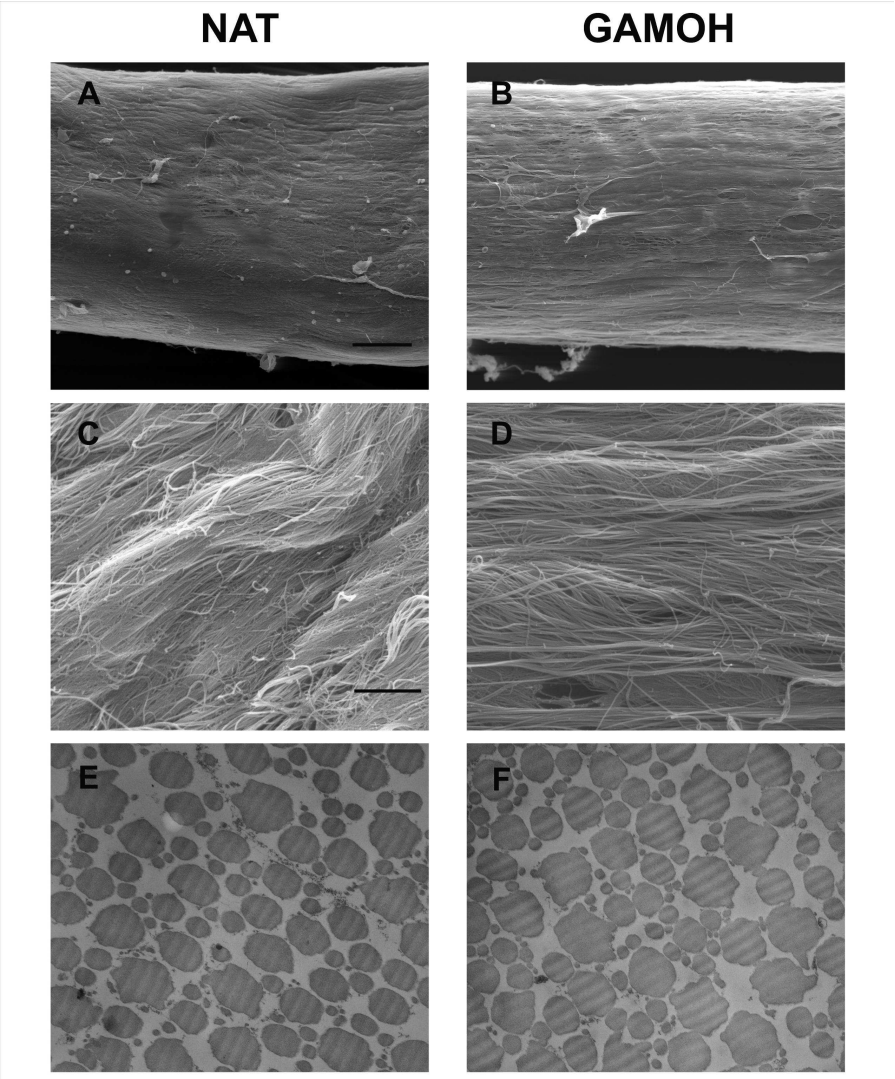

Figure 8: (A-D) Scanning (SEM) and (E,F) transmission electron micrographs (TEM) of rat tail collagen single fibers. (A,C,E) Native collagen fibers (NAT), (B,D,F) γ-irradiated and ethanol treated collagen fibers (GAMOH). Magnification: (A,B) 350x (Bar: 50 µm), (C,D) 10,000x (Bar 2 µm), and (E,F) 20,000x (Bar: 0.4 µm).

Morphologically, it can be seen that the collagen fibrils have a bimodal distribution as the fibrils had both large and small diameters (Figure 9). Both the untreated and GAMOH groups had uniformly small collagen fibril diameters. No differences in the structure and the diameter of the collagen fibers were found between all the groups.

2.3.2 Biomechanical testing

A typical load-elongation curve of the tensile strength was observed during the experiments (Figure 7C). In agreement with Vice Dean Prof. T. Dandekar some results are not shown here due to a patent application in preparation. The diameter of the collagen fibers was about 0.35 to 0.45 mm and the resulting area was about 0.10 and 0.16 mm², respectively.

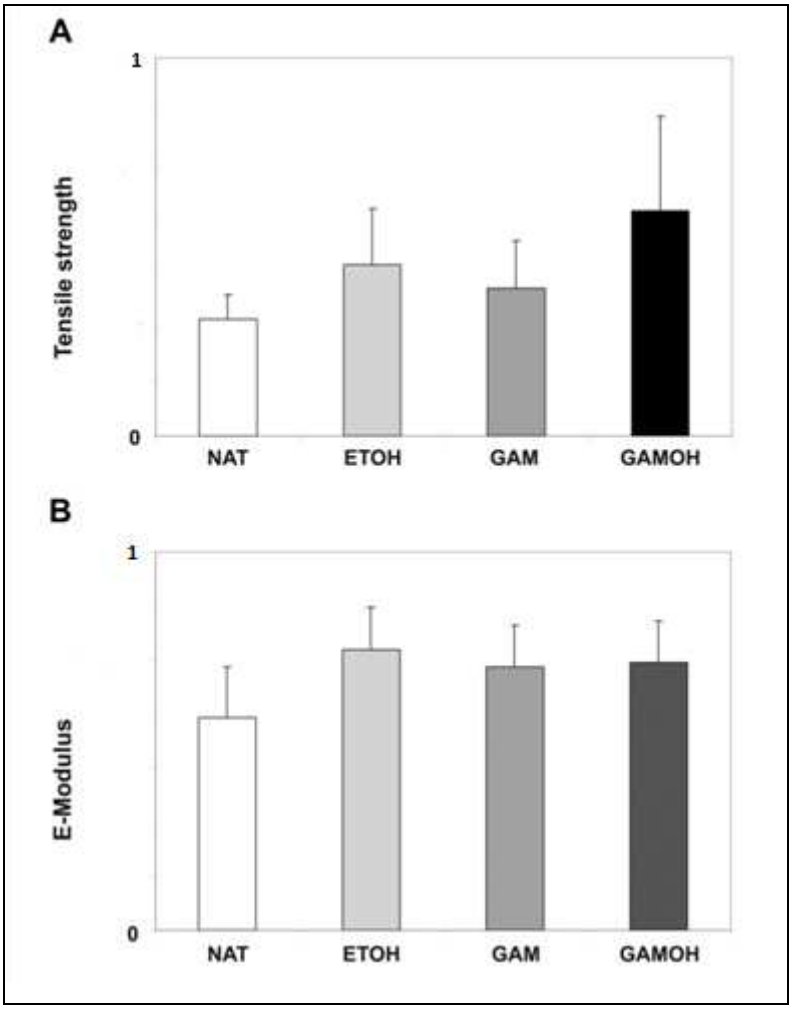

Figure 9: (A) Load to failure diagram and (B) E-Modulus of the collagen fibers after different sterilization methods compared to native fibers. Mean value ± SD (n=10).

2.4 Discussion

Numerous studies have attempted to determine the effect of various scaffolds such as silk, small intestinal submucosa (SIS), chitosan based scaffolds, PGA, PLLA (Altman et al., 2002a; Cooper et al., 2006; Dejardin et al., 2001; Laurencin and Freeman, 2005; Lu et al., 2005). In comparison to these materials, the use of collagen fibers features considerable advantages. Given that collagen is the largest component of tendon and ligament tissue, the most commonly used natural scaffold are primary composed of collagen (Awad et al., 2000; Gentleman et al., 2003; Meaney Murray et al., 2003; Murray and Spector, 2001b). Collagen fibers are an optimal substrate for cell adhesion, locomotion, and function (Chvapil et al., 1993).

The use of rat tail collagen fibers posed the questions to sterilization, stabilization, and immunological response. Gamma irradiation is one of the most effective sterilization methods. A gamma irradiation dose of more than 25 kGy assured total inactivation of all pathogens, including resistant bacterial spores, HIV, and hepatitis, and without altering their biological properties (Grieb et al., 2006). . In regard to the immunological response a clinical multicenter study with collagen hydrogel from rat tail collagen fibers showed no antibody reaction.

Allografts with an ultimative load between 628 and 1216 N depending on the tendon, which are used in less than 10%, may cause an immunological response (LaPrade et al., 2005). Additionally, allografts exhibit a slower healing and remodeling compared to autografts because of adverse, but necessary, sterilization and cross-linking procedures (Dahlstedt et al., 1989; Good et al., 1989; Jackson et al., 1990; Pinkowski et al., 1989).

Furthermore, the femur-ACL-tibia complex reached an ultimative load (tensile strength) of 2160 ± 157 N, an approved treatment after ACL rupture is the transplantation of bone-patellar-bone autografts with an ultimative load of 1784 ± 580 N and quadrupled semitendinosus and gracilis tendon autografts with 4090 ± 295 N, respectively (Woo et al., 2006c). While the majority of ACL reconstructions yielded good short term clinical results, at least 20-25% of the patients showed complications. For autografts, the key limitation problem is the donor site morbidity, with pain, muscle atrophy, loss of functionality, and rupture of the tendon (Cooper et al., 2006; Wang et al., 2006). In this case, the collagen fiber based ACL construct could be an alternative because no additional donor site is necessary. Furthermore,

implantation of cell-free collagen fiber based constructs could make sense, because autografts undergo necrosis after transplantation. Different studies have reported on necrosis of allografts and autografts (free and vascularized) shortly after transplantation, because fibroblast-seeded ligament may not be able of long-term survival in the knee joint (Butler et al., 1989; Kleiner et al., 1989). Ligament analog seeded with fibroblasts of intrasynovial origin, however, may survive and proliferate in the knee joint since they are accustomed to a moderately blood supply (Arnoczky, 1985; Butler et al., 1989). Additionally, synovial fluid may provide nutrition to transplanted ligament analogs in the early postoperative period (Amiel et al., 1986a; Dahlin et al., 1991; Fulkerson et al., 1990). Therefore, collagen fibers based ACL grafts could exhibit the structural element and the scaffold over which fibroblasts attach, migrate, and deposit new connective tissue. Dunn et al. showed the attachment of cells such as ACL fibroblasts to collagen fibers (Dunn et al., 1995). These fibroblasts align in columns along the direction of the collagen fibers (Doroski et al., 2007).

The complexity of ACL architecture was to resist the composite forces experienced about the knee. The fibroblasts within the ACL are exposed to dynamic stress, and the structural properties of the ligament are influenced by these forces. Whereas the fibroblasts themselves do not comprise a large volume of ACL tissue, they are responsible for secreting and maintaining the extracellular matrix.

Chapter 3

Intratendinous injection of mesenchymal stem cells after rotator cuff repair - an experimental study in rabbits

Abstract

The fatty infiltration of the rotator cuff is one of the most frequent musculoskeletal diseases and has important economic and social consequences, including substantial costs and loss of productivity. Different surgical methods were used from endoscope to the point of shoulder prosthesis. In the most cases, a complete regeneration of the function after surgical reconstruction is not possible. The cell based therapy provides an opportunity for the reconstruction of defects. Besides the injection of tendon fibroblasts and muscle-derived cells, mesenchymal stem cells could be very important for the treatment of the fatty infiltration of the rotator cuff. In this study, the intratendinous injection of the mesenchymal stem cell (MSC) was investigated for the treatment of a fatty infiltrated musculus supraspinatus (SSP).

3.1 Introduction

Rotator cuff diseases represent a musculoskeletal disorder with a high prevalence and enormous socioeconomic relevance (Olley and Carr, 2008). Rotator cuff tears can result from intrinsic and extrinsic factors. Among these are age-related and structural changes, as well as disturbed blood flow (Hashimoto *et al.*, 2003). Many tears are correlated with unsatisfactory results after surgical repair due to tendon retraction and structural changes, such as degeneration and fatty infiltration. (Goutallier et al., 2003a). Degeneration and fatty infiltration are irreversible and are important predictive factors for the clinical outcome and the recurrence of tears (Goutallier et al., 2003a)

Fatty infiltration of the rotator cuff muscles can be observed as early as 6 weeks after the occurrence of a tear or surgical detachment of the tendon (Matsumoto et al., 2002; Uhthoff et al., 2003). It has been shown that fatty infiltration and degeneration of muscle fibers cannot be reversed, even if rotator cuff surgery was successful (Gerber *et al.*, 2004). Studies in rabbits revealed that an early reattachment of the rotator cuff was not able to reverse the infiltration or fat accumulation (Uhthoff et al., 2003). Furthermore, it was not possible to reverse fatty infiltration with slow continuous musculotendinous traction (Meyer *et al.*, 2006).

Cell based therapies have opened new perspectives for the reconstruction of diseased or damaged tissue. In particular, the application of autologous mesenchymal stem cells (MSCs) might play an important role for the treatment of musculoskeletal diseases (Caplan, 2005). In rotator cuff repair, these cells might be injected into the subacromial space, intratendinously, or into the glenohumeral joint. So far, only few experimental cell based studies for rotator cuff repair have been performed, using mostly tendon fibroblasts. A rabbit study from Funakoshi et al., in which infraspinatus defects were augmented with tenocyte-seeded chitosan based hyaluronan scaffolds, revealed an enhanced collagen type I production and increased mechanical strength in the regenerated tissue (Funakoshi *et al.*, 2005). In another rabbit study, the implantation of porcine small intestine submucosa (SIS) or collagen type I/III scaffolds seeded with tendon fibroblasts, resulted in a better rotator cuff tendon healing and remodeling (Chen *et al.*, 2007). Platelet derived growth factor-β (PDGF-β) and insulin-like growth factor-1 (IGF-1) transduced rat tendon fibroblasts seeded on polyglycolic acid (PGA) showed an enhanced healing after

reconstruction of the injured rotator cuff (Dines et al., 2007; Uggen et al., 2005). Pelinkovic et al. performed a study in which genetically engineered muscle-derived cells (MDCs) were injected into the supraspinatus (SSP) tendon of rats (Pelinkovic *et al.*, 2003). The β-galactosidase transfected MDCs were detectable in the surrounding tissue and differentiated towards a fibroblastic phenotype. No study using bone marrow-derived MSCs for the treatment of rotator cuff repair has been performed so far.

In this study, the effect of bone marrow-derived MSCs injected into the reconstructed SSP tendon was determined in a rabbit model. Therefore, a rotator cuff defect was induced by detaching the SSP tendon and preventing spontaneous reattachment until the occurrence of a fatty infiltration was observed using magnetic resonance imaging (MRI). After 9 weeks, the SSP was reattached and half of the animals were treated with an intratendinous MSC injection. Six weeks after reattachment, histochemical analyses and qualitative MRI were performed to analyze the repair tissue and the degree of fatty infiltration.

3.2 Material & Methods

3.2.1 Surgical procedure

All surgical procedures and experimental protocols were approved by the local authorities. Fourteen 6 months-old female New Zealand White rabbits (Harlan Winkelmann, Borchen, Germany) with body weights between 3 and 4 kg were used. General anesthesia was induced intravenously with sodium pentobarbital (30 mg/kg) via the left marginal auricular vein. A size 1 laryngeal mask was inserted and the animals were artificially ventilated with a mixture of oxygen and air (1:1) to a tidal volume of 25 ml and a respiratory rate of 35/min (Harvard apparatus rodent ventilator; Hugo Sachs Elektronik, March-Hugstetten, Germany). Anesthesia was maintained by isoflurane (2.1%; Forene, Abbott GmbH, Wiesbaden, Germany) and monitored by recurrent testing of palpebral reflexes and hind paw withdrawal.

A bone marrow aspiration of the iliac crest was performed to harvest MSCs, as previously described (Pascher *et al.*, 2004). After shaving and skin disinfection a longitudinal anterolateral skin incision was made over the right shoulder. The omovertebral and deltoid muscle were retracted to expose the SSP upon its insertion at the greater tuberosity. The SSP was transected close to its insertion and any fibrocartilaginous tissue attached to the greater tuberosity was removed. The proximal stump of the SSP was wrapped with a polyvinylidine fluoride (PVDF) membrane (Durapore7 SVLP; Millipore, Bedford, MA, USA) of 125 µm in thickness and 5 µm of pore size to prevent spontaneous reattachment (Matsumoto *et al.*, 2002; Koike *et al.*, 2005). The wound was closed in layers and the animals wear allowed full weight-bearing immediately after surgery and were housed in free range. Postoperative analgesia was carried out with metamizol (30 mg/kg i.v.). In addition, buprenorphine (0.02 mg/kg s/c) was given 1 h before, 8 and 16 h after surgery and every 12 h on days 2 and 3.

After 6 and 9 weeks the degree of fatty infiltration of the SSP was visualized using MRI. After 10 weeks, the SSP was reattached to the greater tuberosity in all animals. Therefore, the previous incision was used to reach the tendon stump. The PVDF membrane was removed and the SSP was mobilized. Three drill holes were made with a 1 mm diameter drill bit at the lateral aspect of the greater tuberosity into a prepared bone groove. Two horizontal mattress sutures with non-absorbable, monofilament 3-0 prolene (Ethicon, Norderstedt, Germany) were placed. Each suture

was passed through a lateral drill hole, through the tendon, and was exiting through the drill hole in the middle. The sutures were tied over the lateral cortical bone, thus pulling the tendon stump to the greater tuberosity. Half of the animals were injected with 3.6×10^6 MSCs in 1 ml of PBS into the first third of the SSP using 5 single injections of 0.2 ml and a 23-gauge needle (+MSC). The other half was injected in the same manner with 0.2 ml of PBS (–MSC). The non operated SSP of the left side was used as a control. All animals were sacrificed 16 weeks after the first surgery and the removed right and left SSP were photographed for macroscopical evaluation.

3.2.2 Cell culture

The cells of the aspirated bone marrow were counted with a hemocytometer (Neubauer improved chamber, Superior Marienfeld GmbH & Co. KG, Lauda-Königshofen, Germany) and plated in 75 cm^2 tissue culture flasks (TPP, Trasadingen, Switzerland) at a density of 0.5×10^6. Non-adherent cells were removed after 3 days and attached cells were rinsed twice with phosphate buffered saline (PBS). The culture medium consisted of DMEM supplemented with 10% fetal bovine serum (FBS), 1 U/ml penicillin and 10 g/ml streptomycin (all PAA, Linz, Austria), and 50 µg/ml ascorbate-2-phoshate (Sigma-Aldrich, Taufkirchen, Germany). When cells reached 70 to 80% confluency, they were detached with 0.25% trypsin containing 1 mM EDTA (PAA, Linz, Austria). Detached cells were frozen in a concentration of 1×10^6 cells/ml using 10% Dimethylsulfoxide (DMSO; Applichem, Darmstadt, Germany), 50% FBS, and 40% culture medium. One week before the second surgical procedure with the reattachment of the SSP, cells were thawed, centrifuged at 1200 rpm for 5 min, and suspended in culture medium. For all animals MSCs at passage 3 were used.

3.2.3 MSC labeling with VSOPs

For later identification of the injected MSCs, the cells were labeled with very small superparamagnetic iron oxide particles (VSOPs; C200, Ferropharm, Teltow, Germany). The labeling was performed as previously described (Stroh *et al.*, 2005, Heymer et al., 2008). When the cells reached 70 to 80% confluency, culture medium containing VSOPs at a concentration of 1.5 mM was added. After incubation for 90 min at 37℃ and 5% CO_2, cells were washed 3 times with PBS to remove any

VSOPs, which were not incorporated by endocytosis. Adherent cells were detached with 0.25% trypsin-EDTA, centrifuged, and counted. For the injection of VSOP-labeled MSCs, 3.6 x 10^6 cells in 1 ml of PBS were drawn up in a 1 ml plastic syringe.

3.2.4 Magnetic resonance imaging (MRI) experiments

In vivo MRI was performed using a 1.5 T clinical whole body scanner (Avanto, Siemens Healthcare, Erlangen, Germany). Under isoflurane anesthesia, images were taken one week before, 6 weeks, and 9 weeks after detaching the SSP. Additional MRI was performed 3 and 6 weeks after reconstructing the tendon. The MR images were acquired using 2D multislice FLASH and Turbo-Spin-Echo (TSE) sequences with the following parameters: echo time T_E = 10 and 15 ms, repetition time T_R = 444 and 4000 ms (FLASH / TSE). In all cases, 4 averages and a field-of-view (FOV) of 160 x 160 mm^2 and a slice thickness of 1.5 mm were used, with a matrix size of 256^2 and 512^2 image points (FLASH/TSE). This led to isotropic nominal in-plane resolutions of 0.625 mm and 0.313 mm, respectively. During the image post-processing, a zero filling by a factor of 2 was applied in both dimensions. For the detection of the fatty infiltration within the SSP, the experiments were performed with and without fat suppression (fat saturation = fs). TR was increased to 934 ms for the FLASH sequence with fat saturation. The fat content of the SSP was evaluated according to Goutallier et al. by three independent reviewers using blinded data (Goutallier *et al.*, 1994). In this classification, the fatty infiltration is divided in five stages: stage 0 = complete muscle is normal, stage 1 = muscle contains some fatty streaks, stage 2 = more muscle than fat tissue, stage 3 = as much fat as muscle, and stage 4 = more fat than muscle (Goutallier *et al.*, 1994).

3.2.5 Histochemical analyses

The SSP was cut in 3 equal parts, the insertion with the musculotendinous fraction, the intermediate part, and the medial part. The tissue was embedded in Tissue Tek® (Sakura, Zoeterwoude, Netherlands) and frozen in liquid nitrogen. Sections of 6 µm were cut, air dried overnight, washed with 0.5 mol/l Tris(hydroxymethyl-aminoethan)-solution, and stained for H&E. VSOPs were detected by Prussian blue staining. Therefore, after washing with distilled water, slices were incubated with 1%

potassium ferrocyanide in 1% hydrochlorid acid for 30 min, washed, and counterstained with nuclear fast red for 5 min (Heymer et al., 2008).

To quantify the amount and distribution of fatty infiltration in the SSP, the fat was extracted with ethanol in histochemical sections of H&E. The area of the empty spaces (former fat in the infiltrated tissue) were measured and compared to the total area of the muscle with the image analysis software AxioVision 4.6 (Carl Zeiss, Göttingen, Germany). For quantitative evaluation, 3 cross sections of each region (insertion, intermediate part, and medial part) of all SSPs were analyzed. Furthermore, within each cross section measurements were performed at 3 different sites. For statistical analyses, the Bonferroni test was applied to identify significant differences. P values less than 0.05 were considered statistically significant (*). Data were verified by analysis of variance and are shown as means ± standard deviations (SD).

3.3 Results

3.3.1 Gross examination

Macroscopic appearance of the dissected SSPs revealed differences between the group treated without cells (–MSC) and the cell-treated group (+MSC) compared to the non operated control group (Table 4 and Figure 11 upper row). The control group showed a typical appearance with a natural red muscle tissue and a short whitish tendon (*) at the insertion (Figure 11A and B, lower row). In contrast, all operated animals showed a fatty degeneration of the SSP, which could be visualized macroscopically as a less intense red muscle tissue along with an atrophic muscle (Figure 11A and B). In the –MSC group, the fatty degeneration affected the complete SSP in 3 animals, as shown in 2 representative specimens in Figure 11A.

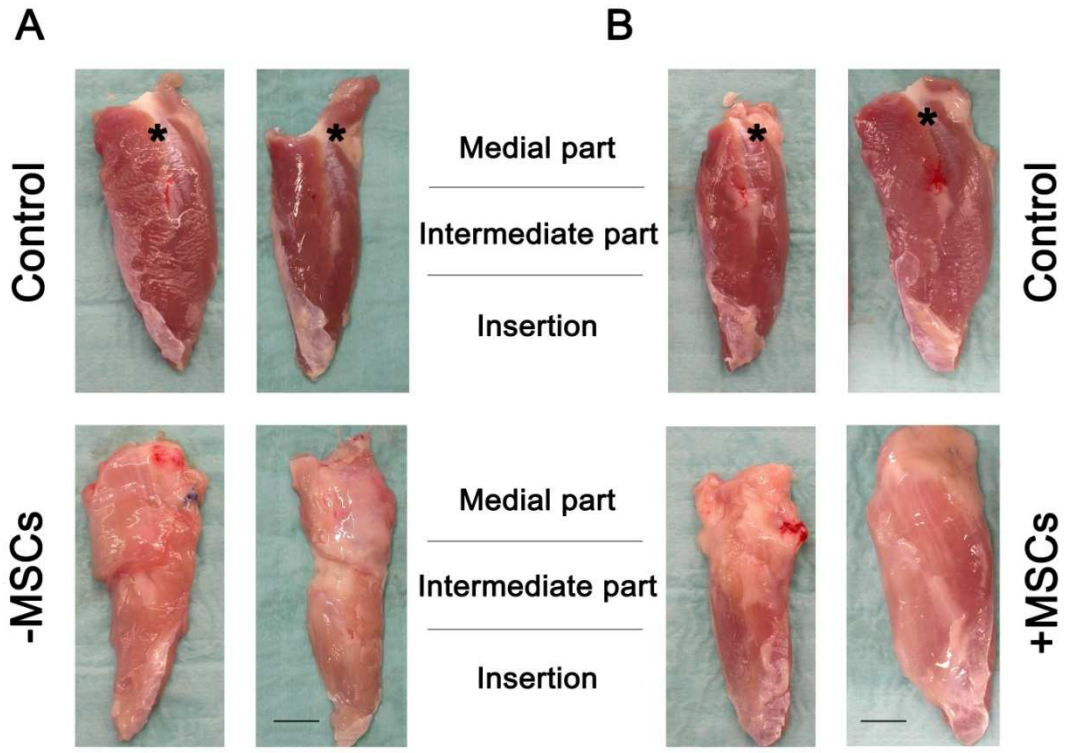

Figure 10: Macroscopical appearance of the non operated left SSP (control) and the corresponding operated right SSP of the same animals 16 weeks after first surgery. (A) PBS (-MSC) and (B) VSOP labeled MSCs (+MSC) were injected into the first third (insertion) of the muscle. In all operated animals a fatty degenerated atrophic SSP could be observed compared to the non operated control group. The distribution of the fatty degeneration was different in the –MSC group compared to the +MSC group (see text and Table 1). Bar = 1 cm.

Table 3: Distribution of the fatty infiltration in the –MSC and the +MSC group evaluated macroscopically.

	fatty infiltration	
	-MSC group (n=7)	**+MSC group (n=7)**
medial part	7	7
intermediate part	7	2
insertion	3	none

In all other cases in this group, only the medial part and the intermediate part were affected by a fatty degeneration. In the +MSC group, 2 specimens showed macroscopically a fatty degeneration at the medial part and the intermediate part of the SSP (Figure 11B, left SSP). In all other specimens, the fatty degeneration was restricted to the medial part (Figure 11B, right SSP). The macroscopic findings are summarized in Table 1.

3.3.2 MRI

Sagittal (Figure 12A,C, and E) and coronal (Figure 12B,D, and F) MR images were performed without (Figure 12A and B) and with fat saturation (Figure 12C and D). MRI images showed that 9 weeks after detaching the SSP, a distinct fatty infiltration of the SSP could be observed (Figure 12). The fatty infiltration was typically seen as streaks and spots close to the fossa supraspinata (Figure 12). In some specimens, also the ISP and SSC developed a partial fatty infiltration.

After 16 weeks only slight differences between the –MSC and the +MSC group could be observed. In Figure 13 a distinct fatty infiltration in the medial part, intermediate part, and insertion could be observed, despite reattachment and reconstruction of the SSP. The Goutallier staging (Goutallier *et al.*, 1994) of MR images acquired 9 weeks after the SSP detachment revealed a fatty degeneration of stage 2.3 ± 0.6 (coronal) and 2.3 ± 1.0 (sagittal) in the -MSC group. The fatty degeneration in this group increased to a value of 2.7 ± 0.9 (coronal) and 2.8 ± 1.0 (sagittal) after 16 weeks. For the +MSC group a fatty degeneration of stage 2.4 ± 0.5 (coronal) and 2.4 ± 0.5

(sagittal) was observed after 9 weeks and increased to values of 2.7 ± 0.7 (coronal) and 2.7 ± 0.9 (sagittal) after 16 weeks. After semi-quantitative evaluation according to Goutallier (Goutallier *et al.*, 1994), the single values of the fatty infiltration ranged coronal from 2 to 4 and sagittal from 1 to 4, respectively.

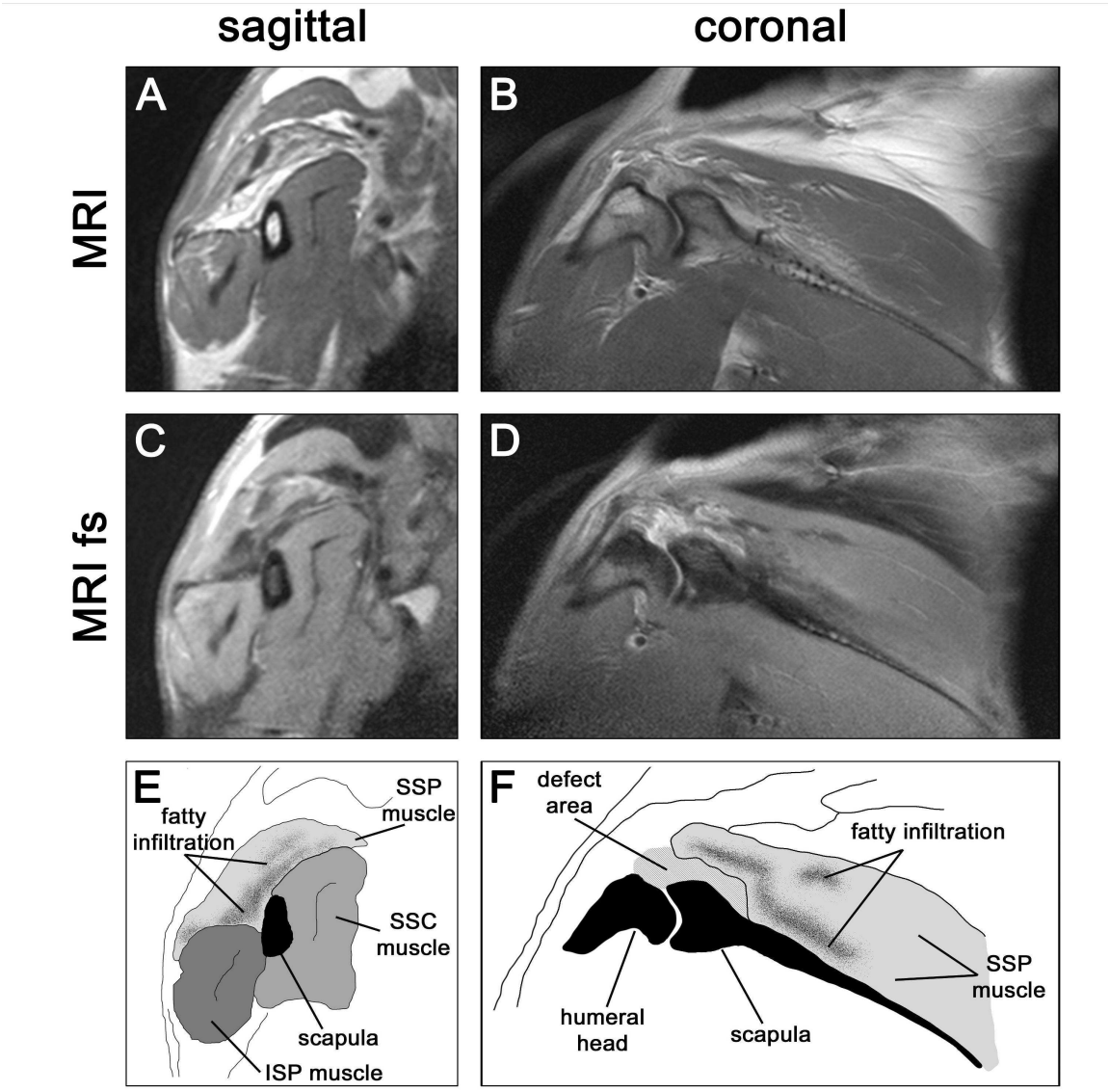

Figure 11: MR images of the rotator cuff 9 weeks after detachment of the SSP and before reconstruction. (A and C) Sagittal and (B and D) coronal images. Images were performed without (MRI; A and B) and with fat saturation (MRI, fat sat.; C and D). After 9 weeks the fatty infiltration (FI, arrows) of the SSP was clearly visual. (E and F) Sketch of the anatomy of a sagittal and a coronal MR image. 2D multislice Turbo-Spin-Echo experiment, FOV = 160 x 160 mm², TE = 15 ms, and TR = 4000 ms. SSP = supraspinatus muscle, ISP = infraspinatus muscle, SSC = subscapularis muscle.

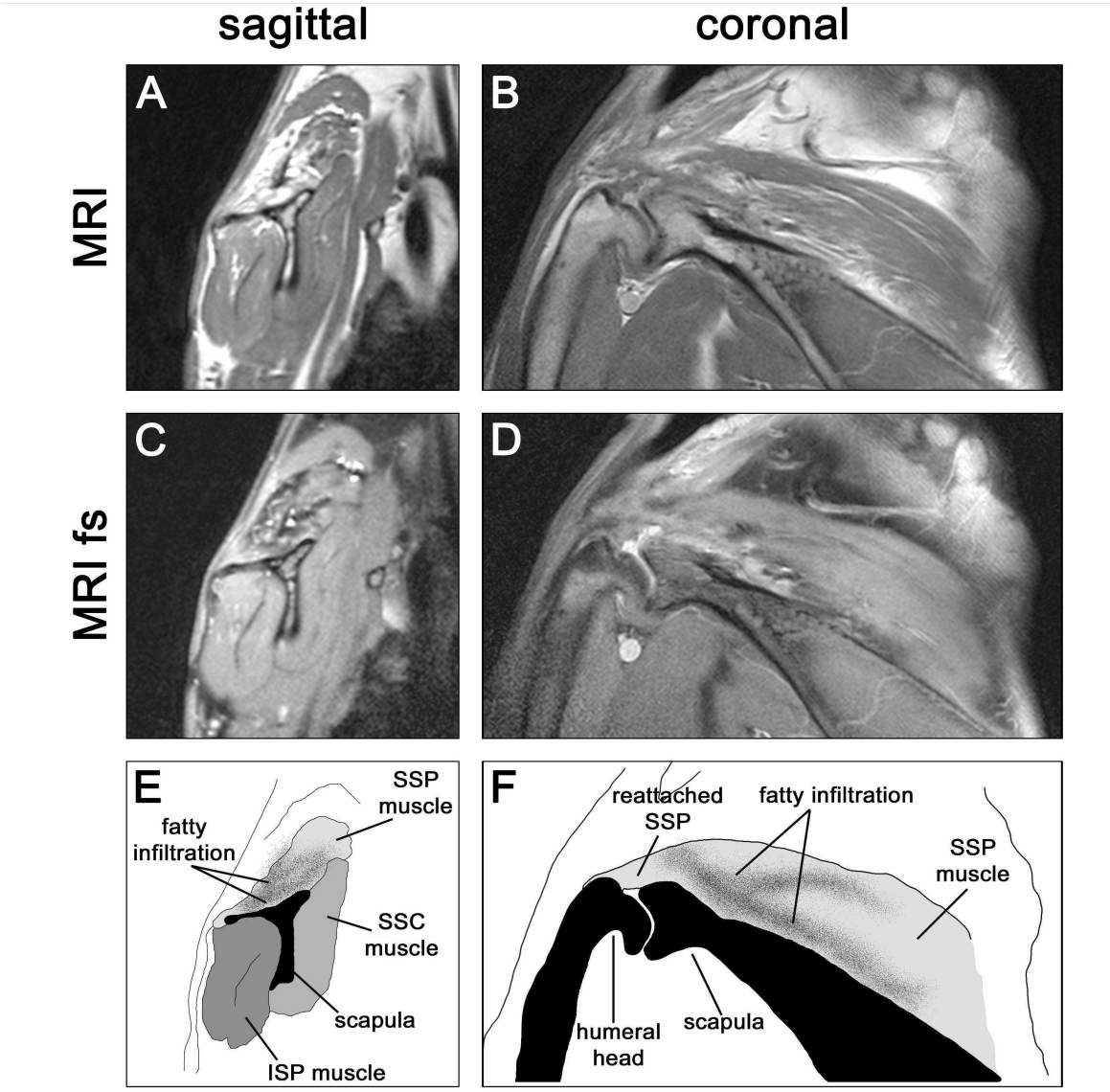

Figure 12: MR images of the rotator cuff 16 weeks after detachment of the SSP and 6 weeks after reconstruction. (A and C) Sagittal and (B and D) coronal MR images were performed (MRI; A and B) without and (MRI, fat sat.; C and D) with fat saturation. Despite reattachment and reconstruction of the SSP, a distinct fatty infiltration was observed in the medial part, intermediate part, and insertion of the SSP. (E and F) Sketch of the anatomy of a coronal and a sagittal MR image. 2D multislice Turbo-Spin-Echo experiment, FOV = 160 x 160 mm^2, TE = 15 ms, and TR = 4000 ms. SSP = supraspinatus muscle, ISP = infraspinatus muscle, SSC = subscapularis muscle.

3.3.3 Histochemical analyses

Six weeks after the second surgery, cryosections of the control group (Figures 14A-C), the group treated without cells (–MSC; Figure 14D-F), and the cell-treated group (+MSC; Figure 14G-I) were stained with H&E. In both, the –MSC and the +MSC

group, the accumulation of the fat took place between the muscle bundles, whereas the muscle fibers showed no evidence of a fatty infiltration. In the control group few adipocytes were found in the medial part, in the intermediate part, and the insertion (Figure 14A-C). The fatty infiltration in the –MSC group (Figure 14D-F) was distributed on the complete SSP. In the +MSC group, the medial part showed a readily increased fat content in comparison to the intermediate part and the insertion (Figure 14G-I).

The different parts (medial part intermediate part, and insertion) of the SSP showed no differences in the control group (Figure 15A).

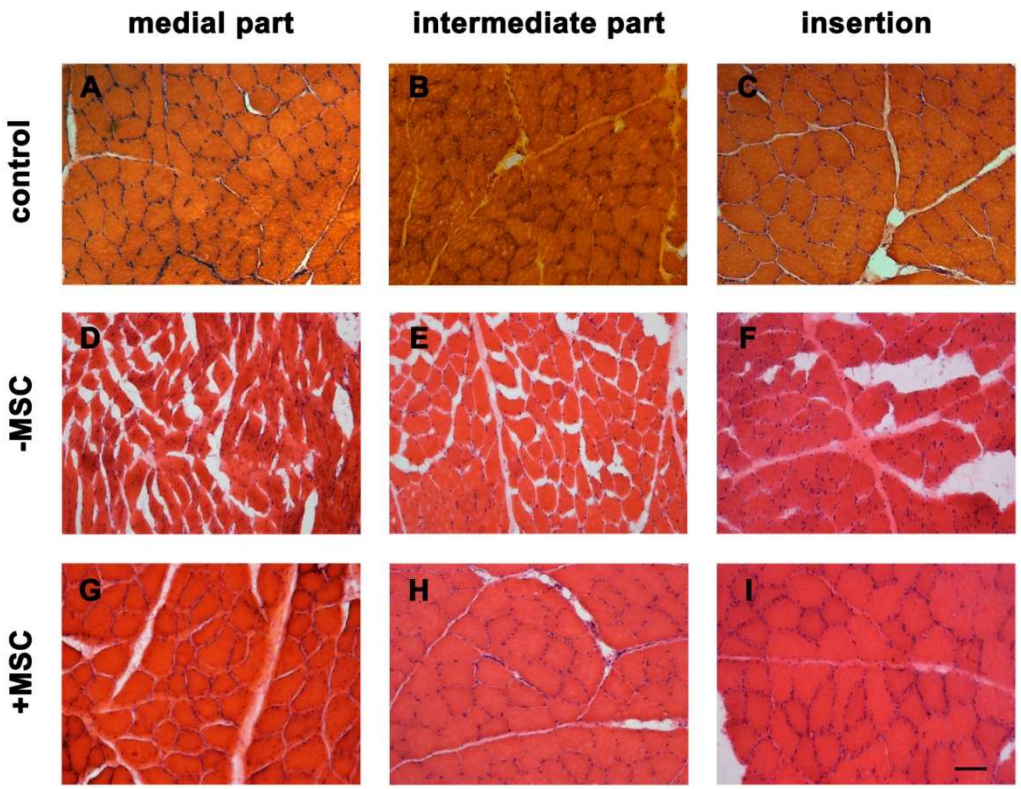

Figure 13: Cross-sections of the medial part, the intermediate part, and the insertion of the SSP muscles stained with H&E 6 weeks after reconstruction of the defect. (A-C) Non operated control group; (D-F) Group treated without cells (–MSC); (G-I) Cell-treated group (+MSC). Bar = 100 µm. Original magnification: 100x.

The fat content of the control was 3.6 ± 2.5% at the insertion, 3.7 ± 2.3% at the intermediate part, and 3.1 ± 2.9% at the medial part. In contrast, the amount of fat in the –MSC group was higher at the medial part (14.2 ± 7.8%), the intermediate part (11.0 ± 5.4%), and at the insertion (14.3 ± 6.0).

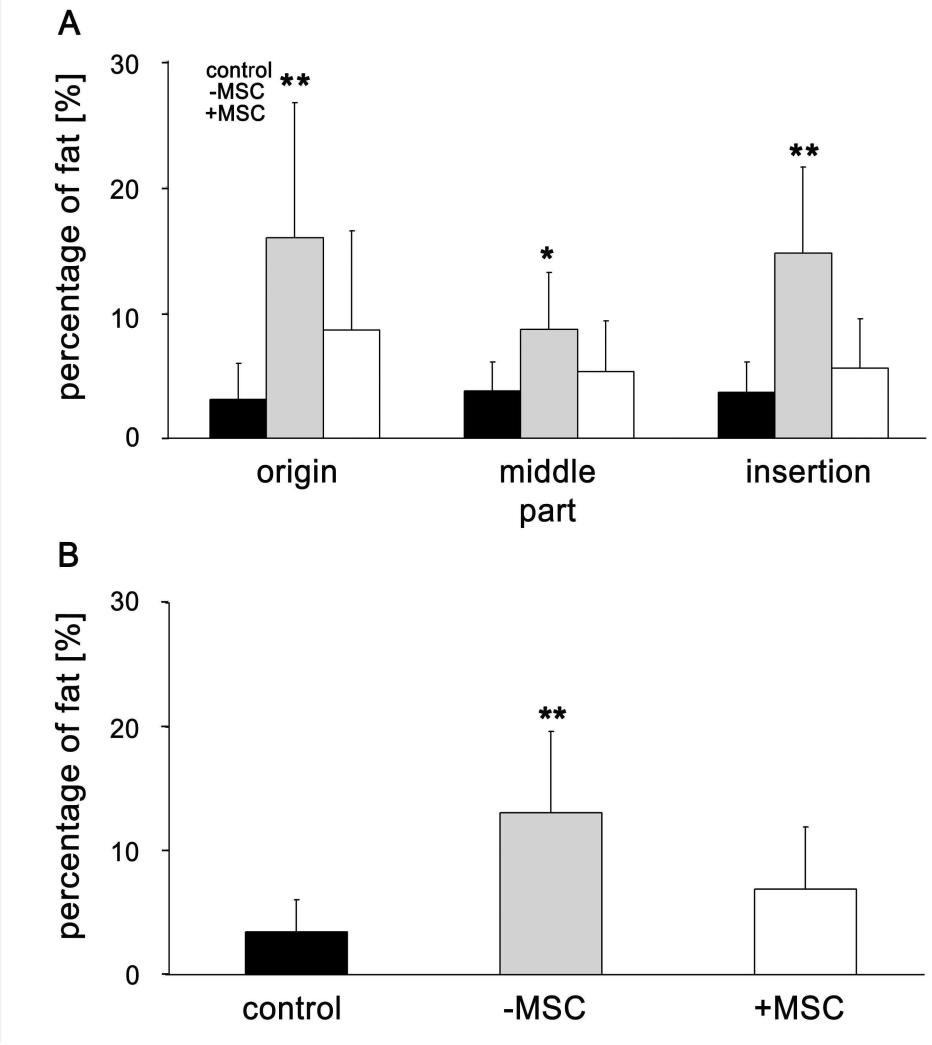

Figure 14: Quantitative analyses of the percentage of fat as determined by histomorphometry using HE staining. (A) The fat content of the medial part, the intermediate part, and the insertion was compared in the SSPs of the control, the –MSC, and the +MSC groups. The percentage of fat in the control group was very low. In contrast, the –MSC group showed a much higher fat content in the SSPs. The +MSC group revealed a distinct lower fat content than the –MSC group. (B) All measurements of the medial part, the intermediate part, and the insertion were pooled. Mean ± SD of 3 areas, respectively in the medial part, the intermediate part, and the insertion of all SSPs (control group: n = 12; –MSC group: n = 5, and +MSC group: n = 8). Asterisks (*) indicate a significant difference between the +MSC group, the –MSC group, compared to the control group (*: $p < 0.05$; **: $p<0.001$).

The fat content in the +MSC group was 7.7 ± 6.4% at the medial part, 6.4 ± 4.0% at the intermediate part, and 6.7 ± 4.4% at the insertion of the muscle. The statistical analyses showed significant differences between the different parts of the SSP in the –MSC group compared to the control group (Figure 15A; medial part $p<0.001$; intermediate part $p<0.003$; insertion $p<0.001$). In contrast, no statistical differences in all three parts of the SSP between the +MSC group and the control group were

found. Furthermore, the comparison of the –MSC with the +MSC group, revealed significant differences in the medial part ($p<0.02$), the intermediate part ($p<0.003$), and the insertion ($p<0.001$) of the SSP muscle.

For a comparison with the clinically used Goutallier staging, the data of all three parts of each muscle was averaged. The overall histomorphometrical data of the muscles (Figure 15B) showed, that the fat content of the -MSC group was 13.1 ± 6.6%, which was significantly higher compared to the control group (3.5 ± 2.6; $p<.001$; Figure 15B). In contrast, the +MSC group (6.9 ± 5.0%) showed here significant statistical differences compared to the control group. Furthermore, the comparison between the –MSC and the +MSC group revealed significant differences in the fat content for the pooled data of the whole SSP ($p<0.001$).

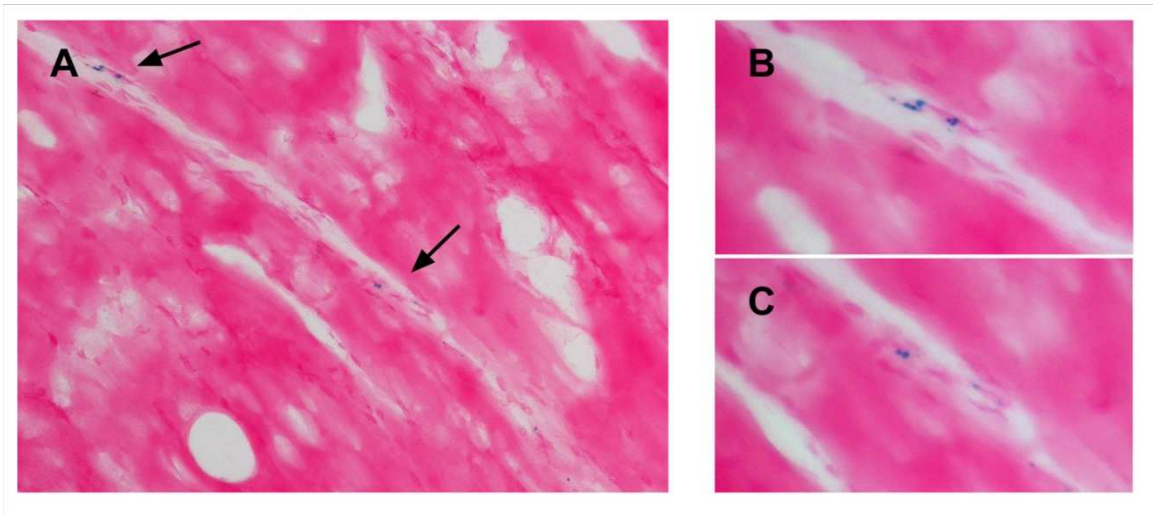

Figure 15: Prussian blue staining for the detection of VSOP labeled MSCs 6 weeks after injection in the reconstructed SSPs of the animals. Per animal 3.6 x 10^6 cells in 1 ml PBS were injected in the defect area of the SSPs. The VSOP labeled MSCs were mainly found in the medial part of the reconstructed SSPs. Original magnification: (A) 200x; (B and C) 400x.

Prussian blue staining of the +MSC group revealed the VSOP-labeled MSCs in the area of the injections, hence only at the medial part and at the intermediate part of the SSP. The labeled MSCs were found mainly at the border from normal muscle tissue to the fatty infiltration. The VSOP nanoparticles were found exclusively within the cytoplasm of the labeled MSCs (Figure 16). The appearance of the labeled MSCs was comparable to elongated fibroblast-like cells.

3.4 Discussion

Cell based therapies have been reported to be an innovative approach in regenerative medicine and orthopedic surgery. Bone marrow-derived MSCs are best investigated in this context, because they are easy to harvest and to expand (Tuan et al., 2003; Caplan, 2005; Noth et al., 2008; Ozawa et al., 2008). Muscle-derived stem cells (MDSCs) which have been used in experimental studies for rotator cuff diseases so far (Pelinkovic *et al.*, 2003), are only available in low concentrations and are difficult to expand. Thus, MDSC yield is normally very low and the use of bone marrow-derived MSCs therefore favorable.

The application of the bone marrow-derived MSCs can be performed via a simple injection or matrix based via a scaffold. Scaffolds, such as collagen for MSC delivery have already been used in experimental settings for healing of the patellar tendon (Awad *et al.*, 2003; Butler *et al.*, 2007; Kuo and Tuan, 2008). For rotator cuff repair so far studies have been performed with acellular dermal matrix, a variety such as small intestinal submucosa (SIS) (Dejardin *et al.*, 2001; Iannotti *et al.*, 2006; Chen *et al.*, 2007; Rotini *et al.*, 2008; Ide *et al.*, 2009). In a clinical study the treatment of chronic two-tendon rotator cuff tears using SIS as an augmentation showed no improved healing (Iannotti *et al.*, 2006). The use of SIS in a MR-controlled study also showed no favorable results (Sclamberg *et al.*, 2004). Funakoshi et al. described the use of an acellular nonwoven chitin fabric for the reconstruction of the ISP in rabbits and the enhancement of a biologic and mechanical regeneration of the tendons (Funakoshi *et al.*, 2006). None of these acellular techniques has lead to a good reconstruction and therefore the addition of cells might be beneficial (Dines *et al.*, 2007; Moffat *et al.*, 2009).

In contrast to matrix based approaches direct injection of MSCs is technically the simplest approach and therefore interesting for a possible clinical application. The injection of bone marrow-derived MSCs for the treatment of acute and chronic Achilles tendon injuries in horses has already been reported and showed evidence of rapid healing (Smith *et al.*, 2003; Smith and Webbon, 2005; Smith, 2008). In rotator cuff diseases, theoretically MSCs might be injected directly intratendinously, into the subacromial space, or even into the glenohumeral joint. The latter two exhibit disadvantages and therefore direct intratendinous injection was chosen in our study.

The atrophy and fatty infiltration of the rotator cuff have been described in the rat, rabbit, dog, and sheep model, whereas the rat is the most extensively studied model (Dejardin *et al.*, 2001; Matsumoto *et al.*, 2002; Pelinkovic *et al.*, 2003; Uhthoff *et al.*, 2003; Gerber *et al.*, 2004; Dines *et al.*, 2007; Rubino *et al.*, 2007). Pelinkovic et al. showed that after intratendinous injection of MDCs the cells can differentiate into fibroblasts by the expression of vimentin (Pelinkovic *et al.*, 2003). Furthermore, IGF-1 transduced cells seeded onto a nonwoven PGA scaffold revealed an enhanced rotator cuff healing in a rat model (Dines *et al.*, 2007). However, no significant fatty infiltration was observed in the rat model after setting a defect (Gupta and Lee, 2007). In our opinion, the rat is an unsuitable animal model for rotator cuff tears because of the small size of the rotator cuff and the spontaneously healing of almost all defects in rats. In contrast, a study from Uhthoff and colleagues showed that the rabbit model is ideal to investigate the degeneration and fatty infiltration of the rotator cuff using histochemical analyses (Uhthoff *et al.*, 2003). The sheep model used in a study performed by Gerber et al. has limits if tendon healing is the focus of interest because the tendon will heal spontaneously (Gerber *et al.*, 2004).

The aim of our study was to reduce the fatty infiltration of the rotator cuff by intratendinously MSC injection and to identify the injected MSCs. The fatty degeneration was induced by detaching the SSP surgically and preventing a spontaneous self healing by covering the SSP stump with a polyvinyl sheet. The occurrence of fatty infiltration was monitored non invasively using MRI. Nine weeks after surgery, a distinct fatty infiltration was observed. Our macroscopic analyses showed differences between the +MSC group, the -MSC group, and the control group (Figure 11). Histochemical analyses revealed the accumulation of fat in the -MSC group (Figure 14). Similar to the study of Matsumoto (Matsumoto *et al.*, 2002), we have quantified the intramuscular fat content in relation to the muscle tissue using an image analysis software. Histomorphometrical evaluation with different stainings (H&E, van Gieson, Masson Goldner, and Oil Red O) methods confirmed the results (Figure 15). In previous analyses, Masumoto et al. have described an equal fat content for the untreated control (Matsumoto *et al.*, 2002). The determination of the different SSP areas showed that the fatty tissue was mainly distributed and accumulated at the medial part, the so-called musculotendinous unit. Comparable observations were seen by Matsumoto et al. (Matsumoto *et al.*, 2002). In all areas, the fat content of the SSPs in the group treated without cells was higher compared to

the control and the cell- treated group. The pooling of all results offered that the SSPs of the cell-treated group exhibit a lower fat content compared to the group treated without cells. In comparison, more than 4 months after detaching the SSP in rabbits, a completely untreated rotator cuff tear offers a fat accumulation between 30 and 40% (Rubino *et al.*, 2007). The quantitative analyses of the fatty infiltration in the -MSC group correlates with the defect area. These results could mean that fatty infiltration was formed slower or was reversible due to the injection of MSCs. This phenomenon appears to be driven by the interplay of MSCs with myogenic cells. The exact mechanisms are unknown, but it is clear that MSCs secrete a broad spectrum of bioactive molecules that have immunoregulatory and regenerative activities such as transforming growth factor, insulin growth factor, basic fibroblast growth factor (Tuan *et al.*, 2003; Bobis *et al.*, 2006; Chen *et al.*, 2006; Kan *et al.*, 2007; Uccelli *et al.*, 2007; Winkler *et al.*, 2008). Bioactive factors secreted by MSCs have been revealed to inhibit tissue scaring, suppress apoptosis, stimulate angiogenesis, and enhance mitosis of tissue-intrinsic stem or progenitor cells (Caplan and Dennis, 2006). The complex, multifaceted effects resulting from the secretory activity of MSCs have been referred to as trophic activity and are distinct from the direct differentiation of MSCs into repair tissue (Caplan and Dennis, 2006; Caplan, 2007). Additionally, several approaches confirmed, that mimicry of the mechanical and chemical microenvironment is apparently necessary for the development of the MSCs (Bobis *et al.*, 2006; Hoffmann and Gross, 2006).

Furthermore, in the histochemical analyses, the VSOP labeled MSCs were mainly observed at the insertion of the SSP which means that the MSCs did not migrate. Since the MSCs stayed at the injection site, one can speculate about the reasons for the lack of the usual homing tendency or a possible homing signal originating from defect zone in the rotator cuff (Barry, 2003; Barry and Murphy, 2004). After cell death of the labeled MSCs, the VSOPs could no be detected. The phagocytosis of iron particles from dead or alive magnetically labeled cells may cause a problem in the in vivo tracking of the labeled MSCs. For this, the cells must be double labeled for example with VSOPs and GFP. Our own previous *in vitro* results showed that VSOPs have no influence to the viability, proliferation, and chondrogenic, adipogenic, and osteogenic differentiation behavior of the MSCs. The presence of iron in VSOP-labeled MSCs could be observed over 9 cell cycles (Heymer *et al.*, 2008). It is

therefore likely that the VSOP-labeling did not interfere with the homing tendency of the MSCs.

To monitor the course of muscle degeneration and fatty infiltration and to characterize the development of new cell based therapies non-invasive and repeatable imaging methods are necessary. Also in humans, the formation of the fatty infiltration can already be detected as early as 6 weeks after rupture of the SSP. In our study, qualitative MRI was used as an effective non-invasive method to monitor the course of the fatty infiltration *in vivo*. Different time points for the formation of a fatty infiltration in rabbits have been discussed previously. These varied between 4, 6 and 12 weeks (Matsumoto *et al.*, 2002; Uhthoff *et al.*, 2003; Rubino *et al.*, 2007). In our study, MRI monitoring 6 weeks after setting the defect did not show a satisfying fatty infiltration whereas the MR images acquired after 9 weeks revealed the development of a distinct fatty infiltration in all animals (Figure 2). The evaluation according to Goutallier et al. reached a value of 2.3 in our experiments (Goutallier *et al.*, 1994). This means that the muscle contains distinct fatty streaks whereas the muscle content is higher than the fat content. In addition, a fatty infiltration of lower degree could be observed in some cases in the infraspinatus muscle (ISP) and the subscapularis muscle by MRI. Reason for this could be a pain related reflex atrophy of the shoulder of the rabbits.

The qualitative approach used in this study led to inhomogeneous results which was mainly attributed to the semi-quantitative character of the Goutallier evaluation (Kenn, 2002; Oh *et al.*, 2009) based on a subjective staging process. Since the fatty tissue was also distributed inhomogeneously along the SSP, it was especially difficult to characterize the whole muscle with a single value based on a number of slices through the muscle. To quantify the fatty infiltration of rotator cuff muscles after injection of MSCs non-invasively in future studies, 2D SPLASH spectroscopy will be used (Kenn *et al.*, 2004). The protocol then consists of an imaging sequence and a newly implemented SPLASH sequence, which allows an exact quantification of the fat/water ratio with a high spatial resolution in an arbitrarily shaped region of interest (ROI). This leads to a more complex experimental protocol and longer measurement times per animal, but the percentage of fat in the rotator cuff muscles can then be determined more accurately, while still preserving the non invasive measurement.

In summary, the rabbit model is suitable for the fatty infiltration of the rotator cuff and the injection of cells, particularly for the intratendinous injection. Histological and

histomorphometrical data exhibit a lower fatty infiltration of the SSP after reconstruction and intratendinous injection of autologous MSCs compared to SSPs which were only reconstructed. However, the mechanism of this phenomenon is unclear. Additionally, this phenomenon must be controlled with a higher number of cases and if necessary in the sheep model. Because of the enhanced healing capacity in the animal models it could not be infer to the human.

Furthermore, the MRI technology allows monitoring the time course of the fatty infiltration and muscle atrophy. The detection of cells and a quantitative evaluation of the fatty infiltration could be enhanced by the use of a 2D SPLASH spectroscopy.

Acknowledgement

We are grateful to Christa Amrehn, Viola Monz, and Martina Regensburger for their excellent technical assistance. This study was supported by the German Society for Shoulder and Elbow Surgery (DVSE) to U. Nöth, O. Rolf, and F. Gohlke and the foundation of the Orthopaedic clinic König-Ludwig-Haus Würzburg.

Chapter 4

BMP-12 and BMP13 gene transfer induce ligamentogenic differentiation in mesenchymal progenitor and anterior cruciate ligament cells

Abstract

To date there are only very few data available on the ligamentogenic differentiation capacity of mesenchymal stem/progenitor cells (MSCs) and anterior cruciate ligament (ACL) fibroblasts. Here we describe the *in vitro* potential of MSCs and ACL cells to undergo ligamentogenic differentiation upon transduction with adenoviral vectors encoding the human cDNAs for bone morphogenetic protein (BMP) 12 and BMP13, also known as growth and differentiation factor (GDF) 6 and 7, respectively. Transgene expression for at least 14 days was confirmed by western blot analyses. After 21 days of cell culture within collagen type I hydrogels, histochemical (H&E, Azan, van Gieson), immunohistochemical, and PCR analyses of the genetically-modified constructs of both cell types revealed elongated, viable fibroblast-like cells embedded in a ligament-like matrix rich in collagens, vimentin, fibronectin, decorin, elastin, scleraxis, tenascin, and tenomodulin. Thus, it appears that both the MSCs and ACL fibroblasts are capable of ligamentogenic differentiation with these factors. This information may aid in the development of biologic approaches to repair and restore the ACL after injury.

4.1 Introduction

The incidence of anterior cruciate ligament (ACL) ruptures is approximately 1/1000, and reconstruction with autologous tendon grafts is currently the gold standard of treatment (Lawhorn and Howell, 2007; Schoderbek *et al.*, 2007). However, ACL reconstruction still has complications of donor site morbidity, loss of knee function, recurrent instability and particularly premature osteoarthritis in large numbers of patients with this injury (Anderson, 2004; Cooper *et al.*, 2006; Gentleman *et al.*, 2006; Hairfield-Stein *et al.*, 2007).

In an effort to improve the care of patients with ACL injuries, tissue engineering approaches have been explored using different scaffold materials including collagen, silk, biodegradable polymers, and composite materials seeded with fibroblasts or mesenchymal progenitor cells (Laurencin and Freeman, 2005; Noth *et al.*, 2005; Heckmann *et al.*, 2006; Liu *et al.*, 2008). Remarkably, it has been shown that cells seeded in collagen hydrogels can degrade and reorganize the surrounding extracellular matrix (Noth *et al.*, 2005; Murray *et al.*, 2006a), while specific culture conditions including biomechanical stimulation (Altman *et al.*, 2002b; Noth *et al.*, 2005; Kuo and Tuan, 2008) or matrix cross-linking (Redden and Doolin, 2003) could be used to elicit a longitudinal orientation of the cells in a contracted collagen network.

For further enhancement of ligament tissue regeneration, the use of growth factors including transforming growth factor-β1 (TGF-β1), insulin-like growth factor-I and –II (IGF-I/II), platelet-derived growth factor-B (PDGF-B), and basic fibroblast growth factor (bFGF) have been described (Evans, 1999; Fu *et al.*, 2003; Molloy *et al.*, 2003; Tsai *et al.*, 2003; Heckmann *et al.*, 2007; Jenner *et al.*, 2007). However, most of these factors have been described to increase cell proliferation and ligament matrix synthesis of fibroblasts, but only few have been found to induce ligamentogenic differentiation of mesenchymal progenitor cells. Recombinant growth and differentiation factor (GDF) 6 (bone morphogenetic protein (BMP) 13) and GDF7 (BMP12), members of the TGF-β superfamily, have been found to induce tendon and ligament formation following ectopic (Wolfman *et al.*, 1997; Helm *et al.*, 2001), or orthotopic (Aspenberg and Forslund, 1999; Lou *et al.*, 2001; Rickert *et al.*, 2001; Majewski *et al.*, 2008) implantation. Therefore, the purpose of this work was to study

the influence of BMP12 and 13 gene transfer on ligamentogenic differentiation of MSCs and ACL fibroblasts seeded into collagen hydrogel constructs.

4.2 Material and Methods

4.2.1 Generation and amplification of recombinant adenoviral vectors

First generation (ΔE1ΔE3) serotype 5 adenoviral vectors, carrying the cDNA of the human BMP12, or the BMP13 gene, respectively, were kindly provided by Wyeth Inc. (Madison, NJ, USA). The resulting adenoviral vectors were designated Ad.BMP12 and Ad.BMP13, respectively. For generation of high titer preparations, adenoviral vectors were amplified in 293 cells (ATCC, Manassas, VA, USA), purified on 3 rounds of CsCl density gradients, and dialyzed with viral titers being determined by optical density and standard plaque assay as described earlier (Palmer et al., 2003b).

4.2.2 Isolation and cell culture of MSCs and ACL fibroblasts

All chemicals were purchased from Sigma (Steinheim, Germany) unless stated otherwise. After approval of the Institutional Review Board of the University of Würzburg, isolation of MSCs was performed from the femoral head of patients undergoing total hip arthroplasty (all because of osteoarthritis) using a protocol first described by Haynesworth et al. (Haynesworth et al., 1992) and modified by Nöth et al. (Noth et al., 2002) as described previously. MSCs were isolated from four patients (35-, and 65-year-old male, 58-, and 81-year-old female), which had no diseases other than osteoarthritis of the hip and no medication, except occasionally nonsteroidal anti-inflammatory drugs for pain relief. The culture medium consisted of DMEM high glucose supplemented with 10% fetal bovine serum (FBS; Gibco BRL, Darmstadt, Germany), 1 U/mL penicillin and 100 µg/mL streptomycin (PAA, Linz, Austria), and 50 µg/mL ascorbate 2-phosphate (standard medium).

ACL tissue was retrieved from patients undergoing total knee arthroplasty. Institutional Review Board (University of Würzburg) approval was obtained prior to obtaining these ligaments. ACL fibroblasts were isolated by collagenase digestion as described earlier (Chen et al., 2004a). For theses experiments, ACLs were harvested from four patients (61-, 66-, and 77-year-old male, and 70-year-old female), the bony attachment sites and the synovial sheath were removed, and the ligament fascicles were dissected, minced , and digested by 0.1% (w/v) collagenase type I solution (Serva Electrophoresis GmbH, Heidelberg, Germany) for 18 h. ACL fibroblasts were

recovered by filtration through a 70-µm nylon mesh cell strainer (Falcon, Beckton Dickinson Labware, Franklin Lakes, NJ, USA), and centrifugated at 1500 rpm for 10 min. Then the cell pellets were resuspended in standard medium, counted and seeded in 75 cm^2 tissue flasks (TPP). The medium was changed every 3 to 4 days and second passage ACL fibroblast cultures were used in all experiments. When the cells reached confluence (after 10–14 days), the cells were detached with 0.25% trypsin containing 1 mM EDTA (PAA) and used for further experiments.

4.2.3 Adenoviral transduction and fabrication of collagen hydrogel constructs

For the experiments, MSCs and ACL fibroblasts were seeded at $3.6x10^6$ cells/175 cm^2 flask and transduced at 10 or 100 multiplicities of infection (MOI) of Ad.BMP12, or Ad.BMP13, respectively, in 5 mL of serum-free medium, as indicated in the respective experiments. One day after transduction, the cells were trypsinized for the cell proliferation assay or production of the collagen hydrogel constructs, with marker gene (green fluorescent protein (GFP)/firefly luciferase (Luc)) or untransduced cells serving as comparative controls.

For collagen hydrogel construct fabrication, $3x10^5$ cells were suspended in 100 µL of a neutral buffer solution,, followed by the addition of 100 µL collagen type I stock solution (Arthro Kinetics AG, Esslingen, Germany) as earlier described (Noth et al., 2005; Steinert et al., 2008). After polymerization the constructs were transferred into a 48-well plate and 500 µL culture medium was added. Medium was changed every 2-3 days throughout the 21-day culture period. All constructs were evaluated biochemically, histologically, immunohistochemically, and by semi-quantitative RT-PCR after 21 days.

4.2.4 Transgene expression analyses

At day 3, 7, and 14 cell lysates of the BMP12 and -13 transduced MSCs in the hydrogel constructs were collected and frozen at -80℃. The protein content of each lysate was determined using the Rotiquant according to the instructions of the supplier (Carl Roth GmbH, Karlsruhe, Germany). Twenty µg of protein were boiled for 5 min in SDS-polyacrylamide gel electrophoresis buffer (10 mM Tris, pH 6.8; 7.5% glycerol, 1& SDS, 0.025% bromphenol blue). Afterward the protein was separated by

12% SDS-PAGE and electrotransferred to nitrocellulose membranes. To inhibit non-specific binding, the membranes were treated with buffer containing 0.1% Tween 20, 2% horse serum, 2.5% bovine serum albumin (BSA), 2.5% milk powder in PBS for 2 h. Then, the membranes were incubated overnight at 4℃ in 0.1% Tween 20, 1% horse serum and 1% milk powder in PBS with the primary antibody anti-BMP-12 and anti-BMP-13 (1:100; Acris Antibodies GmbH, Hiddenhausen, Germany). After 3 wash steps in washing solution (10 mM Tris, pH 7.5m 140 mM NaCl, 2 mM EDTA, 0.1% Triton X-100, 1% horse serum, 1% BSA, and 1% milk powder), the membrane was incubated for 1 h with horseradish peroxidase-conjugated anti-rabbit IgG (1:2000; Sigma-Aldrich) using a solution containing in 0.1% Tween 20, 1% horse serum, 1% BSA, and 1% milk powder in PBS. Then the membrane was washed another time with washing solution. Signals were detected by chemiluminescence using the ECL system (Amersham Biosciences, GE Healthcare Life Sciences, Freiburg, Germany).

4.2.5 Cell proliferation assay

Proliferation of monolayer cells was determined using the CellTiter-Glo Luminescent Cell Viability Assay (ATP assay; Promega GmbH, Mannheim, Germany). Detection is based on using luciferase reaction to measure the amount of ATP from viable cells. The ATP amount in the cells is a function of the viability of the cells. For this, BMP12 or BMP13 transduced cells were plated in 100 µl cell culture medium in 96-well plates (1000 cells/well) with clear bottom, with untransduced or GFP-modified cultures serving as comparative controls. At the respective time points, 100 µl of CellTiter-Glo Reagent was added in each well, followed by shaking for 2 min on a shaking plate and incubation for 10 min at room temperature in the dark. The luminescence was recorded with an Orion II Luminometer (Berthold Detection System, Pforzheim, Germany) for 0.25 s/well integration time. The proliferation of the cells was measured after 1, 2, 3, 4, 5, 6, and 7 days.

4.2.6 Cell viability and apoptosis assay

Cells within collagen hydrogel constructs were evaluated for cell viability and apoptosis after 21 days by the use of the apoptosis detection kit Annexin V-Cy3 (Sigma, Steinheim, Germany). Annexin V-Cy3 binds to phosphatidylserine present in the outer leaflet of the plasma membrane of early apoptotic cells. Additionally, 6-

carboxyfluorescein diacetate (6-CFDA) was used to label viable cells (Martin et al., 1995). Collagen hydrogel constructs were incubated with 50 µl of the double labeling staining solution for 10 min at room temperature. After staining, gels were washed 5 times with 50 µl of 1x binding buffer, rinsed twice with PBS, fixed overnight in PBS-buffered 4% paraformaldehyde, dehydrated through a series of ethanols, infiltrated with isoamyl acetat (Merck, Hohenbrunn, Germany), and embedded in paraffin. Sections of 1 µm were cut through the center of the gels. The apoptotic and living cells were observed on the respective mid-sections using a fluorescence microscope (Zeiss, Ulm, Germany).

4.2.7 Histological and immunohistochemical analyses

After 21 days, hydrogel constructs were washed twice with PBS, fixed overnight in PBS-buffered 4% paraformaldehyde, dehydrated through a series of ethanols, infiltrated with isoamyl acetate, and embedded in paraffin. Sections of 1 µm were cut through the center of the gels and stained with hematoxylin/eosin (H&E), Azan, Van Gieson, and Masson-Goldner.

For immunohistochemistry, all sections were pre-treated by boiling in 10 mM citric acid (pH 5.5) for 10 min. Thereafter, the sections were incubated for 1 h at room temperature with the Dako REALTM Antibody Diluent (Dako) using primary antibodies for collagen type III (COL III; AB 747, Chemicon, Temecula, USA), elastin (ELA; MAB 1681, Calbiochem, San Diego, USA), vimentin (VIM; M0725, Dako, Hamburg, Germany) fibronectin (FN; F0916 Sigma), and tenascin (TN; CBL213; Chemicon). The slides were rinsed with PBS and visualized by treatment with AdvanceTM HRP Link and AdvanceTM HRP Enzyme for 20 min (Dako) followed by diaminobenzidine staining (DAB kit; Dako) for 10 min. The slides were finally counterstained with hemalaun (Merck, Darmstadt, Germany). For all immunohistochemical analyses controls without the primary antibody were performed.

4.2.8 Total RNA extraction and semi-quantitative RT-PCR analyses

After 21 days, 5 human hydrogel constructs per group were pooled, minced with scissors and homogenized using a pellet pestle. Total RNA was subsequently extracted with an additional purification step using a RNA isolation kit (Marcherey-

Nagel, Düren, Germany) according to the manufacturer instructions. The RNA was quantified spectrophotometrically and reverse transcribed using random hexamer primers (GE Healthcare, Munich, Germany) and Bioscript reverse transcriptase (Bioline, Luckenwalde, Germany). Equal amounts of each cDNA synthesized (100 ng), were used as templates for PCR amplification in a 50 µL reaction volume using Taq DNA polymerase (Bioline) and 50 pmol of ligament gene specific primers (Noth et al., 2005). In Table 4 the sequences, annealing temperatures, number of cycles, and product sizes of forward and reverse primers are listed for biglycan (BGN), collagen type III (COL III), decorin (DCN), elastin (ELA), fibronectin (FN), scleraxis (SCL) tenascin-C (TN-C), tenomodulin (TNMD), vimentin (VIM), and elongation factor 1α (EF1α) as internal control.

Table 4: RT-PCR primer sequences for semi-quantitative RT-PCR

Gene	*RT-PCR primer sequences (5'-3')*	Cycle number	Annealing Temp (℃)	Product size (bp)
EF1α	Sense: AGGTGATTATCCTGAACCATCC Antisense: AAAGGTGGATAGTCTGAGAAGC	27	54	234
BGN	Sense: GAGAGGCTTCTGGGACTTCA Antisense: AGGTGGGTGTGACAGAGTCC	27	58	113
COL III	Sense: GCGGAGTAGCAGTAGGAG Antisense: GTCATTACCCCGAGCACC	27	56	173
DCN	Sense: AATTGAAAATGGGGCTTTCC Antisense: GCCATTGTCAACAGCAGAGA	27	53	220
ELA	Sense: GCAGTGCCTGGGGTCCTTGGAG Antisense: GCTGCTTTAGCGGCTGCAGCTGG	35	58	211
FN	Sense: TGGAACTTCTACCAGTGCGAC Antisense: TGTCTTCCCATCATCGTAACAC	30	58	451
SCL	Sense: CCTGAACATCTGGGAAATTTAATTTTAC Antisense: CGCCAAGGCACCTCCTT	37	56	111
TN-C	Sense: TCAAGGCTGCTACGCCTTAT Antisense: TCAAGGCTGCTACGCCTTAT	40	57	230
TNMD	Sense: CCATGCTGGATGAGAGAGGT Antisense: CTCGTCCTCCTTGGTAGCAG	40	58	123
VIM	Sense: GACCGCTTCGCCAACTACATCGAC Antisense: GGTCATCGTGATGCTGAGAACTTCG	40	65	1060

The RT-PCR products were electrophoretically separated on 1.5% agarose gels containing ethidium bromide and visualized using the Bio Profile software (LTF, Wasserburg, Germany). The densities of the PCR bands were analyzed with the Bio 1D/Capt MW software (LTF) and the mean ratio (x-fold change) normalized to the EF1α housekeeping gene expression and related to the controls was calculated from three bands (one per patient).

4.2.9 Statistical analyses

For each set of experiments described m=4 replicates with cells from different MSC or ACL donors were performed, with n=3 pellets per group per replicate. Data from cell proliferation and RT-PCR analyses were expressed as mean ± standard deviation (SD). Statistical significance between groups was determined by the Mann-Whitney test using the PASW Statistic software (SPSS GmbH Software, Munich, Germany). A level of $p<0.05$ was considered significant.

4.3 Results

4.3.1 BMP12 and BMP13 detection

By means of western blot analyses BMP12 and BMP13 could be detected in Ad.BMP12 and -13 transduced MSCs (Figure 15A) as well as ACL fibroblast (data not shown) at a dose of MOI 100.

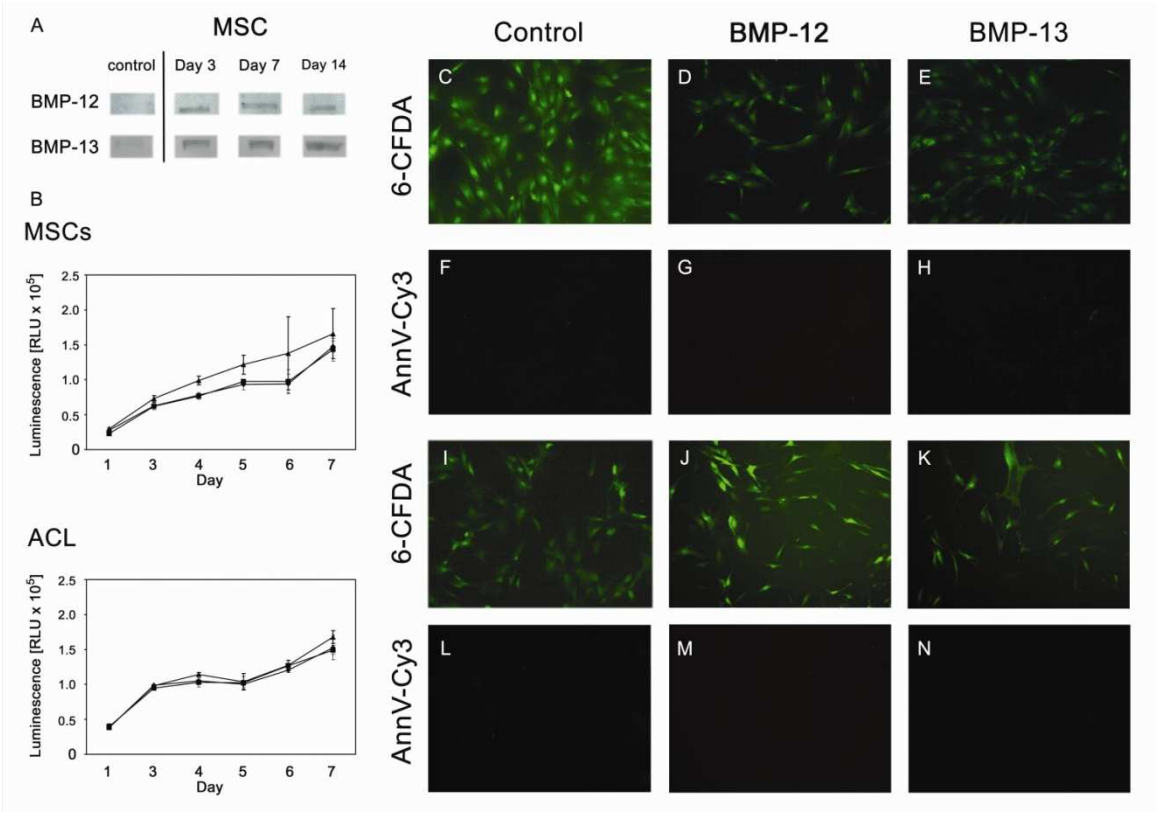

Figure 16: Cell proliferation and viability in BMP12 and BMP13 modified ligament constructs. **(**A) Western blot analyses to detect BMP12 and BMP13 in Ad.BMP12 and Ad.BMP13 transduced MSCs at a dose of MOI 100 after 3, 7, and 14 days. (B) Time course of cell proliferation by MSCs and ACL fibroblasts following transduction with adenovirus encoding BMP12 and BMP13. Analyses of cell vitality and apoptosis in MSCs (C-H) and ACL fibroblasts (I-N) 3 days after transduction with Ad.BMP12 (D,G) and Ad.BMP13 (E,H) compared to the control (C,F). The cells were double-stained with 6-CFDA and annexin V-Cy3, allowing for discrimination of living cells stained green with 6-CFDA, necrotic cells stained red with annexin V-Cy3, and apoptotic cells stained for both. Bar 20 µm. Original magnifications: 100x.

4.3.2 Effects of BMP12 or BMP13 gene transfer on cell proliferation, viability and apoptosis

No differences in proliferation rate could be observed for the Ad.BMP12 and -13 transduced MSCs (Figure 17B). No differences in proliferation were found for the ACL fibroblasts either (Figure 17B) at a MOI 100. The transduction with Ad.BMP12 and 13 seems to have no influence to the proliferation kinetics of MSCs and ACL fibroblast compared to controls.

Double fluorescence staining with AnnV-Cy3 and 6-CFDA allowed differentiation between viable (only green), early apoptotic (green and red), and necrotic cells (only red). Three days after transduction, the high levels of green fluorescence found in all groups revealed that the respective transductions of the MSCs (Figures 17C-E) and ACL fibroblasts (Figures 17I-K) did not affect cell viability compared to controls. Only very small proportions of cells appeared to be apoptotic or necrotic in all groups, as evidenced by red fluorescence (Figures 17F-H and L-N). For MSCs and ACL fibroblasts in monolayer culture transduced with lower MOI similar results were observed (data not shown).

4.3.3 Histochemical and immunohistochemical analyses

After 21 days, staining with H&E showed a homogenous cell distribution of both MSCs and ACL fibroblasts within the hydrogel constructs (Figure 18A). Moreover, the BMP12 and BMP13 modified constructs revealed, that the cells of both types were embedded in a dense collagenous matrix compared to controls where less collagenous matrix was seen, as evidenced by matrix staining with Azan (Figure 18B) and Van Gieson (Figure 18C).

Furthermore, immunohistochemical stainings after 21 days were performed for collagen type III, fibronectin, tenascin, and vimentin (Figure 19). MSCs revealed somewhat more intense stainings for collagen type III in the Ad.BMP12 and Ad.BMP13 transduced hydrogel constructs compared to corresponding control specimen or ACL fibroblasts, where no brown staining of the matrix was detectable (Figure 19A). Fibronectin could be observed in all MSC and ACL fibroblast collagen hydrogel constructs, with Ad.BMP12 transduced constructs showing most intense staining, followed by the BMP-13 modified constructs. However, the marker gene transduced controls of both cell types had only weak matrix staining (Figure 19B).

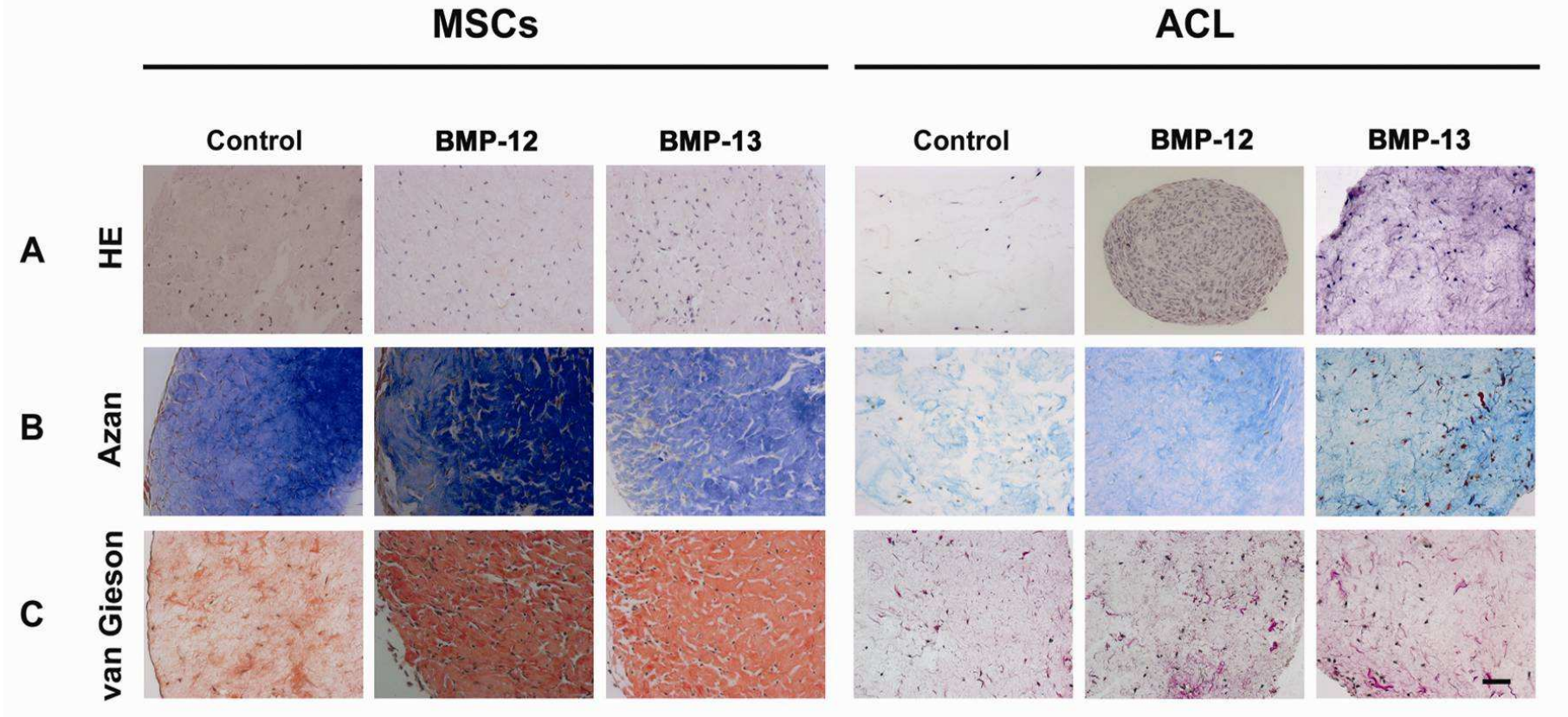

Figure 17: Histochemical analyses of BMP12 and BMP13 modified MSC and ACL hydrogel constructs. (A) H&E staining, (B) Azan staining, and (C) Van Gieson staining. Bar = 100 µm. Original magnifications: 200x.

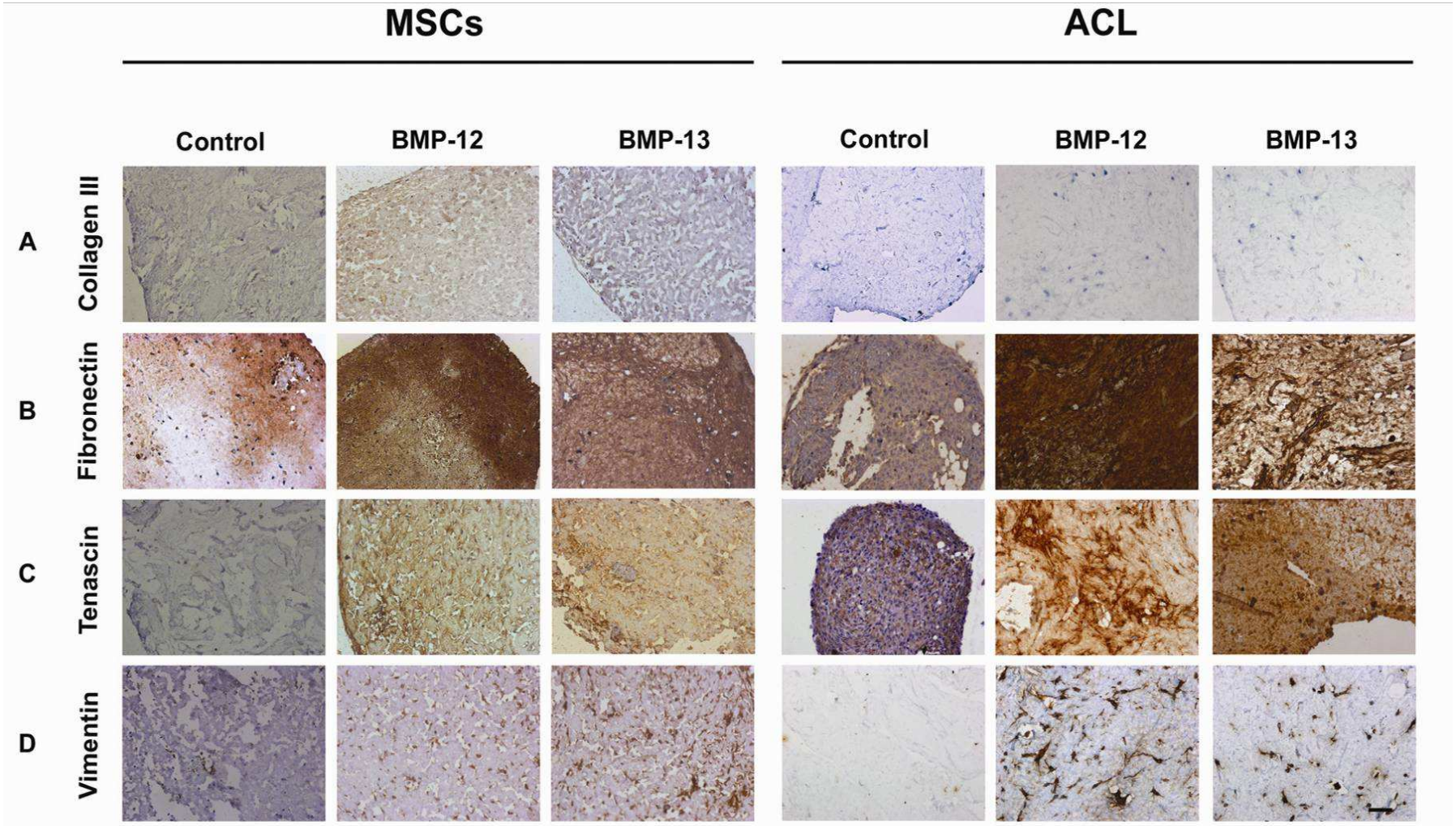

Figure 18: **Immunohistochemical analyses of BMP12 and BMP13 modified MSC and ACL hydrogel constructs. Staining for (A) collagen type III, (B) fibronectin, (C) tenascin, and (D) vimentin.** Positive immunostainings are indicated by the brown-colored network in the vicinity of the blue-colored cells (stained with hematoxylin). Bar = 100 µm. Original magnifications: 200x.

Staining for tenascin in the MSC control and vimentin in the MSC and ACL fibroblast control was negative. Positive stain for tenascin (Figure 19C) and vimentin (Figure 19D) was detected in the Ad.BMP12 and Ad.BMP13 transduced MSC and ACL fibroblast hydrogel constructs, while vimentin staining was absent in the controls and tenascin only weakly present in the ACL constructs. Major differences between groups of different vector doses could not be observed. For each stain, controls were performed without primary antibody, which were negative in all cases (not shown).

4.3.4 Semi-quantitative RT-PCR analyses

Semi-quantitative RT-PCR analyses revealed the gene expression of BGN, COL3, DCN, ELA, FN, SCL, TN-C, TNMD, and VIM in all samples after 21 days (Figure 20). In the following, x-fold change calculated by densitometry was normalized to the EF-1α housekeeping gene and related to the respective control (Figures 20A-D). In the Ad.BMP12 modified MSC hydrogel constructs the gene expression at doses of MOI10 and 100 of the following ligament-associated matrix proteins was equal or less than the control (Figure 20A): BGN (1.02- and 0.94-fold), COL3 (0.97- and 0.94-fold), DCN (0.84- and 0.93-fold), ELA (1.08- and 0.89-fold), FN (0.89- and 0.90-fold), TN-C (0.91- and 0.96-fold), and TNMD (1.01- and 0.97-fold). In contrast, VIM (1.05- and 1.18-fold) showed a slightly increased gene expression (Figure 20A). SCL was only higher at MOI 100 (0.94- and 1.10-fold).

The Ad.BMP13 modified MSC hydrogel constructs revealed distinct differences between MOI 10 and MOI 100. RT-PCR analyses showed higher gene expression level for the ligament-associated matrix proteins BGN (1.38-fold), DCN (1.18-fold), FN (1.31-fold), and VIM (1.04-fold) at a dose of MOI 100 (Figure 20C) compared to the untransduced control. Both at MOI 10 and 100 COL3 (1.01- and 1.58-fold), ELA (1.00- and 1.58-fold), SCL (1.35- and 2.38-fold), TN-C (1.03- and 1.36-fold), and TNMD (1.26- and 1.41-fold) were equal or higher than the control.

In the Ad.BMP12 modified ACL fibroblast hydrogel constructs at a dose of MOI 100 the transgene expression of the ligamentogenic matrix proteins BGN (1.38-fold), COL3 (1.66-fold), DCN (1.36-fold), and TN-C (2.16-fold) was higher than the control (Figure 20B). In contrast, TNMD (1.61-fold), ELA (1.24), SCL (1.04-fold), and VIM (1.10-fold) showed a higher gene expression at MOI 10 (Figure 20B). However, the matrix protein FN (0.65- and 0.92-fold) was always less compared to the control.

As shown in Figure 20D, the gene expression of the Ad.BMP13 modified ACL fibroblast hydrogel constructs revealed distinct differences between MOI 10 and MOI 100. The gene expression for BGN (1.58- and 2.18-fold), DCN (1.37- and 2.75-fold), COL3 (0.93- and 1.46-fold), FN (1.22- and 1.45-fold), and TN-C (3.22- and 1.76-fold) was higher for MOI 10 and 100 than the control. SCL (1.54- and 1.51-fold) was clearly higher than the control but showed no differences between MOI 10 and 100. ELA (0.95- and 0.89-fold) showed also no differences between MOI10 and 100 but was lower than the control. The gene expression of TNMD (1.65- and 0.87-fold) and VIM (1.41- and 0.76-fold) was highest for MOI 10 (Figure 20D).

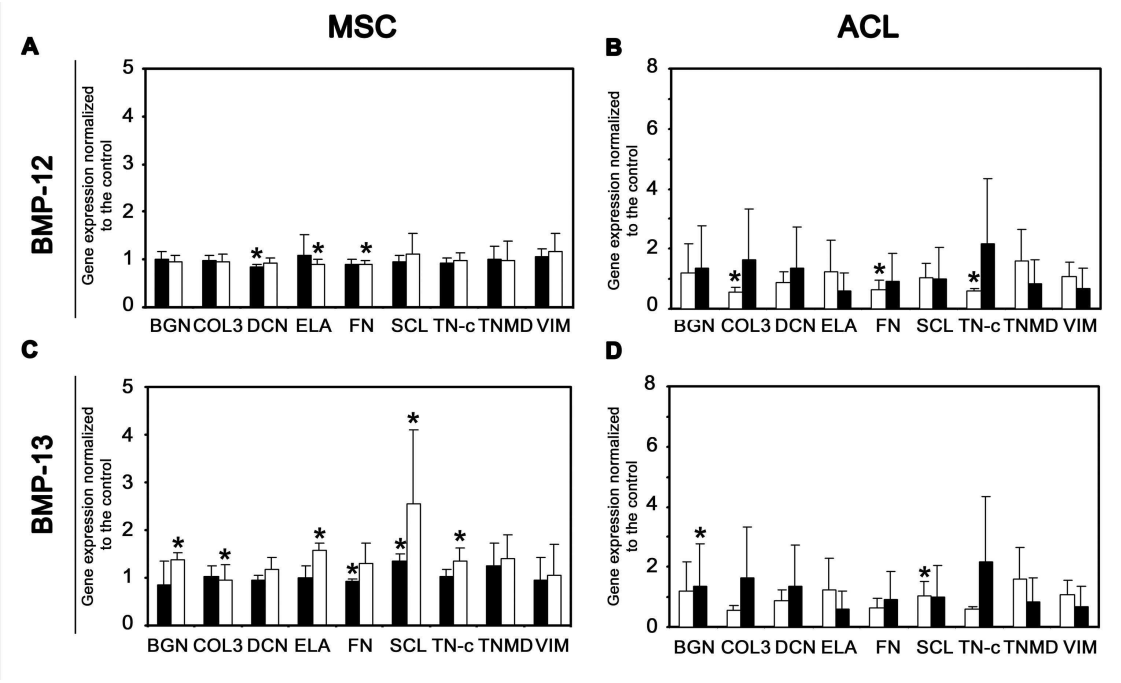

Figure 19: RT-PCR analyses of ligament-specific marker gene expression of BMP12 and BMP13 modified MSC (left) and ACL fibroblast (right) collagen hydrogel constructs. Densitometry of PCR products of Ad.BMP12 (A,B) and Ad.BMP13 (C,D) transduced MSC (A,C) and ACL fibroblast (B,D) collagen hydrogel constructs. X-fold changes of BGN, COL 3, COL 5, DCN, ELA, FN, SCL, TN-C, TNMD, and VIM are shown. Gene expression was normalized to the house keeping gene EF1α and related to controls. Mean values ± SD are derived from three patients. Differences compared to the control were calculated significant for $p<0.05$ (*). EF1α = elongation factor 1α, BGN = biglycan, COL 3 = collagen type III, COL 5 = collagen type V, DCN = decorin, ELA = elastin, FN = fibronectin, SCL = scleraxis, TN-C = tenascin c, TNMD = tenomodulin, VIM = vimentin.

4.4 Discussion

For biologic ligament repair approaches, a well balanced interplay between matrix material, cells, biological and biomechanical factor(s) is of key importance. The ideal matrix material is not only suitable for promoting the presence of cells but also of the bioactive factors involved. Here we chose to use a collagen type I hydrogel for two reasons. First the hydrogel is well characterized, its use is standardized, and collagen type I is the primary matrix found in ligament and tendon (Kuo and Tuan, 2008). Additionally, it could be demonstrated that collagen type I hydrogels were effective carriers of adenoviral vectors and transduced cells (Steinert et al., 2008). Different studies indicate that cells initiate a reparative response after an ACL rupture when a collagen hydrogel is placed between the ruptured ends of an ACL *in vitro* (Pascher et al., 2004) or *in vivo* (Murray et al., 2007).

In our approach, the bioactive factors were delivered via cells transduced by adenoviral vectors encoding BMP12 or BMP13 leading to ligament matrix formation in the respective constructs (Figures 18-20). Notably, transductions at even high viral doses (100 MOI) were not detrimental for cell viability and proliferation (Figure 17). Our study is consistent with findings of others using recombinant human BMP12 (Fu et al., 2003), or BMP13 (Heckmann et al., 2008) protein, in that we also report the induced formation of a ligament-tissue like matrix when these factors re added to undifferentiated precursor cells *in vitro*.

Remarkably, several studies have shown somewhat stronger ligament/tendon formation in response to ectopic (Wolfman *et al.*, 1997; Forslund and Aspenberg, 2001; Helm *et al.*, 2001; Hoffmann and Gross, 2006) or orthotopic (Aspenberg and Forslund, 1999; Lou *et al.*, 2001; Rickert *et al.*, 2001; Majewski *et al.*, 2008) implantation of BMP12 and BMP13 *in vivo*. In this respect it is important to note that our *in vitro* study presented here is limited to static cultures, and that stronger effects might have been observed in an environment where additional biomechanical stimulation was present such as in a bioreactor or *in vivo*.

However, it could be shown that BMP12 and -13 gene transfer into MSCs and ACL fibroblasts induce ligamentogenesis. Although there is no single specific marker for ligamentogenesis, we evaluated the expression of scleraxis, a basic helix-loop-helix (bHLH) transcription factor as one indicator of ligament and tendon development (Hoffmann and Gross, 2006). Despite its multiple functions during early embryonic

development, scleraxis marks the tendon progenitor population that forms the fourth somitic compartment the syndectome and is continuously expressed through differentiation into the mature tenocytes and ligament cells (Schweitzer *et al.*, 2001; Murchison *et al.*, 2007). Schweitzer et al. could show that the later expression of scleraxis is specific to the developing connective tissue that mediates the attachment of muscle to bone including tendons, as well as ligaments mediating the connection between bones (Schweitzer et al., 2001). Murchison et al. revealed that the scleraxis function is required for the normal force-transmitting tendons (Murchison et al., 2007). In our study, the PCR results revealed a distinct SCL expression in Ad.BMP12 and 13 transduced MSCs and ACL fibroblasts at MOI 100 compared to the control.

Another important marker for ligament and tendon development is tenomodulin, a member of new family of type II transmembrane glycoproteins (Docheva et al., 2005). A distinct higher TNMD expression in Ad.BMP13 transduced MSCs at MOI 100 and in Ad.BMP12 and 13 transduced ACL fibroblasts at MOI 10 was detected in comparison to the controls. Furthermore, BMP12 transduction resulted in an increase of the SCL and VIM expression in MSCs, and BGL, COL3, DCN, and TN-C expression for ACL fibroblasts, respectively (Fig 20A, C). Genetic modification with BMP13 at MOI 100 enhanced also the expression of BGL, COL3, DCN, ELA, FN, TN-C, and VIM for MSCs and BGL, COL3, DCN, FN, and TN-C for ACL fibroblasts (Figures 20B, D).

These findings confirm that expression of BMP12 and, particularly, BMP13 enhanced certain aspects of the ligament and tendon healing response when high doses of vectors were used. In general, ACL fibroblasts offered a higher expression of specific markers of ligament and tendon in comparison to the controls (Figure 20). This is consistent with the immunohistochemical analyses, which revealed the presence of fibronectin, tenascin, and vimentin, but not collagen type III in the BMP12 and 13 transduced cells (Figure 19), with stainings in the ACL fibroblast cultures being more intense than in the MSCs. Therefore, it might be that BMP12 and BMP13 are more effective in mediating ligamentogenesis in more committed cell types, such as in the ACL cells, but might be less powerful inducers of ligamentogenesis in uncommitted precursors.

In summary, we have shown that BMP12 and BMP13 gene transfer into MSCs and ACL fibroblasts induce ligamentogenic differentiation, with the ACL fibroblasts being more powerful responders. Therefore, ACL cell populations might be therefore better

candidates for ligamentogenic induction using BMP12 and BMP13 compared with undifferentiated precursors obtained from bone marrow.

Acknowledgement

We thank Mrs. C. Amrehn, V. Monz, and M. Regensburger for their excellent technical assistance. We are also grateful to Wyeth Inc. for providing the adenoviral vectors for BMP12 and BMP13 and the kind advice from Drs. D. Pittman and J. Archamboult. Support to this research was given by grants from DFG (Grant No. STE1051/1-1 to A.F.S), BMBF (Grant No. 0313386E to U.N.), BayFor (FORZEBRA; TP2/WP5 to A.F.S and U.N.) and NIH (RO1, Grant No. AR 052809 to C.H.E and AR052772 to MMM).

Chapter 5

In situ IGF-1 gene delivery to the anterior cruciate ligament using a collagen type I hydrogel

Abstract

Ruptures of the anterior cruciate ligament (ACL) are common knee injuries that do not heal, even with surgical repair. Our research is directed towards developing novel, biological approaches that enable suture repair of this ligament. One promising strategy involves the insertion of a collagen hydrogel between the severed ends of the ACL. Cells migrate from the damaged ligament into the hydrogel and produce repair tissue. Here we have investigated the potential for augmenting this process by the transfer of insulin like growth factor (IGF) 1 cDNA to the repair cells using an adenovirus vector. The goal is to achieve direct, *in situ* gene delivery by loading the hydrogel with vector prior to its insertion into the defect. In a step-wise approach towards evaluating this process, we confirmed that monolayers of ACL fibroblasts were efficiently transduced by adenovirus vectors and continued to express transgenes when subsequently incorporated into the hydrogel; indeed, transgene expression persisted longer within collagen gels than in monolayer culture. Transfer of IGF-1 cDNA increased the cellularity of the gels and led to the synthesis and deposition of increased amounts of types I and III collagen, elastin, tenascin, and vimentin. The cells remained viable, even when subjected to high viral loads. Similar results were obtained when collagen hydrogels were preloaded with adenovirus prior to insertion into an experimental ACL lesion *in vitro*. These data confirm the promise of using vector-laden hydrogels for the *in situ* delivery of genes to cells within damaged ligaments and suggest novel possibilities for the biological repair of the ACL.

5.1 Introduction

Ruptures of the anterior cruciate ligament (ACL) are among the most common injuries of the knee with an incidence of 1 in 3000 (Frank and Jackson, 1997; Owings and Kozak, 1998; Praemer et al., 1999). The sequelae of chronic anterior knee instability have been well described and include pain, chondral and meniscal damage and inevitably lead to premature degenerative joint disease (Caborn and Johnson, 1993; Frank and Jackson, 1997). As initial suture repair approaches performed in the 1950s and 1960s failed (Feagin and Curl, 1976), the ACL is currently replaced by tendon grafts (West and Harner, 2005). Although this surgical procedure results in good clinical outcome in terms of restoration of knee stability and return to full sports activity (Freedman et al., 2003), the complex architecture, proprioception, and biomechanics of the ACL are not restored, resulting in radiographic changes consistent with osteoarthritis in more than 50% of the patients (Aglietti *et al.*, 1992; Anderson *et al.*, 1994). Synthetic ACL substitutes have been evaluated as well since the early 1970s, but these have had very limited clinical success due to insufficient material properties and severe inflammatory reactions that lead to graft failure (reviewed in(Ge et al., 2006; Petrigliano et al., 2006)).

These limitations have prompted research aimed to develop a tissue engineered ACL repair technique that addresses the shortcomings of existing strategies (Hutmacher *et al.*, 2004; Vunjak-Novakovic *et al.*, 2004; Ge *et al.*, 2006; Petrigliano *et al.*, 2006). Data from Murray and colleagues (Murray *et al.*, 2000b; Murray and Spector, 2001b; Spindler *et al.*, 2006; Murray *et al.*, 2007)suggest that the ACL has a latent repair capacity that becomes active when an appropriate scaffold is placed between the ruptured ends of the ACL. Under these conditions, cells migrate into the scaffold and initiate repair processes. Based upon this finding, past research efforts have focused on the development of a scaffold that permits ingress of cells from the cut ends of the ACL *in vitro* (Murray *et al.*, 2000a; Murray and Spector, 2001a) and *in vivo* (Murray *et al.*, 2006b; Spindler *et al.*, 2006; Murray *et al.*, 2007). There is considerable evidence to suggest that ligament repair can be augmented by certain growth factors, and we have previously argued that transfer of their cognate cDNAs offers an expeditious method for delivering them in a sustained and focused fashion (Evans *et al.*, 1993; Schmidt *et al.*, 1995; Gerich *et al.*, 1996, 1997; Scherping *et al.*, 1997; Evans, 1999; Hildebrand *et al.*, 1999). Present research thus focuses on the development of an

enhanced suture repair of the ACL by employing a reinforced collagen type I (COL I) hydrogel-containing recombinant adenovirus vectors. These vectors were selected because they transduce a wide variety of cell types very efficiently without the need for cell division; they are straightforward to produce at high titers, and they do not integrate (Evans et al., 2005). We have previously shown that collagen hydrogels can be used as means to deliver genes to ligaments, and that it was possible to modulate cell behavior *in situ* using the TGF-β1 cDNA (Pascher et al., 2004). Such an approach obviates the need for cell culture, thereby offering a technology that is potentially more economical and clinically expedient than traditional tissue engineering approaches (Evans et al., 2007). Promising preliminary results encouraged us to undertake this more detailed study to characterize further the parameters of gene delivery within this collagen hydrogel in terms of persistence of adenoviral infectivity, duration of transgene expression and the biological effects of other transgenes. IGF-1 was selected as the transgene for these studies because the protein is known to stimulate the survival and division of ligament cells, and to promote matrix synthesis. Moreover, Provenzano et al. (Provenzano et al., 2007) have shown that systemic administration of IGF-1 enhances ligament healing. Therefore, in this work, we tested the two following hypotheses: (1) the collagen hydrogel could be used to effectively deliver gene products of interest to ACL cells; and (2) that this delivery would result in significant changes in biologic function of the ACL cells in a simulated wound site.

5.2 Materials and Methods

5.2.1 Experimental approach

As depicted in Figure 21, two experimental strategies were used. An *ex vivo* (indirect) approach was used to expedite the study of transduced ACL derived cells within hydrogels. For this, the cells were cultured as monolayers, transduced with the relevant adenovirus vectors and their properties examined. Monolayer-transduced cells were then incorporated into hydrogels. Confirmatory experiments were then conducted using the *in vivo* (direct) approach in which vectors were loaded into hydrogels which were then placed in between severed ends of ACL, as an *in vitro* model of injury and repair (Pascher et al., 2004).

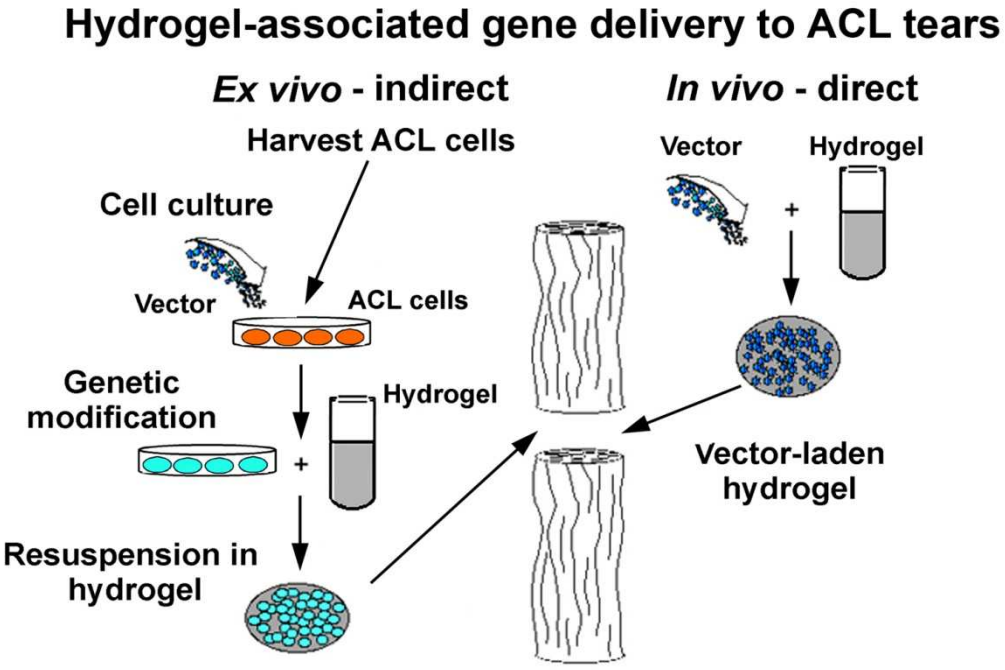

Figure 20: Schematic illustration of hydrogel-associated gene delivery approaches to ACL tears. In the first, ACL fibroblasts are harvested, transduced with the vector of interest, and may be subsequently selected and amplified. The genetically modified ACL cells are seeded into a collagen hydrogel, before the construct is transplanted to the site of ACL injury (left). The second approach entails placement of a vector-laden hydrogel between the ruptured ends of the ACL. ACL cells become transduced as they migrate into the hydrogel and express the foreign transgene (right).

5.2.2 Generation and amplification of recombinant adenoviral vectors

First-generation (DE1DE3) serotype 5 adenoviral vectors, carrying the cDNA of the human IGF-1; The green fluorescent protein (GFP) from jellyfish; or the firefly luciferase (Luc) gene, were constructed by cre-lox recombination as described earlier, and propagated in 293/Cre8 cells the resulting adenoviral vectors were designated Ad.IGF-1; Ad.GFP or Ad.Luc, respectively. For generation of high titer preparations, adenoviral vectors were amplified in 293 cells (ATCC, Manassas, VA, USA), purified on three rounds of CsCl density gradients (1.2/1.4 mg/mL) and dialyzed against buffer (10 mM Tris–HCl, 150 mM NaCl, 10 mM $MgCl_2$ and 4% sucrose, pH 7.8) (Palmer et al., 2003a). Virus titers were estimated between 10^{12} and 10^{13} viral particles (vp)/mL by optical density and adenoviral infectivities were approximated between 10^{10} and 10^{11} infectious particles (ip)/mL by standard plaque assay (Palmer et al., 2003a).

5.2.3 ACL tissue harvest, fibroblast isolation and cell culture

Human intact ACLs were harvested aseptically from 6 male 50–65-year-old patients undergoing total knee arthroplasty (after informed consent and as approved by the local institutional review board of the University of Würzburg) and rinsed twice with serum-free Dulbecco's modified Eagle's medium (DMEM; Invitrogen, Carlsbad, CA, USA) containing 2% antibiotic/antimycotic solution (Invitrogen). After removal of the bony attachment sites and the synovial sheath, the ligament fascicles were dissected, minced into pieces of about 2 mm^3, and digested subsequently for 12 h in 0.1% (w/v) collagenase 1 and 3 solution (all Invitrogen). ACL fibroblasts were recovered from the digest solutions by filtration through a 40-mm nylon mesh cell strainer (Falcon, Beckton Dickinson Labware, Franklin Lakes, NJ, USA), and centrifuged at 1500 rpm for 10 min. Then the cell pellets were resuspended in complete medium consisting of DMEM supplemented with 10% fetal bovine serum (FBS), 2 mmol L-glutamine, 1% antibiotic/antimycotic solution (all Invitrogen), and 50 mg/mL ascorbate-2-phosphate (Sigma, St. Louis, MO, USA), counted and seeded at a density of 10^4 cells/cm^2 in 225 cm^2 tissue culture flasks (Falcon). The medium was changed every 3–4 days and second passage ACL fibroblast cultures were employed in all experiments using monolayers or ACL cell-seeded hydrogels.

5.2.4 Adenoviral transduction in monolayer culture and incorporation into collagen hydrogels

For the monolayer experiments, ACL fibroblasts were seeded at 1 x 10^5 cells/well in 24-well plates (Falcon) and transduced 24 h later in 100 µL serum-free medium for 2 h with doses of Ad.IGF-1 as indicated in the respective experiments. Control cultures received Ad.GFP, or recombinant IGF-1 protein (Invitrogen) at a concentration of 10 ng/mL, or remained uninfected. Following incubation, the supernatant was aspirated and replaced with complete DMEM every 3-4 days throughout the 14-day culture period. At day 3, 7, and 14, monolayer cultures were harvested and analyzed for transduction efficiencies, cell proliferation and collagen production rates.

Transduction of ACL monolayer fibroblasts to be incorporated within collagen hydrogels was conducted similarly, except that cells were seeded at 3.6x10^6 cells/75 cm^2 flask (Falcon) and transduced with 300 ip/cell of Ad.IGF-1, or Ad.GFP, or different doses of Ad.Luc, in 750 mL of serum-free medium, as indicated in the respective experiments. Twenty-four hours after transduction, the cells were trypsinized, and aliquots of 3x10^5 cells were spun and resuspended in 200 mL of a collagen hydrogel. The collagen hydrogels were created by mixing a solution of acid-soluble bovine COL I (ICN Biomedicals Inc., Aurora, OH, USA) with double distilled water, 10xF12 media and FBS (both Invitrogen). The mixture spontaneously gels when neutralized to a pH of 7.4 with $NaHCO_3$ and warmed to 37°C. No specific cross-linking agent is used. For cell-seeded gels, the cell pellet is resuspended in the cold neutralized collagen solution prior to warming and gelation. After cell-seeding, the gels were immediately placed in semi-tubular silicone molds of 5mm diameter and 2 cm length (Cole-Parmer Instrument Company, Vernon Hills, IL, USA), with a nylon mesh being fixed at opposite ends for attachment. After 30 min the gels solidified, and the constructs including the molds were transferred into 12-well plates (Falcon) and cultured in 2 mL of complete DMEM each with media changes every 2–3 days. The Ad.Lucmodified constructs were examined for dose-responsiveness of transgene expression, the Ad.GFP modified constructs were monitored for persistence of transgene expression, the Ad.IGF-1-transduced constructs were evaluated biochemically, histologically, immunohistochemically, and by semi-quantitative RT-PCR after 21 days, with Ad.Luc-transduced and –untransduced constructs serving as negative controls.

5.2.5 Fabrication of vector-laden hydrogels and ACL in vitro repair model

Collagen type I hydrogels were prepared as above and then mixed before gelling with the adenoviral stock solution of Ad.GFP, Ad.Luc, or Ad.IGF-1 as indicated to a final concentration of $1x10^9$ ip/mL of vector-laden hydrogel each.

The ACL tissue pieces were placed in an *in vitro* repair model as described previously (Pascher et al., 2004). Briefly, fascicles of approximately 3 mm diameter were dissected longitudinally from 3 ACLs, bisected transversely, and cut into pieces of approximately 3 mm length, representing a proximal and distal group of explants. Then proximal and distal pieces were placed at opposite ends of 5 mm diameter semi-tubular silicone molds (Cole-Parmer Instrument Company), leaving a 5 mm gap, and fixed in place with 25 gauge needles (Beckton Dickinson Labware, Franklin Lakes, NJ, USA). The gap between the explants was then subsequently filled with approximately 100 mL collagen hydrogel containing 10^8 ip of Ad.GFP, Ad.Luc, or Ad.IGF-1, or no virus, respectively. After solidification of the hydrogels, explant constructs were placed into 12-well plates (Falcon) and cultured for 21 days as stated above, with media changes every 3–4 days. The Ad.GFP-containing constructs were closely monitored by fluorescence microscopy for transgene expression, and all constructs were fixed in 4% phosphate-buffered paraformaldehyde for histological processing at the end of the culture period.

5.2.6 Assessment of adenoviral infectivity and retention within type I collagen hydrogels

A series of experiments was conducted to compare the stability and infectivity of recombinant adenovirus as a free suspension with that incorporated into the hydrogel (see also illustration Figure 27A). To do this, cell-free hydrogels of 100 mL volume were prepared as described above, containing 10^8 ip of Ad.GFP or Ad.Luc. Control gels contained no viral particles. The vector-laden (virus gel) or the empty gel controls were then incubated for 21 days in 300 mL serum-free medium in 48-well plates (Falcon) at 37℃. For comparison, equal amou nts of free adenoviral vectors (Ad.GFP, Ad.Luc) were placed in solution (virus solution; 10^8 ip/300 mL serum-free medium), and were incubated in parallel over the time course together with a control containing only serum-free medium.

At the designated end time points, the hydrogels were removed and the elution medium was collected to assess vector elution from the hydrogels (virus elution medium). The hydrogels were solubilized in 400 mL of 1% collagenase type I (Invitrogen) solution in serum-free medium for 30 min. The parallel vector solutions and vector elution media, together with the respective controls, were also mixed with collagenase type I (2%, 200 mL) in order to obtain comparable suspensions for subsequent infections. To determine the infectivity of the viral particles recovered in this manner, whole suspensions of all experimental groups were placed on top of confluent monolayer cell cultures in 24-well tissue culture plates (Falcon; approximately $2x10^5$/well) for 2 h. Ad.Luc-containing suspensions were placed on the ACL fibroblast cultures, to measure transduction efficiencies over the time course, and Ad.GFP-containing suspensions were placed onto 293 cells for highly sensitive detection of infectious virus. After the 2 h infection time, the medium was changed to complete DMEM, and cultures were analyzed for transgene expression 48 h later. All experiments for each vector, experimental group, and time point were performed in triplicate and repeated three times (n=3, m=9 per group and time point).

5.2.7 Evaluation of transgene expressions

5.2.7.1 GFP transgene expression

GFP transgene expression was visualized by fluorescence microscopy and quantified by flow cytometry. Green fluorescent cells were observed in tissue culture using a fluorescence microscope (Model Axioscope 2; Carl Zeiss, Göttingen, Germany), and photographed with a digital camera (AxioCam MRc; Carl Zeiss). For quantitative assessment of dose-responsive GFP-transgene expression rates, ACL monolayer cultures, transduced at different doses of Ad.GFP (n=3, m=9 per group) were harvested at day 3 of culture, pelleted, washed with PBS, resuspended in 100 mL of PBS and immediately subjected to flow cytometric analyses using a Cytomics FC 500 (Beckman, Coulter, Fullerton, CA, USA). Ad.Luc and untransduced monolayer cultures served as controls.

5.2.7.2 Luciferase expression

To determine Luc transgene expression of monolayer cultures in 24-well plates, the cells were washed once in PBS, incubated for 2 min in 200 µL of lysis reagent (Bright-Glo Luciferase Assay System, Promega, Madison, WI, USA), homogenized by pipetting, and the Luc activity assayed.

For measurement of Luc, collagen hydrogels were mixed with 500 mL PBS and homogenized using a motorized homogenizer; 100 mL of the homogenate was reserved for assay of total protein content. Following incubation for 15 min with an equal volume of lysis buffer (Bright-Glo Luciferase Assay System, Promega, Madison, USA), the homogenate was centrifuged at low speed in a tabletop clinical centrifuge. Then 350 mL of the supernatant was mixed with an equal volume of lysis reagent, incubated for 2 min at room temperature, and the Luc activity was measured in an Autolumat Plus luminometer (Berthold Detection Systems, Oak Ridge, TN, USA). Total protein concentration of the homogenate was determined using the Bradford reagent as directed by the supplier (Sigma, St. Louis, MO, USA).

5.2.7.3 IGF-1 expression

At time points indicated, media conditioned by monolayer and hydrogel cultures for 24 h (n=3, m=9 per group and time point) were collected and stored at –20℃ until testing for IGF-1 concentration using Quantikine Human Immunoassay kits (R&D Systems, Minneapolis, MN, USA) according to the manufacturer's instructions.

5.2.8 Cell proliferation, collagen synthesis and DNA content assays

Cell proliferation rates in ACL monolayer cultures were determined by [^{3}H] thymidine incorporation, and collagen production rates were approximated by [^{14}C] proline uptake as described and performed previously (Peterkofsky and Diegelmann, 1971; Marui *et al.*, 1997a; Meaney Murray *et al.*, 2003; Murray *et al.*, 2006a). Briefly, at days 3, 7, and 14 of monolayer culture, each separate set of per treatment and control group (n=3, m=9 for all tests) were radiolabeled, with 2 µCi/mL of [^{3}H] thymidine and 2 µCi/mL of [^{14}C] proline (New England Nuclear, Boston, MA, USA) per well. After 24 h of incubation, the radiolabeled ACL monolayers were washed with 1mL of PBS containing unlabeled proline each, and placed in a rocking incubator at 4℃ for 15 min. The washes were repeat ed four times total. Thereafter,

the cells were trypsinized, digested overnight at 60℃ in a proteinase K solution (1 µg/mL; Sigma), resuspended in 5 mL of scintillation fluid (HIONIC FLUOR, 6013319; Meriden, CT, USA), and counted using a Tri-Carb liquid scintillation counter (Model 4640; Packard Instrument Company, Downers Grove, IL, USA) for both [^{3}H] and [^{14}C] with compensation for the beta emission overlap accounted for the analysis software as described previously (Meaney Murray et al., 2003; Murray et al., 2006a). The final wash was also analyzed and found to contain less than 0.001% of the radioactivity of the original labeling medium.

For DNA measurement, ACL monolayer cells or ACL cell hydrogelconstructs were harvested and incubated in 1mL of proteinase K digest solution (1 µg/mL; Sigma) at 60℃ for 12 h. An aliquot of the proteinase K diges t was read fluorometrically (Hoefer Scientific Instruments, San Francisco, CA, USA) using Hoechst dye no. 33258 (Sigma) dissolved in 2 mL of Tris–EDTA–NaCl buffer. The DNA concentration was determined from a standard curve of calf thymus DNA (Sigma), and values of cell-free collagen hydrogel controls were subtracted from the sample values. A total of n=3 replicates per group was performed at the end of the 21 days culture period in all experiments tested, and the whole experiment was repeated three times (m=9).

5.2.9 Total RNA extraction and semi-quantitative RT-PCR analyses

After 21 days, 10 human hydrogel-constructs per group were pooled, minced with scissors, and homogenized using a pellet pestle and repeated tituration in 1mL of Trizol reagent (Invitrogen) as previously described (Noth et al., 2005). Total RNA was subsequently extracted using Trizol reagent with an additional purification step using RNeasy separation columns (RNeasy kit; Qiagen, Hilden, Germany) according to the manufacturer's instructions. RNA from each group of constructs (2 µg each group) was used for random hexamer primed cDNA synthesis using MoMLV-H reverse transcriptase (Promega). Equal amounts of each cDNA synthesized (100 ng), were used as templates for PCR amplification in a 50 µL reaction volume using Taq DNA polymerase (Amersham, Piscataway, NJ, USA) and 50 pmol of gene-specific primers, which were used to detect mRNA transcripts characteristic of human ligament tissue as previously described (Noth et al., 2005). The sequences, annealing temperatures, number of cycles, and product sizes of forward and reverse primers used for COL I and collagen type III (COL III), elastin (ELA), vimentin (VIM), and fibronectin (FN) are listed in Table 5, with elongation factor 1 a (EF1α) serving as

housekeeping gene and internal control. The RT-PCR products were electrophoretically separated on 1.5% agarose gels containing 0.1 µg/mL ethidium bromide and visualized using the Bio Profile software (LTF, Wasserburg, Germany). The densities of the PCR bands were analyzed with the Bio 1D/Capt MW software (LTF) and the mean ratio (x-fold change) normalized to the EF1α housekeeping gene expression was calculated from 3 bands (one per patient).

Table 5: RT-PCR primer sequences and product sizes for semi-quantitative RT-PCR.

Gene	*RT-PCR primer sequences (5'-3')*	Cycle number	Annealing Temp (℃)	Product size (bp)
EF1α	Sense: AGGTGATTATCCTGAACCATCC Antisense: AAAGGTGGATAGTCTGAGAAGC	24	54	234
COL I	Sense: GGACACAATGGATTGCAAGG Antisense: TAACCACTGCTCCACTCTGG	30	54	461
COL III	Sense: GCGGAGTAGCAGTAGGAG Antisense: GTCATTACCCCGAGCACC	35	56	483
ELA	Sense: GCAGTGCCTGGGGTCCTTGGAG Antisense: GCTGCTTTAGCGGCTGCAGCTGG	35	58	211
VIM	Sense: GACCGCTTCGCCAACTACATCGAC Antisense: GGTCATCGTGATGCTGAGAACTTCG	35	65	1060
FN	Sense: TGGAACTTCTACCAGTGCGAC Antisense: TGTCTTCCCATCATCGTAACAC	32	58	451

5.2.10 Histological and immunohistochemical analyses

Histological and immunohistochemical analyses of ACL cell-seeded hydrogels, and ACL explant cultures were performed after 21 days (Noth et al., 2005). Briefly, the constructs were washed twice with PBS, embedded in Tissue Tek (Sakura, Horgen, Switzerland) and cryosections of 10 µm were performed. For histochemical analyses, sections were fixed for 10 min in acetone and stained with haematoxylin/eosin (H&E) for evaluation of cellularity, and with Azan, Van Gieson (Gieson), or Masson-Goldner (Goldner) to assess collagen accumulation. For immunohistochemistry of elastin, sections were pre-treated for 15 min with 6 M guanidine HCL/50 mM DTT in 20 mM Tris-buffer, followed by washes with Tris-buffer and 15 min incubation with 100 mM iodoacetamide. For all immunohistochemical analyses, sections were treated for 15 min with H_2O_2 in Trisbufferand were incubated overnight at 4℃ with the primary antibodies diluted in 0.5% BSA. Primary antibodies for COL III (AB 747; Chemicon,

Temecula, CA, USA), elastin (ELA, MAB 1681; Calbiochem, San Diego, CA, USA), tenascin (TEN, CBL213; Chemicon), and vimentin (VIM, M0725; Dako, Hamburg, Germany) were used. Immunostainings were visualized by treatment with peroxidase-conjugated antibodies (Dako) followed by diaminobenzidine staining (DAB kit; Sigma). The slides were finally counterstained with hemalaun (Merck, Darmstadt, Germany). For all immunohistochemical analyses controls with non-immune IgG (Sigma) instead of the primary antibodies were performed.

5.2.11 ACL cell viability within collagen hydrogels

Distribution of live, apoptotic and necrotic cells within the gels after 21 days was visualized using the Annexin V-Cy3 apoptosis detection kit (Sigma) as directed by the supplier. The kit uses the dye Cy3.18 as red fluorochome conjugated with annexin V (AnnV-Cy3) for apoptosis detection through binding to phosphatidylserine epitopes on the plasma membrane of early apoptotic cells, and the hydrolyzation of the nonfluorescent 6-carboxyfluorescein diacetate (6-CFDA) to the green fluorescent compound 6-carboxyfluorescein by the esterases of living cells to label viable cells. Collagen hydrogels constructs (n=3) per group were incubated with 50 µL of the double labeling staining solution for 10 min at room temperature. After staining, gels were washed five times with 50 µl of 1x binding buffer, rinsed twice with PBS, fixed overnight in PBS-buffered 4% paraformaldehyde, dehydrated, infiltrated with isoamylacetate (Merck, Hohenbrunn, Germany), embedded in paraffin, and sectioned to 4 µm. Viable and non-viable cells were observed on the respective midsections using a fluorescence microscope.

5.2.12 Statistical analysis

The data from the ELISA, Luc expression, thymidine, and proline uptake, DNA content, and RT-PCR analyses were expressed as mean values ± standard deviation (SD) and subjected to variance analysis (one- or two-factor ANOVA). Each experiment was performed in triplicate and repeated at least three times. Statistical significance was determined by Fisher post hoc or t-testing, and level of $p<0.05$ was considered significant.

5.3 Results

5.3.1 Ad.IGF-1 transduction and monolayer cultures of primary ACL fibroblasts

The initial set of experiments was performed to determine the efficiencies and transgene expression patterns after adenoviral transduction of primary ACL fibroblasts in monolayer culture, as well the effects of IGF-1 gene delivery on cell proliferation and matrix production. Therefore primary ACL cell cultures were infected with Ad.GFP or Ad.IGF-1 at doses of 10, 100, and 300 ip/cell, remained uninfected, or received recombinant IGF-1 protein at a concentration of 10 ng/mL as control. After 3 days, cultures were analyzed using fluorescence microscopy and flow cytometry. As shown in Figure 22, there was a viral dose-dependent increase of GFP-positive (GFP+) cells, with no GFP+ cells in the untransduced cultures (A), and average transduction efficiencies of 5.7% at 10 ip/cell (B), 53.0% at 100 ip/cell (C), and 97.0% at 300 ip/cell (D). Green fluorescence in all groups declined gradually after day 3, and had almost disappeared in all cultures at the end of the culture period at day 15 (data not shown).

IGF-1 transgene expression was evaluated during the 15-day time course using ELISA (Figure 22E). Cell proliferation was measured by means of [^{3}H] thymidine incorporation (Figure 22F), and DNA content analyses (Figure 22G). Collagen production was determined using [^{14}C] proline uptake (Figure 22H). IGF-1 treatment led to a significant increase in IGF-1 levels in the culture media compared to untransduced or Ad.GFP-transduced controls (p<0.05 for all groups and time points). At day 3, a peak value of 75.71 ± 4.4 ng/mL (mean ± SD) was seen in the Ad.IGF-1-infected cultures at 300 ip/cell, and by day 15, the levels of transgene expression had decreased significantly in all groups transduced with Ad.IGF-1 (Figure 22E). The concentrations of IGF-1 in media, to which 10 ng/mL rhIGF-1had been added 24 h before, remained at relatively constant levels between 4.8 and 7.8 ng/mL during the time course. Transduction with Ad.IGF-1 at doses of 100 and 300 ip/cell was accompanied by an increase in cell proliferation as measured by [^{3}H] thymidine incorporation (Figure 22F) and DNA content (Figure 22G) (p<0.05 for all comparisons).

The corresponding collagen synthesis rates were significantly increased in the Ad.IGF-1-transduced cultures only at doses of 100 and 300 ip/cell at all time points

compared to controls and all other groups, where no statistically significant differences could be identified.

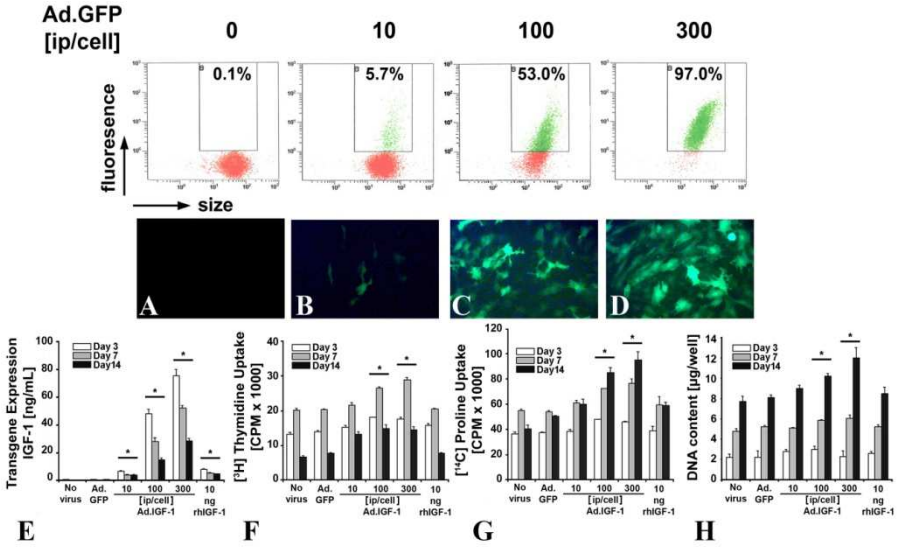

Figure 21: Adenovirus-mediated gene transfer to ACL fibroblasts in monolayer culture. Fluorescence microscopy and flow cytometry of ACL monolayer cultures following 3 days of Ad.GFP-transduction at doses of 0 (A), 10 (B), 100 (C), and 300 (D) infectious particles (ip)/cell revealed a dose-dependent increase in green fluorescence. Levels of transgene expression in Ad.IGF-1-transduced ACL cultures were assayed by ELISA (E). Cell proliferation was assessed by measurement of [^{3}H] thymidine incorporation (F) and DNA content (H). Collagen production rates (G) were estimated using [^{14}C] proline uptake measurements. Untransduced and Ad.GFP-transduced monolayer cultures served as controls. The results are expressed as means ± SD. Asterisks indicate values that are statistically different for each time and group compared to the untransduced control cultures (p<0.05). Original magnifications (A–D): 100x.

5.3.2 Persistent marker gene expression within collagen hydrogels

Having determined previously that ACL fibroblasts can express foreign transgenes after incorporation in collagen hydrogels for a period of 21 days (Pascher et al., 2004), this experiment was designed to evaluate dose-responsiveness and persistence of marker gene expressions of ACL cells within collagen hydrogels over a 10-week period *in vitro*. For this, ACL cell-seeded hydrogels were placed in semi-tubular silicone molds to avoid excessive cell contraction, and a typical macroscopic appearance is shown in Figure 23A. The constructs transduced with Ad.Luc at doses of 1, 10, 100, and 1000 ip/cell revealed all significantly elevated levels of transgene expression throughout the 21 days of culture compared to controls, and also interestingly between all groups at all time points (Figure 23B; p<0.05 for all

comparisons). Within the respective groups, levels of Luc transgene decreased during the time course of the experiment. At 3 weeks, Luc expression remained at more than 1000-fold above background levels in all groups (Figure 23B).

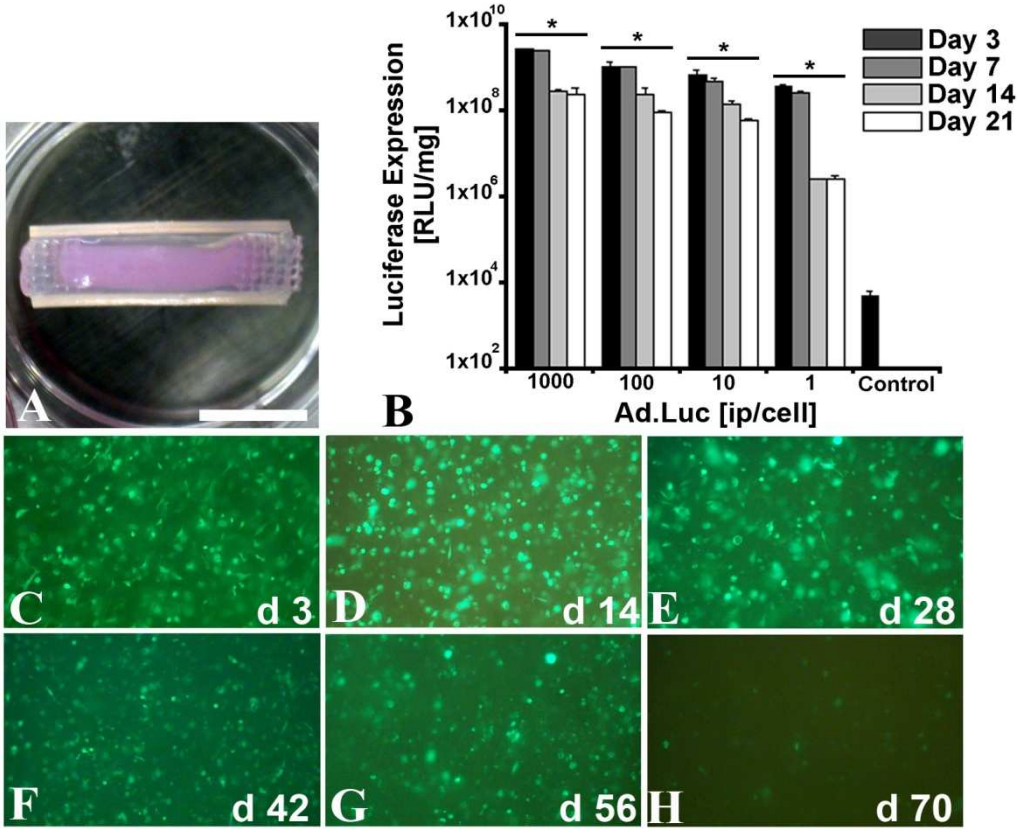

Figure 22: Persistence of markergene expression in collagen hydrogels. Cells were transduced prior to incorporation into the gels. Macroscopic appearance of a collagen type I hydrogel construct-containing ACL cells within a semi-tubular silicone mold that was placed in a 12-well plate (A). Time course of luciferase transgene expression by ACL cells following transduction with different doses of Ad.Luc and seeding into hydrogels (B). Values represent mean levels of luciferase activity in relative light units per mg of protein (n=3, m=9 per time point). Untransduced and Ad.GFP-modified ACL hydrogel constructs at 300 ip/cell served as controls. Fluorescence microscopy of hydrogels seeded with Ad.GFP-modified ACL fibroblasts showed a gradual decline in GFP expression over time (C–H), with GFP expression being evident in the hydrogel cultures for up to 10 weeks (H). Asterisks indicate values that are statistically different for each time in culture compared to the untransduced controls. Bar in (A) = 7 mm. Original magnifications (C–H): 100x.

To examine further the duration of transgene expression of ACL cells within the collagen hydrogel *in vitro*, constructs were modified with Ad.GFP at a medium dose of 100 ip/cell, and monitored in culture by fluorescence microscopy for the time of persistence of green fluorescence (Figure 23C–F). As shown in Figure 23, levels of

transgene expression remained high (bright green fluorescence) until day 14 (C, D), and gradually declined thereafter (E–G) until almost all green fluorescent cells disappeared by week 10 of culture (H), when the cultures were terminated.

5.3.3 Effects of IGF-1 gene delivery on ACL cell-seeded constructs

5.3.3.1 IGF transgene expressions, DNA content, and RT-PCR analyses

Having demonstrated the ability of the hydrogel to support sustained marker gene expression for a periods of time compatible with repair, the effects of IGF-1 transgene expression on the behavior of ACL cells was evaluated. To this end, ACL cells were transduced with 100 ip/cell Ad.IGF-1, Ad.GFP, or Ad.Luc and maintained for 21 days in hydrogel culture. In contrast to the control cultures, which showed constantly low levels of IGF-1 production, the Ad.IGF-1-modified ACL cell-seeded hydrogels revealed significantly elevated expression levels at all time points (Figure 24A).

The highest level of IGF-1 secretion in the medium was seen on day 3 in the Ad.IGF-1-modified cultures (72.9 ± 2.2 ng/mL), and continuously declined thereafter until the end of the 21-day culture period (Figure 24A). This resulted in significantly increased cellularity in the Ad.IGF-1-modified constructs at day 21 as evidenced by DNA content analyses compared to the Ad.GFP-transduced group (Figure 24B). RT-PCR analyses revealed higher expression of genes encoding matrix proteins associated with ligaments, including COL I (1.5-fold) and III (1.4-fold), ELA (2.6-fold), VIM and FN (1.4-fold) in the Ad.IGF-1-modified constructs compared to Ad.GFP controls (Figure 24C). Semiquantitative analyses of n=3 replicates are shown, with EF1a serving as internal control.

5.3.3.2 Histological and immunohistochemical analyses

Increased cellularity in hydrogels seeded with Ad.IGF-1-transduced ACL cells was confirmed by H&E staining in which the constructs appeared much more cellular, in particular on the surface of the construct, than the Ad.Luc controls (Figure 23A).

Furthermore, the Ad.IGF-1-modified constructs showed more elongated fibroblast-like (Figure 25A) cells embedded in a dense collagenous matrix (Figure 25B–D) compared to controls where no orientation of cells and collagenous matrix was seen,

as evidenced by collagen matrix stainings with Azan (B; blue), Van Gieson (C; red), and Masson-Goldner (D; green).

As further shown in Figure 26, immunohistochemical stainings were performed for COL III (A), ELA (B), TEN (C), and VIM (D) revealed more intense stainings of these ligamentogenic matrix components in the Ad.IGF-1-transduced hydrogel cultures, compared to corresponding control specimen. Notably, the intensities of brown-colored staining of extracellular matrix proteins in the Ad.IGF-1 group increased from panels A to D (COL III<ELA<TEN<VIM). For each staining controls were performed without primary antibody, which were negative in all cases (not shown).

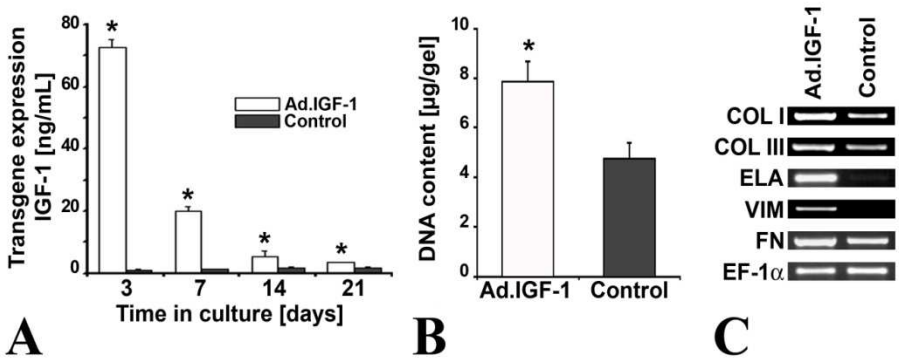

Figure 23: Transgene expression (A) and DNA content (B) and RT-PCR analyses (C) of Ad.IGF-1 modified ACL-hydrogel constructs, which were cultured for 3 weeks. Each error bar represents mean values ± SD, and asterisks indicate values that are statistically different compared to the Ad.GFP transduced control cultures (A, B). RT-PCR analyses of ligament-specific marker gene expression of Ad.IGF-1 modified constructs compared to Ad.GFP controls. COL I = collagen type I, COL III = collagen type III, ELA = elastin, VIM = vimentin, FN = fibronectin, EF1α = elongation factor 1 α.

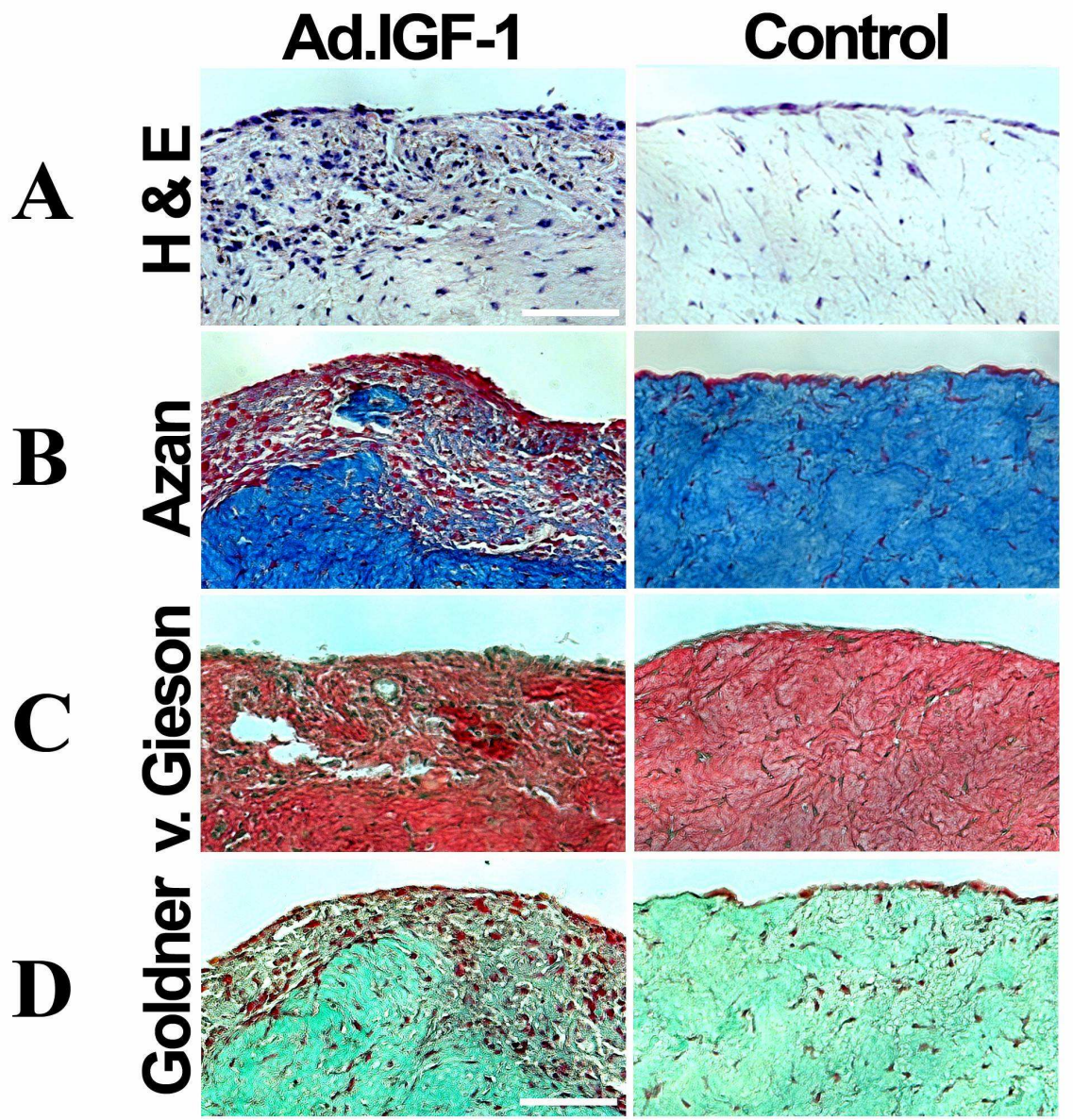

Figure 24: Histochemical analyses of Ad.IGF-1 modified ACL hydrogel constructs after 21 days compared to Ad.GFP controls. Cells were transduced prior to incorporation into the gels. Cellularity of the constructs was evaluated by (A) H&E staining, and collagen accumulation was assessed by (B) Azan (blue), (C) Van Gieson (Gieson; red), or (D) Masson-Goldner (Goldner; green) staining. Bars in (A) and (D) = 100 µm. Original magnifications (A–D): 200x.

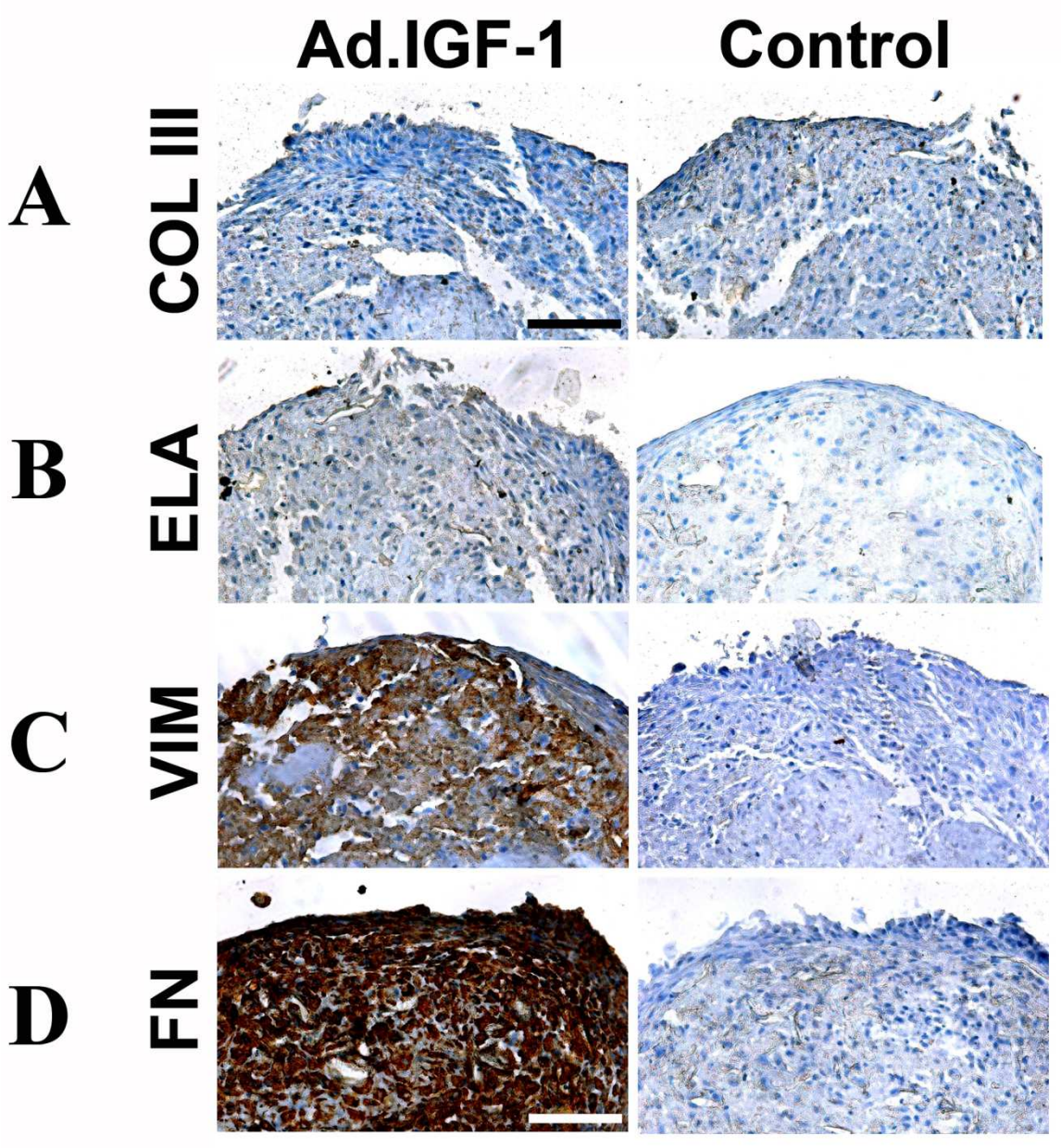

Figure 25: Immunohistochemical analyses of Ad.IGF-1 modified ACL hydrogel constructs after 21 days compared to Ad.GFP controls. Cells were transduced prior to incorporation into the gels. Immunostainings were performed for the ligament matrix components (A) collagen type III (COL III), (B) elastin (ELA), (C) tenascin, and (D) vimentin (VIM). Positive immunostaining is indicated by the brown-colored network in the vicinity of the bluecolored cells (stained with haematoxylin). Bars in (A) and (D) = 100 µm. Original magnifications (A–D): 200x.

5.3.3.3 Cell viability and apoptosis

Double fluorescence staining with AnnV-Cy3 and 6-CFDA allowed viable (only green), early apoptotic (green and red), and necrotic cells (only red) to be distinguished. The high levels of green fluorescence found in the Ad.IGF-1 (Figure

25A) and control group constructs (Figure 25B) revealed high viability in both groups, with a higher cellularity in the Ad.IGF-1 constructs after 21 days. Only a small proportion of cells appeared to be apoptotic or necrotic in either group, as evidenced by red fluorescence (Figures 25C and D).

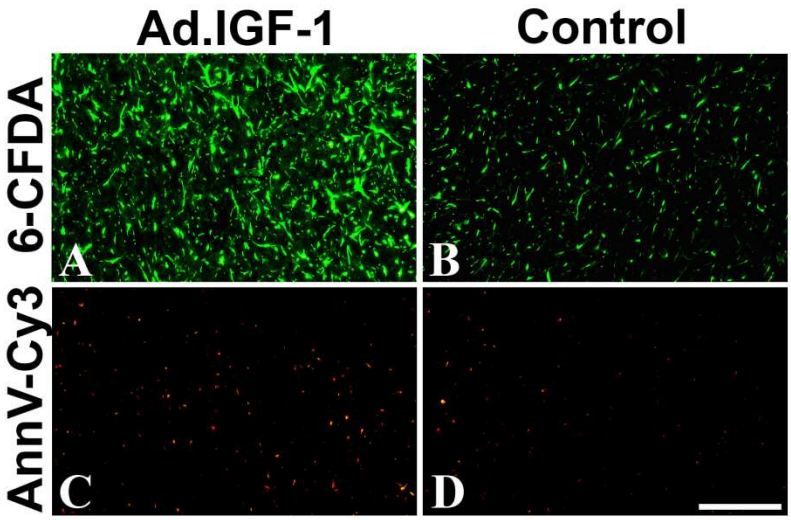

Figure 26: Analyses of viable ACL cells after 3 weeks of hydrogel culture. ACL hydrogel constructs modified with Ad.IGF-1 (A,C), or Ad.Luc (B,D) were double-stained with 6-CFDA (A,B) and annexin V-Cy3 (AnnCy3; C,D), and visualized with fluorescence microscopy. Living cells were stained green with 6-CFDA and necrotic cells red with annexin V-Cy3. Apoptotic cells stained for both, annexin V-Cy3 (red) and 6-CFDA (green). Bar in (D) = 200 µm. Original magnifications (A–D): 100x.

5.3.4 In situ gene IGF-1 transfer to ACL tissue in vitro

To deliver genes to the ACL cells as they migrate into the defect site vectors were incorporated into the scaffold. To this end, we used an *in vitro* explant culture model of ACL repair developed by Murray and colleagues (Pascher *et al.*, 2004; Murray *et al.*, 2006b), and tested the responses of Ad.IGF-1, Ad.GFP or Ad.Luc vector-laden hydrogels in this system. A typical macroscopic appearance of a control construct with mold after 7 days is shown in Figure 28A. At that time considerable number of green fluorescent ACL cells were seen in the gel (Figure 28B), and the number of GFP+ cells increased progressively until the end of the culture period at day 21, confirming results obtained previously (Pascher et al., 2004). IGF-1 transgene expression by Ad.IGF-1-modified explant constructs increased significantly between days 3 and 14 to peak values of 55.275.2, and decreased thereafter (Figure 28C). However, expression levels were significantly higher at all time points than in the

controls, with the difference being still more than 35-fold at day 21 (Figure 28C). This led to significantly increased DNA levels in the Ad.IGF-1-modified explants at day 21 compared with the Ad.GFP-transduced group (Figure 28D).

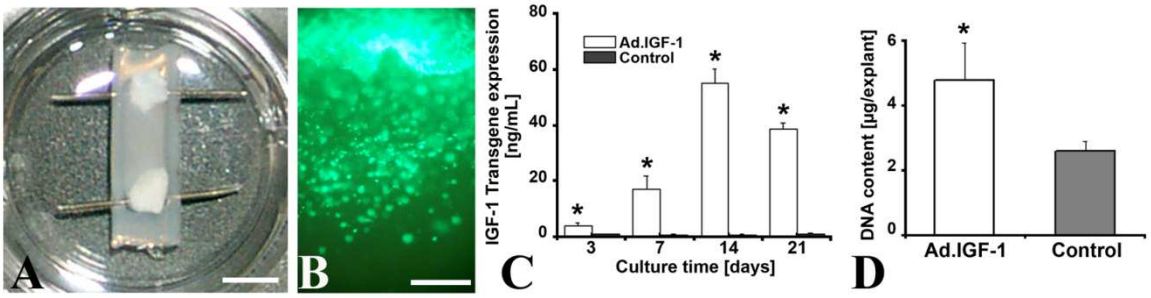

Figure 27: Effect of *in situ* delivery of Ad.IGF-1 in an *in vitro* ACL repair model. Vector-laden collagen gels containing Ad.GFP or Ad.IGF-1 were placed between the cut ends of two 3x3 mm ACL fascicle pieces from the proximal and distal ends of the ligament. A macroscopic view of a representative control explant after 1 week is shown (B). At that time, considerable number of cells had migrated from the bulk ACL tissue, entered the hydrogel and become transduced by the vector (Ad.GFP), as indicated by green fluorescence. IGF-1 transgene expression by Ad.IGF-1-modified constructs compared to the controls (Ad.GFP) over 21 days is shown in panel C, and DNA content analyses at day 21 in panel D. The results are expressed as mean values ± SD and asterisks indicate values that are statistically different compared to controls. Bar in (A) = 5 mm and (B) = 200 µm. Original magnification (B): 100x.

5.3.5 Persistence of adenoviral infectivity within collagen hydrogels

Having observed remarkable the effectiveness of *in situ* transduction of ACL cells from adenovirus-laden gels, we wished to characterize further the bioactivity of the adenoviral vectors when incorporated into collagen hydrogels. Therefore, 10^8 ip of Ad.GFP or Ad.Luc were incorporated into collagen hydrogels and preincubated over a 21-day period, and compared to virus solution and no virus controls (empty), which were maintained in parallel. The experimental design is illustrated in Figure 29A, and experiments were performed as described in the Materials and methods section. ACL fibroblasts were efficiently transduced at all time points with Ad.Luc vectors at significant levels compared to empty controls in all preincubation conditions tested, with the virus solution group showing the highest transgene expression rates (Figure 29B;**). Furthermore, the virus elution medium group revealed higher Luc expression levels at all time points compared to the virus gel group, which reached significance levels only at days 3 and 7 (Figure 29B;*). When Ad.GFP infections were performed on 293 cells and monitored in culture by fluorescence microscopy, a similar pattern of

transgene expression was observed. As shown in Figure 29, levels of transgene expression were highest at all time points (bright green fluorescence) in the virus solution group (C), followed by the virus elution medium group (E) and the virus gel group (D). Although infectivity declined in all cultures with time (C–E), green fluorescent cells were apparent in all Ad.GFP-containing groups at the end of the culture period of 21 days, indicative of persistence of infective recombinant adenovirus in all conditions shown (C–E). Cultures containing no Ad.GFP revealed no green fluorescence (data not shown).

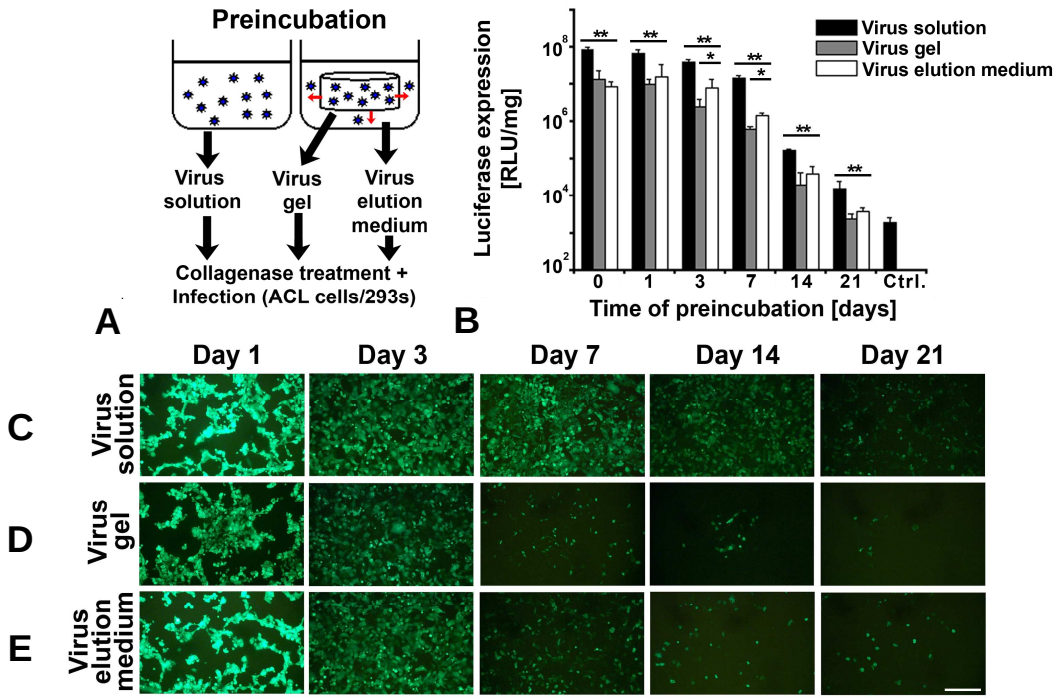

Figure 28: Duration of adenoviral infectivity within the collagen type I hydrogels. The experimental design is illustrated in panel A. 10^8 infectious viral particles of Ad.GFP or Ad.Luc were incorporated into collagen hydrogels and preincubated over a 3-week period. For comparison, equal amounts of vectors were placed in solution (virus solution) and preincubated in parallel, as well as no virus controls. At time points indicated vector-laden hydrogels were removed (virus gel), and the elution medium was collected (virus elution medium) to assess vector leakage from the hydrogels (red arrows; A). Then all groups were treated with collagenase for solubilization and whole suspensions were used for infection of ACL fibroblast cultures (B; Ad.Luc), and 293 cells (C–E; Ad.GFP), with transgene expressions being monitored after 48 h. All luciferase data are expressed as means ± SD (n=3, m=9 per group and time point) and asterisks indicate values that are statistically different compared to controls. Bar in (D) = 200 µm. Original magnification (B): 100x.

5.4 Discussion

Our experiments confirm the ability of first generation adenoviral vectors to transduce ACL cells both in monolayer and in hydrogel culture, and show that ACL fibroblasts are able to express transgenes at elevated levels in a dose-dependent and sustained fashion for at least 10 weeks, when maintained in COL I hydrogels. This is, in contrast to the rapid drop-off of transgene expression seen by day 7 in monolayer culture.

Genetic modification with the IGF-1 transgene at suitable doses increased the cellularity of all culture systems and enhanced the synthesis and deposition of a matrix rich in COL I, III, ELA, TEN, VIM, and FN. This confirms that expression of IGF-1 enhances certain key aspects of the ligament healing response when appropriate doses of vectors are used (Doroski *et al.*, 2007). Transductions at these doses were not detrimental to cell viability (Figure 27). These findings are consistent with the literature (Schmidt *et al.*, 1995; DesRosiers *et al.*, 1996; Evans, 1999; Molloy *et al.*, 2003; Hildebrand *et al.*, 2004; Petrigliano *et al.*, 2006; Provenzano *et al.*, 2007). Whether IGF-1 will be the transgene of choice for enhanced ACL healing remains to be determined. Using the same technology, delivery of the TGF-β1 cDNA also resulted in higher DNA levels and elevated matrix synthesis (Pascher et al., 2004). However, TGF-β1 risks a number of adverse side-effects, particularly those relating to fibrosis. Several other potent growth factors exist and much more research is required to determine the most appropriate factor or combination of factors for this purpose (Evans, 1999; Molloy *et al.*, 2003; Hildebrand *et al.*, 2004; Petrigliano *et al.*, 2006). COL I hydrogels were effective carriers of adenoviral vectors, which preserved infectivity within the gels for time periods compatible with ligament healing (Figures 28 and 29). However, considerable vector leakage from the gel was detected. This is consistent with the findings of Schek et al. (Schek et al., 2004), showing considerable vector leakage from their hydrogels and a reduction of adenoviral infectivity within the observed 4 days of preincubation. According to these investigators, vector leakage rates were dependent on the material chosen (fibrin vs. COL I) and on the concentrations of the materials used to form the hydrogels, with lower concentrations being more susceptible to vector leakage than higher ones. Thus, the high levels of vector leakage in our system might be attributed to the low concentration of COL I used (0.5 mg/mL), which suggests the testing of higher collagen concentrations in

further studies using this system to optimize vector containment within the gel. The stability of the recombinant adenovirus vectors at 37℃ in solution and in gels was sufficient for the proposed eventual clinical use of this technology; there was no difference in the thermal decay of infectivity of free or bound virus. It is interesting that ACL fibroblasts express transgenes for much longer periods of time when incorporated into gels than when in monolayer. Whether this reflects the lower rate of cell division or some other aspect of their biology is unknown. However, it is encouraging that transgene expression persists for periods that are compatible with the probable requirements of ACL repair. Our data are also consistent with those of Dai et al. (Dai et al., 2003) who were able to deliver marker genes to the rat Achilles tendon with an adenovirus vector contained within a gelatin sponge. It remains to be seen whether other matrix materials used in the context of ligament healing (Altman *et al.*, 2003; Cooper *et al.*, 2005; Ge *et al.*, 2006; Petrigliano *et al.*, 2006) will be suitable for these types of *in situ* approach to tissue regeneration (Bonadio, 2000; Schek *et al.*, 2006; Evans *et al.*, 2007; Hu *et al.*, 2007; Park *et al.*, 2007). While biologically active, the collagen hydrogels have very low mechanical strength (on the order of only 60 kPa (Murray et al., 2006a) at the start of culture. Thus, these hydrogels are only useful as adjuncts to a mechanically sound construct. For example, in the case of a torn ACL, the hydrogels could be cast around a suture repair to stimulate the biology of the wound site—a technique that has already shown some promise in one large animal model (Murray et al., 2007). In addition, the properties of the hydrogel over time in culture are likely to be largely dependent on the cell-mediated remodeling of the construct, with increases in hydrogel strength noted when the anabolic function of the cells outweigh the catabolic response and decreases in hydrogel strength noted when the reverse is true. The changes in the mechanical properties of the hydrogel over time *in vitro* were outside the scope of this current work, but certainly deserve further study. It is uncertain whether a first generation adenovirus would be the vector of choice for eventual clinical application of this technology. In our hydrogel system, it was efficient in generating constantly high levels of transgene expression for time periods compatible with ligament healing. Although adenovirus is inflammatory and antigenic, and has caused the death of one subject in a gene therapy trial (Lehrman, 1999; Marshall, 1999), its local, focussed delivery in the manner suggested here should obviate these safety concerns. Of the other vector systems presently available for human gene therapy,

lentiviruses and retroviruses are integrating vectors that are unlikely to be appropriate for uses such as this (Evans et al., 2005). Until last week, AAV was considered a safe vector (Evans et al., 2005), but now that the first death has been reported this will change. Non-viral gene delivery remains the most attractive theoretical possibility but, so far, levels and duration of transgene expression are not sufficient (Evans et al., 2005).

5.5 Conclusions

The ACL has a latent repair capacity that becomes active when a suitable scaffold is placed between the ruptured ends of the ligament. A type I collagen hydrogel laden with adenoviral vectors is able to transduce cells as they migrate into the scaffold and enhance the synthesis of repair tissue. Collagen hydrogels maintained the infectivity of adenoviral vectors for at least 21 days and promoted transgene expression of transduced ACL cells for at least 10 weeks. In response to IGF-1 as the transgene, greater numbers of ACL cells accumulated in the hydrogels, where they synthesized and deposited larger amounts of COL I and III, ELA, TEN, VIM, and FN, while considerable levels of ACL cell apoptosis were not observed. These in vitro data confirm the efficiency of in situ gene delivery to ACL cells using adenoviral vectors and COL I hydrogels, and permit optimism over a possible future clinical application of this technology.

Chapter 6

Discussion

Despite the incidence of severe ligament and tendon injuries, their clinical management is still debated. While a rotator cuff tear or an ACL rupture can be treated surgically, the biomechanical and biochemical properties as well as the histomorphometric appearance of the reconstructed tissue are different to those of normal ligament and tendon tissue.

Therefore, it is inescapable to develop engineered ligaments and tendons. The development of a functional engineered ligament or tendon requires the use of reparative cells with the capacity for proliferation and matrix synthesis, a structural scaffold that facilitates cell attachment and regulatory stimuli. These constituents may be applied in either an *in vivo* or *ex vivo* system (Petrigliano et al., 2006). *In vivo* engineered ligaments and tendons need a scaffold that is designed to be implanted into the patient and advance cell ingrowth and formation of ligamentogenic tissue. A collagen fiber based ACL graft causes no donor site morbidity and the risk of disease transmission or bacterial infections are missing. The native ACL is mainly composed of collagen type I (more than 70% of the dry weight) (Dunn *et al.*, 1995; Woo *et al.*, 2006a). Such a natural scaffold could help to develop a better clinical strategy and improved clinical outcome. Additionally, a biomimetic tissue engineered ligament or tendon can be individually processed. Beside the stability of the collagen fiber-based ACL grafts, the *in vivo* attachment of fibroblasts and matrix synthesis are relevant. Dunn et al. showed that fibroblasts can attach to collagen fibers (Dunn et al., 1995) and tend to oriented along the longitudinal axis (Dunn et al., 1995). Additionally, the material of the graft must produce minimal toxic and immunogenic reactions to the surrounding tissue. The use of a collagen type I hydrogel for articular cartilage repair causes no immunogenic reaction and is in clinical use for ACT for 5 years.

Cell based therapy is another promising method for the healing of ligament and tendon defects. The application of MSCs or bone marrow cells into the defect zone has been described in many studies (Young *et al.*, 1998; Watanabe *et al.*, 2002). To minimize the immune response at the injury site, autologous cells were used for transplantation. The advantage of a MSC based cell therapy is the differentiation into a large number of fibroblasts and the enhancement of the ligament and tendon

healing. In the case of a rotator cuff tear, the *in vivo* study showed a distinct lower fat content in the +MSC group after injection of autologous MSCs in the defect area. The histomorphometric evaluation revealed significant differences in the fat content between the –MSC group (group treated without cells) and the +MSC group (cell-treated group). These results can mean that the healing is enhanced or the fatty degeneration runs slower. The reconstruction of musculoskeletal tissue, e.g. bone, cartilage, muscle, tendons, and ligaments, was described in different *in vivo* studies (Tuan *et al.*, 2003; Calve *et al.*, 2004; Natsu *et al.*, 2004). The reconstruction of a musculus tibialis anterior defect model in Sprague-Dawley rats was described after application of MSCs. This study showed that MSCs enhance the maturation of muscle fibrils. Additionally, the injured muscle reached an almost normal muscular strength 4 weeks after application of the MSCs (Natsu et al., 2004).

Previous studies suggest that in the future the application of autologous MSCs for the therapy of acute and chronic diseases, e.g. Parkinson's disease, diabetes, myocardial infarction, and musculoskeletal diseases could be of vital importance (Tuan *et al.*, 2003; Chen *et al.*, 2004b; Bobis *et al.*, 2006; Noth *et al.*, 2007; Noth *et al.*, 2008). Beside the classical cell based therapy, MSC-biomaterial composites were used for ligament and tendon repair. A study of Awad et al. described that MSC-collagen constructs have a higher capacity to withstand maximum stress (Awad et al., 2003). Furthermore, many strategies try to mimic the micro-environment that may be necessary to maintain MSCs or ligament/tendon-derived cells to differentiate into ligamentocytes/tendocytes. MSCs in a collagen type I hydrogel and under constant load showed 3 months after transplanted, within an Achilles defect, the formation of neo-tendon tissue (Awad et al., 1999; Caplan, 2005).

Growth factors induce and modulate many different processes, e.g. cell migration, proliferation, differentiation, and matrix synthesis. For the application of tissue engineered ligaments and tendons, *in vitro* and *in vivo* studies investigated the role of growth factors for the complex process of ligament and tendon healing. *In vitro* studies have shown that FGF, TGF-β1, PDGF, as well as BMP-12 and -13 can stimulate fibroblast proliferation, collagen and matrix synthesis, whereas the effect of growth factors is dose-independent (Letson and Dahners, 1994; Marui *et al.*, 1997b; Wolfman *et al.*, 1997; Evans, 1999; Hart and Evans, 2000). *In vivo* studies confirmed parts of these results, when injured ligament and tendon were treated with growth factors. The influence of growth factors *in vivo* is often very variable caused by the

method of delivery (Batten *et al.*, 1996; Scherping *et al.*, 1997; Nakamura *et al.*, 1998). Especially the interplay between different growth factors in a specific progression and dose is of high importance. On the one hand, different growth factors require a strict local application to prevent adverse effects of systemic application. On the other hand, growth factors are subjects to fast degradation.

Because of the problems with the application of growth factors, the strategy of local production of growth factors by local cells has been developed. Therefore, gene therapy is an additional approach for ligament and tendon healing. Exogenic genes, which code for a specific growth factor, are transferred into cells. After inclusion and expression of the genes, high levels of the mediator protein can be produced and released to the defect area. Only a few therapeutic genes (e.g. PDGF, HGF, TGF-β, IGF) were transferred into ligamentogenic fibroblasts (Nakamura et al., 2001; Pascher et al., 2004; Steinert et al., 2008). Also, BMP-12 and -13 have been identified to induce the formation of ligament- and tendon-like tissue (Wolfman *et al.*, 1997; Lou *et al.*, 2001; Fu *et al.*, 2003). The transduction of MSCs and ACL fibroblasts with high-doses of BMP-12, -13, and IGF in a collagen type I hydrogel showed particularly the production of FN, TN-C, TNMD, and VIM on protein and RNA level. These *in vitro* results confirm the efficiency of *in situ* gene delivery to ACL fibroblasts and MSCs using adenoviral vectors and collagen type I hydrogels. Despite the promising results, the application of gene-modified cells has to be handled with respect because of safety issues. Due to the changeability of integrating viral vectors into the genome of the target cells, there are risks of side effects including potentially severe consequences, such as mutagenesis, which are unacceptable especially for elective cases (Woo et al., 2004). Nevertheless, gene therapy is not an established method for clinical application. Especially, the missing acceptance of gene therapy strategies for the healing of non-life-threatening ligament and tendon injuries is a social problem.

Finally, tissue engineering and other regeneration strategies to treat injured ligaments and tendons must show that they are safe and more effective than the current clinical standard therapy. The composite of the construct must be arranged in a way that allows the surgeon to easily attach the tissue engineered device to the injured site. Nevertheless, tissue engineering offers a promising new therapy for ligament and tendon injuries.

Chapter 7

7.1 Summary

Ruptures of the anterior cruciate ligament (ACL) and defects of the rotator cuff represent the most common ligament and tendon injuries in knee and shoulder. Both injuries represent significant implications for the patients. After an injury, the ACL and the rotator cuff both exhibit poor intrinsic healing capacities. In order to prevent further defects such as arthritis of the knee and fatty infiltration of the rotator cuff, surgical interaction is essential. In both cases, the currently used surgical techniques are far from optimal because even after the therapy many patients report problems ranging from pain and reduced mobility to complete dysfunction of the involved joint and muscles. Tissue engineering may be a possible solution. It is a promising field of regenerative medicine and might be an advantageous alternative for the treatment of musculoskeletal injuries and diseases in the near future.

In this thesis, different tissue engineering based approaches were investigated. For the reconstruction of damaged or diseased ligaments and tendons, the use of MSCs and gene therapy with growth factors is especially suitable and possesses a great therapeutic potential. Therefore, the first method studied and tested in this thesis was the development of a biomaterial based construct for the repair of a ruptured ACL. The second approach represents a cell based strategy for the treatment of the fatty infiltration in the rotator cuff. The third approach was a combined cell, biomaterial, and growth factor based strategy for ACL ruptures.

Biomaterial based ACL construct

The implant is currently tested in a preclinical *in vivo* study in mini pigs. This proof-of-principle study is performed to validate the functional capability of the collagen fiber based implant under load *in vivo* and its population with fibroblasts which produce a ligamentogenic matrix.

Cell based treatment of the fatty infiltration in the rotator cuff

Regarding the treatment of the fatty infiltration of the rotator cuff in a rabbit model, the *in vivo* results are also promising. The group treated with autologous MSCs (+MSC

group) showed a lower fat content than the untreated group (–MSC group) 6 weeks after the treatment. Furthermore, the SSP muscle of the MSC-treated animals revealed macroscopically and microscopically only few differences compared to the healthy control group. The exact underlying mechanisms leading to the positive results of the treatment are not yet fully understood and have therefore to be further investigated in the future.

Cell, biomaterial, and growth factor based treatment of ACL ruptures

Studies described in current literature show that collagen hydrogel scaffolds are not ideal for a complete ligament or tendon reconstruction, because of their insufficient mechanical stability. Introduced as an alternative and superior therapy, the combined strategy used in this thesis proves that the cultivation of BMP-12, -13, and IGF-1 transduced MSCs and ACL fibroblasts in a collagen hydrogel is successful. The results of the performed *in vitro* study reveal that the cells exhibit a fibroblastic appearance and produce a ligamentogenic matrix after 3 weeks. Furthermore, the adenoviral transduction of MSCs and ACL fibroblasts showed no negative effects on proliferation or viability of the cells nor was apoptosis caused. Therefore, the application of these cells represents a possible future therapy for a partial ligament and tendon rupture where the mechanical stability of the remaining ligament or tendon is sufficient and the healing can be improved substantially by this therapy.

In general, prospective randomized clinical trials still have to prove the postulated positive effect of MSCs for the treatment of various musculoskeletal diseases, but the results obtained here are already very promising. Ideally, the treatment with MSCs is superior compared to the standard surgical procedures. Because of current safety issues the use of genetically modified cells cannot be expected to be applied clinically in the near future.

In summary, the different tissue engineering approaches for novel therapies for musculoskeletal injuries and diseases invested in this thesis showed very promising results and will be further developed and tested in preclinical and clinical trials.

7.2 Zusammenfassung

Kreuzbandrupturen und Defekte im Bereich der Rotatorenmanschette stellen die häufigsten Band- und Sehnenverletzungen im Kniegelenk bzw. in der Schulter dar. Beide Verletzungen haben erhebliche Auswirkungen für den Patienten. Sowohl das Kreuzband als auch die Rotatorenmanschette weisen ein sehr schlechtes Heilungspotential nach einer Verletzung auf. Um weiteren Schäden wie einer Kniegelenksarthrose oder einer Verfettung der Rotatorenmanschette vorzubeugen, ist ein operativer Eingriff erforderlich. In beiden Fällen sind die zurzeit verwendeten Behandlungsstandards nicht optimal, da auch nach einer Therapie viele Patienten über Beschwerden klagen, die von Schmerzen und einer eingeschränkten Mobilität bis hin zu einer kompletten Dysfunktion des betroffenen Gelenks und Muskels reichen.
Tissue Engineering ist ein zukunftsträchtiges Feld der Regenerativen Medizin und kann ein möglicher Lösungsansatz sein. Vor allem bei der Behandlung von muskuloskelettalen Verletzungen und Erkrankungen kann es zukünftig eine vorteilhafte Behandlungsalternative darstellen.

In dieser Doktorarbeit wurden verschiedene Tissue Engineering-basierte Lösungsansätze untersucht. Zur Rekonstruktion von defektem Band- und Sehnengewebe sind sowohl der Einsatz von mesenchymalen Stammzellen (MSZ) als auch die Gentherapie mit Wachstumsfaktoren besonders geeignet und weisen ein großes therapeutisches Potential auf. Deswegen wurde in der vorliegenden Doktorarbeit als erster innovativer Therapieansatz ein Biomaterial-basiertes Konstrukt für den Ersatz eines gerissenen Kreuzbandes entwickelt und getestet. Der zweite Lösungsansatz stellt eine Zell-basierte Therapie zur Behandlung einer fettigen Atrophie der Rotatorenmanschette dar. Die dritte Methode kombiniert Zellen, Biomaterialien und Wachstumsfaktoren zur Therapie von Kreuzbandrupturen.

Biomaterial-basiertes Kreuzbandkonstrukt

Das Implantat wird zurzeit in einer präklinischen *in vivo* Studie am Mini Pig getestet. Diese Proof-of-Principle Studie wird durchgeführt, um die Funktionsfähigkeit der Kollagenfaser-basierten Implantate unter Belastung *in vivo* zu validieren und ihre Besiedelung mit Fibroblasten, die eine ligamentäre Matrix ausbilden, zu beobachten.

Zell-basierte Behandlung der fettig-infiltrieten Rotatorenmanschette

Auch bei der Behandlung der fettigen Infiltration der Rotatorenmanschette im Kaninchenmodel, wurden *in vivo* sehr viel versprechende Ergebnisse erzielt. Die mit autologen MSZ (+MSZ-Gruppe) behandelte Gruppe zeigte nach 6 Wochen einen deutlich geringeren Fettanteil als die unbehandelte Gruppe (-MSZ-Gruppe). Des Weiteren wies der SSP-Muskel aller MSZ-behandelten Tiere sowohl makroskopisch als auch mikroskopisch nur geringe Unterschiede im Vergleich zur gesunden Kontrollgruppe auf. Der genaue zugrunde liegende Mechanismus dieser erfolgreichen Behandlung konnte bisher noch nicht genau geklärt werden und muss in zukünftigen Studien weiter untersucht werden.

Zell-, Biomaterial- und Wachstumsfaktor-basierte Behandlung von Kreuzbandrupturen

In der aktuellen Literatur beschriebenen Studien zeigen, dass Kollagenhydrogel-konstrukte aufgrund der fehlenden biomechanischen Stabilität nicht geeignet sind für den kompletten Band- bzw. Sehnenersatz. Als vorteilhafte Behandlungsalternative wurde in der vorliegenden Arbeit eine kombinierte Strategie entwickelt und erfolgreich *in vitro* getestet: Die Kultivierung von BMP-12-, -13- bzw. IGF-1-transduzierten MSZ und Kreuzbandfibroblasten in einem Kollagenhydrogel verlief sehr viel versprechend und ergab, dass die Zellen nach 3 Wochen im Kollagenhydrogel eine fibroblastäre Morphologie aufweisen und eine ligamentäre Matrix ausbilden. Des Weiteren führte die adenovirale Transduktion der Zellen weder zu negativen Auswirkungen auf das Proliferationsverhalten noch auf die Vitalität der Zellen und löste auch keine Apoptose bei den transduzierten Zellen aus. Zukünftig kann der Einsatz dieser Zellen deswegen ein möglicher Ansatz zur Behandlung von Teilrupturen bei Bändern und Sehnen darstellen, bei denen die biomechanische Stabilität ausreichend ist und die Heilung durch die Therapie wesentlich verbessert wird.

Im Allgemeinen müssen prospektive randomisierte klinische Studien zeigen, ob sich der positive Effekt der MSZ bei der Behandlung von Erkrankungen des muskuloskelettalen Systems in der Orthopädie und Unfallchirurgie bewährt, wobei die in der vorliegenden Arbeit erzielten Ergebnisse sehr Erfolg versprechend sind. Idealerweise erweist sich die Behandlung mit MSZ als deutlich vorteilhaft gegenüber

den bisher etablierten chirurgischen Standardverfahren. Aufgrund der bestehenden Sicherheitsrichtlinien für den Einsatz von gentherapeutischen modifizierten Zellen ist mit deren Verwendung zur Behandlung von Band- und Sehnenerkrankungen in naher Zukunft nicht zu rechnen.

Zusammenfassend führte die Untersuchung der unterschiedlichen Tissue Engineering Ansätze, die in dieser Doktorarbeit als neue Therapien zur Behandlung von muskuloskelettalen Verletzungen und Erkrankungen evaluiert wurden, zu sehr viel versprechende Ergebnisse. Diese Therapieansätze sollen weiterentwickelt und in präklinischen und klinischen Studien getestet werden.

Chapter 8

Appendix

8.1 References

AGLIETTI, P., BUZZI, R., D'ANDRIA, S., and ZACCHEROTTI, G. (1992). Long-term study of anterior cruciate ligament reconstruction for chronic instability using the central one-third patellar tendon and a lateral extraarticular tenodesis. Am J Sports Med **20**, 38-45.

ALTMAN, G.H., DIAZ, F., JAKUBA, C., CALABRO, T., HORAN, R.L., CHEN, J., LU, H., RICHMOND, J., and KAPLAN, D.L. (2003). Silk-based biomaterials. Biomaterials **24**, 401-416.

ALTMAN, G.H., HORAN, R.L., LU, H.H., MOREAU, J., MARTIN, I., RICHMOND, J.C., and KAPLAN, D.L. (2002a). Silk matrix for tissue engineered anterior cruciate ligaments. Biomaterials **23**, 4131-4141.

ALTMAN, G.H., HORAN, R.L., MARTIN, I., FARHADI, J., STARK, P.R., VOLLOCH, V., RICHMOND, J.C., VUNJAK-NOVAKOVIC, G., and KAPLAN, D.L. (2002b). Cell differentiation by mechanical stress. Faseb J **16**, 270-272.

ANDERSON, A.F. (2004). Transepiphyseal replacement of the anterior cruciate ligament using quadruple hamstring grafts in skeletally immature patients. J Bone Joint Surg Am **86-A Suppl 1**, 201-209.

ANDERSON, A.F., SNYDER, R.B., and LIPSCOMB, A.B., SR. (1994). Anterior cruciate ligament reconstruction using the semitendinosus and gracilis tendons augmented by the losee iliotibial band tenodesis. A long-term study. Am J Sports Med **22**, 620-626.

ASPENBERG, P., and FORSLUND, C. (1999). Enhanced tendon healing with GDF 5 and 6. Acta Orthop Scand **70**, 51-54.

AWAD, H.A., BOIVIN, G.P., DRESSLER, M.R., SMITH, F.N., YOUNG, R.G., and BUTLER, D.L. (2003). Repair of patellar tendon injuries using a cell-collagen composite. J Orthop Res **21**, 420-431.

AWAD, H.A., BUTLER, D.L., BOIVIN, G.P., SMITH, F.N., MALAVIYA, P., HUIBREGTSE, B., and CAPLAN, A.I. (1999). Autologous mesenchymal stem cell-mediated repair of tendon. Tissue Eng **5**, 267-277.

BARRY, F.P. (2003). Biology and clinical applications of mesenchymal stem cells. Birth Defects Res C Embryo Today **69**, 250-256.

BARRY, F.P., and MURPHY, J.M. (2004). Mesenchymal stem cells: clinical applications and biological characterization. Int J Biochem Cell Biol **36**, 568-584.

BATTEN, M.L., HANSEN, J.C., and DAHNERS, L.E. (1996). Influence of dosage and timing of application of platelet-derived growth factor on early healing of the rat medial collateral ligament. J Orthop Res **14**, 736-741.

BENHARDT, H.A., and COSGRIFF-HERNANDEZ, E.M. (2009). The role of mechanical loading in ligament tissue engineering. Tissue Eng Part B Rev **15**, 467-475.

BOBIS, S., JAROCHA, D., and MAJKA, M. (2006). Mesenchymal stem cells: characteristics and clinical applications. Folia Histochem Cytobiol **44**, 215-230.

BONADIO, J. (2000). Tissue engineering via local gene delivery: update and future prospects for enhancing the technology. Adv Drug Deliv Rev **44**, 185-194.

BRIGHTON, C.T., STRAFFORD, B., GROSS, S.B., LEATHERWOOD, D.F., WILLIAMS, J.L., and POLLACK, S.R. (1991). The proliferative and synthetic response of isolated

calvarial bone cells of rats to cyclic biaxial mechanical strain. J Bone Joint Surg Am **73**, 320-331.

BUTLER, D.L., JUNCOSA-MELVIN, N., BOIVIN, G.P., GALLOWAY, M.T., SHEARN, J.T., GOOCH, C., and AWAD, H. (2007). Functional tissue engineering for tendon repair: A multidisciplinary strategy using mesenchymal stem cells, bioscaffolds, and mechanical stimulation. J Orthop Res.

CABORN, D.N., and JOHNSON, B.M. (1993). The natural history of the anterior cruciate ligament-deficient knee. A review. Clin Sports Med **12**, 625-636.

CALVE, S., DENNIS, R.G., KOSNIK, P.E., 2ND, BAAR, K., GROSH, K., and ARRUDA, E.M. (2004). Engineering of functional tendon. Tissue Eng **10**, 755-761.

CAPLAN, A.I. (2005). Review: mesenchymal stem cells: cell-based reconstructive therapy in orthopedics. Tissue Eng **11**, 1198-1211.

CAPLAN, A.I. (2007). Adult mesenchymal stem cells for tissue engineering versus regenerative medicine. J Cell Physiol **213**, 341-347.

CAPLAN, A.I., and DENNIS, J.E. (2006). Mesenchymal stem cells as trophic mediators. J Cell Biochem **98**, 1076-1084.

CHEN, G., SATO, T., SAKANE, M., OHGUSHI, H., USHIDA, T., TANAKA, J., and TATEISHI, T. (2004a). Application of PLGA-collagen hybrid mesh for three-dimensional culture of canine anterior cruciate ligament cells. Material Science and Engineering C24, 861-866.

CHEN, J.M., WILLERS, C., XU, J., WANG, A., and ZHENG, M.H. (2007). Autologous tenocyte therapy using porcine-derived bioscaffolds for massive rotator cuff defect in rabbits. Tissue Eng **13**, 1479-1491.

CHEN, L.B., JIANG, X.B., and YANG, L. (2004b). Differentiation of rat marrow mesenchymal stem cells into pancreatic islet beta-cells. World J Gastroenterol **10**, 3016-3020.

CHEN, X., ARMSTRONG, M.A., and LI, G. (2006). Mesenchymal stem cells in immunoregulation. Immunol Cell Biol **84**, 413-421.

CHIQUET-EHRISMANN, R., TANNHEIMER, M., KOCH, M., BRUNNER, A., SPRING, J., MARTIN, D., BAUMGARTNER, S., and CHIQUET, M. (1994). Tenascin-C expression by fibroblasts is elevated in stressed collagen gels. J Cell Biol **127**, 2093-2101.

CHIQUET, M., MATTHISSON, M., KOCH, M., TANNHEIMER, M., and CHIQUET-EHRISMANN, R. (1996). Regulation of extracellular matrix synthesis by mechanical stress. Biochem Cell Biol **74**, 737-744.

COOPER, J.A., JR., BAILEY, L.O., CARTER, J.N., CASTIGLIONI, C.E., KOFRON, M.D., KO, F.K., and LAURENCIN, C.T. (2006). Evaluation of the anterior cruciate ligament, medial collateral ligament, achilles tendon and patellar tendon as cell sources for tissue-engineered ligament. Biomaterials **27**, 2747-2754.

COOPER, J.A., LU, H.H., KO, F.K., FREEMAN, J.W., and LAURENCIN, C.T. (2005). Fiber-based tissue-engineered scaffold for ligament replacement: design considerations and in vitro evaluation. Biomaterials **26**, 1523-1532.

DAI, Q., MANFIELD, L., WANG, Y., and MURRELL, G.A. (2003). Adenovirus-mediated gene transfer to healing tendon--enhanced efficiency using a gelatin sponge. J Orthop Res **21**, 604-609.

DEJARDIN, L.M., ARNOCZKY, S.P., EWERS, B.J., HAUT, R.C., and CLARKE, R.B. (2001). Tissue-engineered rotator cuff tendon using porcine small intestine submucosa. Histologic and mechanical evaluation in dogs. Am J Sports Med **29**, 175-184.

DESROSIERS, E.A., YAHIA, L., and RIVARD, C.H. (1996). Proliferative and matrix synthesis response of canine anterior cruciate ligament fibroblasts submitted to combined growth factors. J Orthop Res **14**, 200-208.

DINES, J.S., GRANDE, D.A., and DINES, D.M. (2007). Tissue engineering and rotator cuff tendon healing. J Shoulder Elbow Surg **16**, S204-207.

DOCHEVA, D., HUNZIKER, E.B., FASSLER, R., and BRANDAU, O. (2005). Tenomodulin is necessary for tenocyte proliferation and tendon maturation. Mol Cell Biol **25**, 699-705.

DODDS, J.A., and ARNOCZKY, S.P. (1994). Anatomy of the anterior cruciate ligament: a blueprint for repair and reconstruction. Arthroscopy **10**, 132-139.

DOROSKI, D.M., BRINK, K.S., and TEMENOFF, J.S. (2007). Techniques for biological characterization of tissue-engineered tendon and ligament. Biomaterials **28**, 187-202.

DUNN, M.G., LIESCH, J.B., TIKU, M.L., and ZAWADSKY, J.P. (1995). Development of fibroblast-seeded ligament analogs for ACL reconstruction. J Biomed Mater Res **29**, 1363-1371.

EVANS, C.H. (1999). Cytokines and the role they play in the healing of ligaments and tendons. Sports Med **28**, 71-76.

EVANS, C.H., BANDARA, G., ROBBINS, P.D., MUELLER, G.M., GEORGESCU, H.I., and GLORIOSO, J.C. (1993). Gene therapy for ligament healing. In *In the anterior cruciate ligament: current and future concepts*. D.W. Jackson, ed. (Raven Press, New York, NY) *pp*. 419-422.

EVANS, C.H., GHIVIZZANI, S.C., HERNDON, J.H., and ROBBINS, P.D. (2005). Gene therapy for the treatment of musculoskeletal diseases. J Am Acad Orthop Surg **13**, 230-242.

EVANS, C.H., PALMER, G.D., PASCHER, A., PORTER, R., KWONG, F.N., GOUZE, E., GOUZE, J.N., LIU, F., STEINERT, A., BETZ, O., BETZ, V., VRAHAS, M., and GHIVIZZANI, S.C. (2007). Facilitated endogenous repair: making tissue engineering simple, practical, and economical. Tissue Eng **13**, 1987-1993.

FAN, H., LIU, H., TOH, S.L., and GOH, J.C. (2009). Anterior cruciate ligament regeneration using mesenchymal stem cells and silk scaffold in large animal model. Biomaterials **30**, 4967-4977.

FEAGIN, J.A., JR., and CURL, W.W. (1976). Isolated tear of the anterior cruciate ligament: 5-year follow-up study. Am J Sports Med **4**, 95-100.

FORSLUND, C., and ASPENBERG, P. (2001). Tendon healing stimulated by injected CDMP-2. Med Sci Sports Exerc **33**, 685-687.

FRANK, C.B., and JACKSON, D.W. (1997). The science of reconstruction of the anterior cruciate ligament. J Bone Joint Surg Am **79**, 1556-1576.

FREEDMAN, K.B., D'AMATO, M.J., NEDEFF, D.D., KAZ, A., and BACH, B.R., JR. (2003). Arthroscopic anterior cruciate ligament reconstruction: a metaanalysis comparing patellar tendon and hamstring tendon autografts. Am J Sports Med **31**, 2-11.

FREEMAN, J.W., WOODS, M.D., and LAURENCIN, C.T. (2007). Tissue engineering of the anterior cruciate ligament using a braid-twist scaffold design. J Biomech **40**, 2029-2036.

FU, S.C., WONG, Y.P., CHAN, B.P., PAU, H.M., CHEUK, Y.C., LEE, K.M., and CHAN, K.M. (2003). The roles of bone morphogenetic protein (BMP) 12 in stimulating the proliferation and matrix production of human patellar tendon fibroblasts. Life Sci **72**, 2965-2974.

FUNAKOSHI, T., MAJIMA, T., SUENAGA, N., IWASAKI, N., YAMANE, S., and MINAMI, A. (2006). Rotator cuff regeneration using chitin fabric as an acellular matrix. J Shoulder Elbow Surg **15**, 112-118.

GE, Z., YANG, F., GOH, J.C., RAMAKRISHNA, S., and LEE, E.H. (2006). Biomaterials and scaffolds for ligament tissue engineering. J Biomed Mater Res A **77**, 639-652.

GENTLEMAN, E., LIVESAY, G.A., DEE, K.C., and NAUMAN, E.A. (2006). Development of ligament-like structural organization and properties in cell-seeded collagen scaffolds in vitro. Ann Biomed Eng **34**, 726-736.

GERBER, C., MEYER, D.C., SCHNEEBERGER, A.G., HOPPELER, H., and VON RECHENBERG, B. (2004). Effect of tendon release and delayed repair on the

structure of the muscles of the rotator cuff: an experimental study in sheep. J Bone Joint Surg Am **86-A**, 1973-1982.

GERICH, T.G., KANG, R., FU, F.H., ROBBINS, P.D., and EVANS, C.H. (1996). Gene transfer to the rabbit patellar tendon: potential for genetic enhancement of tendon and ligament healing. Gene Ther **3**, 1089-1093.

GERICH, T.G., KANG, R., FU, F.H., ROBBINS, P.D., and EVANS, C.H. (1997). Gene transfer to the patellar tendon. Knee Surg Sports Traumatol Arthrosc **5**, 118-123.

GOUTALLIER, D., POSTEL, J.M., BERNAGEAU, J., LAVAU, L., and VOISIN, M.C. (1994). Fatty muscle degeneration in cuff ruptures. Pre- and postoperative evaluation by CT scan. Clin Orthop Relat Res, 78-83.

GUPTA, R., and LEE, T.Q. (2007). Contributions of the different rabbit models to our understanding of rotator cuff pathology. J Shoulder Elbow Surg **16**, S149-157.

HAIRFIELD-STEIN, M., ENGLAND, C., PAEK, H.J., GILBRAITH, K.B., DENNIS, R., BOLAND, E., and KOSNIK, P. (2007). Development of self-assembled, tissue-engineered ligament from bone marrow stromal cells. Tissue Eng **13**, 703-710.

HART, D.A., and EVANS, C.H. (2000). Orthopaedic gene therapy. Ligament and tendon. Clin Orthop Relat Res, S260-261.

HAYNESWORTH, S.E., GOSHIMA, J., GOLDBERG, V.M., and CAPLAN, A.I. (1992). Characterization of cells with osteogenic potential from human marrow. Bone **13**, 81-88.

HECKMANN, L., FIEDLER, J., MATTES, T., and BRENNER, R.E. (2006). Mesenchymal progenitor cells communicate via alpha and beta integrins with a three-dimensional collagen type I matrix. Cells Tissues Organs **182**, 143-154.

HECKMANN, L., FIEDLER, J., MATTES, T., DAUNER, M., and BRENNER, R.E. (2008). Interactive effects of growth factors and three-dimensional scaffolds on multipotent mesenchymal stromal cells. Biotechnol Appl Biochem **49**, 185-194.

HECKMANN, L., SCHLENKER, H.J., FIEDLER, J., BRENNER, R., DAUNER, M., BERGENTHAL, G., MATTES, T., CLAES, L., and IGNATIUS, A. (2007). Human mesenchymal progenitor cell responses to a novel textured poly(L-lactide) scaffold for ligament tissue engineering. J Biomed Mater Res B Appl Biomater **81**, 82-90.

HELM, G.A., LI, J.Z., ALDEN, T.D., HUDSON, S.B., BERES, E.J., CUNNINGHAM, M., MIKKELSEN, M.M., PITTMAN, D.D., KERNS, K.M., and KALLMES, D.F. (2001). A light and electron microscopic study of ectopic tendon and ligament formation induced by bone morphogenetic protein-13 adenoviral gene therapy. J Neurosurg **95**, 298-307.

HEYMER, A., HADDAD, D., WEBER, M., GBURECK, U., JAKOB, P.M., EULERT, J., and NOTH, U. (2008). Iron oxide labelling of human mesenchymal stem cells in collagen hydrogels for articular cartilage repair. Biomaterials **29**, 1473-1483.

HILDEBRAND, K.A., DEIE, M., ALLEN, C.R., SMITH, D.W., GEORGESCU, H.I., EVANS, C.H., ROBBINS, P.D., and WOO, S.L. (1999). Early expression of marker genes in the rabbit medial collateral and anterior cruciate ligaments: the use of different viral vectors and the effects of injury. J Orthop Res **17**, 37-42.

HILDEBRAND, K.A., FRANK, C.B., and HART, D.A. (2004). Gene intervention in ligament and tendon: current status, challenges, future directions. Gene Ther **11**, 368-378.

HOFFMANN, A., and GROSS, G. (2006). Tendon and ligament engineering: from cell biology to in vivo application. Regen Med **1**, 563-574.

HU, W.W., WANG, Z., HOLLISTER, S.J., and KREBSBACH, P.H. (2007). Localized viral vector delivery to enhance in situ regenerative gene therapy. Gene Ther **14**, 891-901.

HUTMACHER, D.W., SITTINGER, M., and RISBUD, M.V. (2004). Scaffold-based tissue engineering: rationale for computer-aided design and solid free-form fabrication systems. Trends Biotechnol **22**, 354-362.

IANNOTTI, J.P., CODSI, M.J., KWON, Y.W., DERWIN, K., CICCONE, J., and BREMS, J.J. (2006). Porcine small intestine submucosa augmentation of surgical repair of chronic two-tendon rotator cuff tears. A randomized, controlled trial. J Bone Joint Surg Am **88**, 1238-1244.

IDE, J., KIKUKAWA, K., HIROSE, J., IYAMA, K., SAKAMOTO, H., and MIZUTA, H. (2009). Reconstruction of large rotator-cuff tears with acellular dermal matrix grafts in rats. J Shoulder Elbow Surg **18**, 288-295.

JARMEY, C., and MYERS, T.W. (2006). *The Concise Book of the Moving Body*. (North Atlantic Books, Berkeley).

JENNER, J.M., VAN EIJK, F., SARIS, D.B., WILLEMS, W.J., DHERT, W.J., and CREEMERS, L.B. (2007). Effect of transforming growth factor-beta and growth differentiation factor-5 on proliferation and matrix production by human bone marrow stromal cells cultured on braided poly lactic-co-glycolic acid scaffolds for ligament tissue engineering. Tissue Eng **13**, 1573-1582.

KAN, I., MELAMED, E., and OFFEN, D. (2007). Autotransplantation of bone marrow-derived stem cells as a therapy for neurodegenerative diseases. Handb Exp Pharmacol, 219-242.

KENN, W. (2002). *Kernspintomographische Diagnostik*. (Gerorg Thieme Verlag, Stuttgart).

KENN, W., BOHM, D., GOHLKE, F., HUMMER, C., KOSTLER, H., and HAHN, D. (2004). 2D SPLASH: a new method to determine the fatty infiltration of the rotator cuff muscles. Eur Radiol **14**, 2331-2336.

KIM, S.G., AKAIKE, T., SASAGAW, T., ATOMI, Y., and KUROSAWA, H. (2002). Gene expression of type I and type III collagen by mechanical stretch in anterior cruciate ligament cells. Cell Struct Funct **27**, 139-144.

KUO, C.K., and TUAN, R.S. (2008). Mechanoactive tenogenic differentiation of human mesenchymal stem cells. Tissue Eng Part A **14**, 1615-1627.

LAURENCIN, C.T., and FREEMAN, J.W. (2005). Ligament tissue engineering: an evolutionary materials science approach. Biomaterials **26**, 7530-7536.

LAWHORN, K.W., and HOWELL, S.M. (2007). Principles for using hamstring tendons for anterior cruciate ligament reconstruction. Clin Sports Med **26**, 567-585.

LEE, I.C., WANG, J.H., LEE, Y.T., and YOUNG, T.H. (2007). The differentiation of mesenchymal stem cells by mechanical stress or/and co-culture system. Biochem Biophys Res Commun **352**, 147-152.

LEHRMAN, S. (1999). Virus treatment questioned after gene therapy death. Nature **401**, 517-518.

LETSON, A.K., and DAHNERS, L.E. (1994). The effect of combinations of growth factors on ligament healing. Clin Orthop Relat Res, 207-212.

LIU, H., FAN, H., TOH, S.L., and GOH, J.C. (2008). A comparison of rabbit mesenchymal stem cells and anterior cruciate ligament fibroblasts responses on combined silk scaffolds. Biomaterials **29**, 1443-1453.

LOU, J., TU, Y., BURNS, M., SILVA, M.J., and MANSKE, P. (2001). BMP-12 gene transfer augmentation of lacerated tendon repair. J Orthop Res **19**, 1199-1202.

MAJEWSKI, M., BETZ, O., OCHSNER, P.E., LIU, F., PORTER, R.M., and EVANS, C.H. (2008). Ex vivo adenoviral transfer of bone morphogenetic protein 12 (BMP-12) cDNA improves Achilles tendon healing in a rat model. Gene Ther **15**, 1139-1146.

MARSHALL, E. (1999). Gene therapy death prompts review of adenovirus vector. Science **286**, 2244-2245.

MARTIN, S.J., REUTELINGSPERGER, C.P., MCGAHON, A.J., RADER, J.A., VAN SCHIE, R.C., LAFACE, D.M., and GREEN, D.R. (1995). Early redistribution of plasma membrane phosphatidylserine is a general feature of apoptosis regardless of the initiating stimulus: inhibition by overexpression of Bcl-2 and Abl. J Exp Med **182**, 1545-1556.

MARUI, T., NIYIBIZI, C., GEORGESCU, H.I., CAO, M., KAVALKOVICH, K.W., LEVINE, R.E., and WOO, S.L. (1997a). Effect of growth factors on matrix synthesis by ligament fibroblasts. J Orthop Res **15**, 18-23.

MARUI, T., NIYIBIZI, C., GEORGESCU, H.I., CAO, M., KAVALKOVICH, K.W., LEVINE, R.E., and WOO, S.L. (1997b). Effect of growth factors on matrix synthesis by ligament fibroblasts. J Orthop Res **15**, 18-23.

MATSUMOTO, F., UHTHOFF, H.K., TRUDEL, G., and LOEHR, J.F. (2002). Delayed tendon reattachment does not reverse atrophy and fat accumulation of the supraspinatus--an experimental study in rabbits. J Orthop Res **20**, 357-363.

MEANEY MURRAY, M., RICE, K., WRIGHT, R.J., and SPECTOR, M. (2003). The effect of selected growth factors on human anterior cruciate ligament cell interactions with a three-dimensional collagen-GAG scaffold. J Orthop Res **21**, 238-244.

MOFFAT, K.L., KWEI, A.S., SPALAZZI, J.P., DOTY, S.B., LEVINE, W.N., and LU, H.H. (2009). Novel nanofiber-based scaffold for rotator cuff repair and augmentation. Tissue Eng Part A **15**, 115-126.

MOLLOY, T., WANG, Y., and MURRELL, G. (2003). The roles of growth factors in tendon and ligament healing. Sports Med **33**, 381-394.

MURCHISON, N.D., PRICE, B.A., CONNER, D.A., KEENE, D.R., OLSON, E.N., TABIN, C.J., and SCHWEITZER, R. (2007). Regulation of tendon differentiation by scleraxis distinguishes force-transmitting tendons from muscle-anchoring tendons. Development **134**, 2697-2708.

MURRAY, M.M., FORSYTHE, B., CHEN, F., LEE, S.J., YOO, J.J., ATALA, A., and STEINERT, A. (2006a). The effect of thrombin on ACL fibroblast interactions with collagen hydrogels. J Orthop Res **24**, 508-515.

MURRAY, M.M., MARTIN, S.D., and SPECTOR, M. (2000a). Migration of cells from human anterior cruciate ligament explants into collagen-glycosaminoglycan scaffolds. J Orthop Res **18**, 557-564.

MURRAY, M.M., MARTIN, S.D., and SPECTOR, M. (2000b). Migration of cells from human anterior cruciate ligament explants into collagen-glycosaminoglycan scaffolds. J Orthop Res **18**, 557-564.

MURRAY, M.M., and SPECTOR, M. (2001a). The migration of cells from the ruptured human anterior cruciate ligament into collagen-glycosaminoglycan regeneration templates in vitro. Biomaterials **22**, 2393-2402.

MURRAY, M.M., and SPECTOR, M. (2001b). The migration of cells from the ruptured human anterior cruciate ligament into collagen-glycosaminoglycan regeneration templates in vitro. Biomaterials **22**, 2393-2402.

MURRAY, M.M., SPINDLER, K.P., ABREU, E., MULLER, J.A., NEDDER, A., KELLY, M., FRINO, J., ZURAKOWSKI, D., VALENZA, M., SNYDER, B.D., and CONNOLLY, S.A. (2007). Collagen-platelet rich plasma hydrogel enhances primary repair of the porcine anterior cruciate ligament. J Orthop Res **25**, 81-91.

MURRAY, M.M., SPINDLER, K.P., DEVIN, C., SNYDER, B.S., MULLER, J., TAKAHASHI, M., BALLARD, P., NANNEY, L.B., and ZURAKOWSKI, D. (2006b). Use of a collagen-platelet rich plasma scaffold to stimulate healing of a central defect in the canine ACL. J Orthop Res **24**, 820-830.

NAGATOMI, J., ARULANANDAM, B.P., METZGER, D.W., MEUNIER, A., and BIZIOS, R. (2001). Frequency- and duration-dependent effects of cyclic pressure on select bone cell functions. Tissue Eng **7**, 717-728.

NAKAMURA, N., HART, D.A., FRANK, C.B., MARCHUK, L.L., SHRIVE, N.G., OTA, N., TAIRA, K., YOSHIKAWA, H., and KANEDA, Y. (2001). Efficient transfer of intact oligonucleotides into the nucleus of ligament scar fibroblasts by HVJ-cationic liposomes is correlated with effective antisense gene inhibition. J Biochem **129**, 755-759.

NAKAMURA, N., SHINO, K., NATSUUME, T., HORIBE, S., MATSUMOTO, N., KANEDA, Y., and OCHI, T. (1998). Early biological effect of in vivo gene transfer of platelet-derived growth factor (PDGF)-B into healing patellar ligament. Gene Ther **5**, 1165-1170.

NATSU, K., OCHI, M., MOCHIZUKI, Y., HACHISUKA, H., YANADA, S., and YASUNAGA, Y. (2004). Allogeneic bone marrow-derived mesenchymal stromal cells promote the regeneration of injured skeletal muscle without differentiation into myofibers. Tissue Eng **10**, 1093-1112.

NOTH, U., REICHERT, J., REPPENHAGEN, S., STEINERT, A., RACKWITZ, L., EULERT, J., BECKMANN, J., and TINGART, M. (2007). [Cell based therapy for the treatment of femoral head necrosis]. Orthopade **36**, 466-471.

NOTH, U., SCHUPP, K., HEYMER, A., KALL, S., JAKOB, F., SCHUTZE, N., BAUMANN, B., BARTHEL, T., EULERT, J., and HENDRICH, C. (2005). Anterior cruciate ligament constructs fabricated from human mesenchymal stem cells in a collagen type I hydrogel. Cytotherapy **7**, 447-455.

NOTH, U., STEINERT, A.F., and TUAN, R.S. (2008). Technology Insight: adult mesenchymal stem cells for osteoarthritis therapy. Nat Clin Pract Rheumatol.

NOTH, U., TULI, R., OSYCZKA, A.M., DANIELSON, K.G., and TUAN, R.S. (2002). In vitro engineered cartilage constructs produced by press-coating biodegradable polymer with human mesenchymal stem cells. Tissue Eng **8**, 131-144.

OH, J.H., KIM, S.H., CHOI, J.A., KIM, Y., and OH, C.H. (2009). Reliability of the Grading System for Fatty Degeneration of Rotator Cuff Muscles. Clin Orthop Relat Res.

OWINGS, M.F., and KOZAK, L.J. (1998). Ambulatory and inpatient procedures in the United States, 1996. Vital Health Stat 13, 1-119.

OZAWA, K., SATO, K., OH, I., OZAKI, K., UCHIBORI, R., OBARA, Y., KIKUCHI, Y., ITO, T., OKADA, T., URABE, M., MIZUKAMI, H., and KUME, A. (2008). Cell and gene therapy using mesenchymal stem cells (MSCs). J Autoimmun **30**, 121-127.

PALMER, G., GOUZE, E., GOUZE, J.N., BETZ, O., EVANS, C.H., and GHIVIZZANI, S.C. (2003a). Gene transfer to articular chondrocytes with recombinant adenovirus. Methods Mol Biol **215**, 235-246.

PALMER, G.D., GOUZE, E., GOUZE, J.N., BETZ, O.B., EVANS, C.H., and GHIVIZZANI, S.C. (2003b). Gene transfer to articular chondrocytes with recombinant adenovirus. Methods Mol Biol **215**, 235-246.

PARK, H., TEMENOFF, J.S., TABATA, Y., CAPLAN, A.I., and MIKOS, A.G. (2007). Injectable biodegradable hydrogel composites for rabbit marrow mesenchymal stem cell and growth factor delivery for cartilage tissue engineering. Biomaterials **28**, 3217-3227.

PASCHER, A., STEINERT, A.F., PALMER, G.D., BETZ, O., GOUZE, J.N., GOUZE, E., PILAPIL, C., GHIVIZZANI, S.C., EVANS, C.H., and MURRAY, M.M. (2004). Enhanced repair of the anterior cruciate ligament by in situ gene transfer: evaluation in an in vitro model. Mol Ther **10**, 327-336.

PELINKOVIC, D., LEE, J.Y., ENGELHARDT, M., RODOSKY, M., CUMMINS, J., FU, F.H., and HUARD, J. (2003). Muscle cell-mediated gene delivery to the rotator cuff. Tissue Eng **9**, 143-151.

PETERKOFSKY, B., and DIEGELMANN, R. (1971). Use of a mixture of proteinase-free collagenases for the specific assay of radioactive collagen in the presence of other proteins. Biochemistry **10**, 988-994.

PETRIGLIANO, F.A., MCALLISTER, D.R., and WU, B.M. (2006). Tissue engineering for anterior cruciate ligament reconstruction: a review of current strategies. Arthroscopy **22**, 441-451.

PITTENGER, M.F. (2008). Mesenchymal stem cells from adult bone marrow. Methods Mol Biol **449**, 27-44.

PRAEMER, A., FURNER, S., and RICE, D.P., eds. (1999). *Musculoskeletal Conditions in the United States*. (AAOS, Rosemont).

PROVENZANO, P.P., ALEJANDRO-OSORIO, A.L., GRORUD, K.W., MARTINEZ, D.A., VAILAS, A.C., GRINDELAND, R.E., and VANDERBY, R., JR. (2007). Systemic administration of IGF-I enhances healing in collagenous extracellular matrices: evaluation of loaded and unloaded ligaments. BMC Physiol **7**, 2.

REDDEN, R.A., and DOOLIN, E.J. (2003). Collagen crosslinking and cell density have distinct effects on fibroblast-mediated contraction of collagen gels. Skin Res Technol **9**, 290-293.

RICKERT, M., JUNG, M., ADIYAMAN, M., RICHTER, W., and SIMANK, H.G. (2001). A growth and differentiation factor-5 (GDF-5)-coated suture stimulates tendon healing in an Achilles tendon model in rats. Growth Factors **19**, 115-126.

ROTINI, R., FINI, M., GIAVARESI, G., MARINELLI, A., GUERRA, E., ANTONIOLI, D., CASTAGNA, A., and GIARDINO, R. (2008). New perspectives in rotator cuff tendon regeneration: review of tissue engineered therapies. Chir Organi Mov **91**, 87-92.

RUBINO, L.J., STILLS, H.F., JR., SPROTT, D.C., and CROSBY, L.A. (2007). Fatty infiltration of the torn rotator cuff worsens over time in a rabbit model. Arthroscopy **23**, 717-722.

SCHEK, R.M., HOLLISTER, S.J., and KREBSBACH, P.H. (2004). Delivery and protection of adenoviruses using biocompatible hydrogels for localized gene therapy. Mol Ther **9**, 130-138.

SCHEK, R.M., WILKE, E.N., HOLLISTER, S.J., and KREBSBACH, P.H. (2006). Combined use of designed scaffolds and adenoviral gene therapy for skeletal tissue engineering. Biomaterials **27**, 1160-1166.

SCHERPING, S.C., JR., SCHMIDT, C.C., GEORGESCU, H.I., KWOH, C.K., EVANS, C.H., and WOO, S.L. (1997). Effect of growth factors on the proliferation of ligament fibroblasts from skeletally mature rabbits. Connect Tissue Res **36**, 1-8.

SCHMIDT, C.C., GEORGESCU, H.I., KWOH, C.K., BLOMSTROM, G.L., ENGLE, C.P., LARKIN, L.A., EVANS, C.H., and WOO, S.L. (1995). Effect of growth factors on the proliferation of fibroblasts from the medial collateral and anterior cruciate ligaments. J Orthop Res **13**, 184-190.

SCHODERBEK, R.J., JR., TREME, G.P., and MILLER, M.D. (2007). Bone-patella tendon-bone autograft anterior cruciate ligament reconstruction. Clin Sports Med **26**, 525-547.

SCHWEITZER, R., CHYUNG, J.H., MURTAUGH, L.C., BRENT, A.E., ROSEN, V., OLSON, E.N., LASSAR, A., and TABIN, C.J. (2001). Analysis of the tendon cell fate using Scleraxis, a specific marker for tendons and ligaments. Development **128**, 3855-3866.

SCLAMBERG, S.G., TIBONE, J.E., ITAMURA, J.M., and KASRAEIAN, S. (2004). Six-month magnetic resonance imaging follow-up of large and massive rotator cuff repairs reinforced with porcine small intestinal submucosa. J Shoulder Elbow Surg **13**, 538-541.

SMITH, R.K. (2008). Mesenchymal stem cell therapy for equine tendinopathy. Disabil Rehabil, 1-7.

SMITH, R.K., KORDA, M., BLUNN, G.W., and GOODSHIP, A.E. (2003). Isolation and implantation of autologous equine mesenchymal stem cells from bone marrow into the superficial digital flexor tendon as a potential novel treatment. Equine Vet J **35**, 99-102.

SMITH, R.K., and WEBBON, P.M. (2005). Harnessing the stem cell for the treatment of tendon injuries: heralding a new dawn? Br J Sports Med **39**, 582-584.

SPINDLER, K.P., MURRAY, M.M., DEVIN, C., NANNEY, L.B., and DAVIDSON, J.M. (2006). The central ACL defect as a model for failure of intra-articular healing. J Orthop Res **24**, 401-406.

STEINERT, A.F., WEBER, M., KUNZ, M., PALMER, G.D., NOTH, U., EVANS, C.H., and MURRAY, M.M. (2008). In situ IGF-1 gene delivery to cells emerging from the injured anterior cruciate ligament. Biomaterials **29**, 904-916.

TOYODA, T., MATSUMOTO, H., FUJIKAWA, K., SAITO, S., and INOUE, K. (1998). Tensile load and the metabolism of anterior cruciate ligament cells. Clin Orthop Relat Res, 247-255.

TRACHSLIN, J., KOCH, M., and CHIQUET, M. (1999). Rapid and reversible regulation of collagen XII expression by changes in tensile stress. Exp Cell Res **247**, 320-328.

TSAI, A.D., YEH, L.C., and LEE, J.C. (2003). Effects of osteogenic protein-1 (OP-1, BMP-7) on gene expression in cultured medial collateral ligament cells. J Cell Biochem **90**, 777-791.

TUAN, R.S., BOLAND, G., and TULI, R. (2003). Adult mesenchymal stem cells and cell-based tissue engineering. Arthritis Res Ther **5**, 32-45.

UCCELLI, A., PISTOIA, V., and MORETTA, L. (2007). Mesenchymal stem cells: a new strategy for immunosuppression? Trends Immunol **28**, 219-226.

UHTHOFF, H.K., MATSUMOTO, F., TRUDEL, G., and HIMORI, K. (2003). Early reattachment does not reverse atrophy and fat accumulation of the supraspinatus--an experimental study in rabbits. J Orthop Res **21**, 386-392.

VUNJAK-NOVAKOVIC, G., ALTMAN, G., HORAN, R., and KAPLAN, D.L. (2004). Tissue engineering of ligaments. Annu Rev Biomed Eng **6**, 131-156.

WATANABE, N., WOO, S.L., PAPAGEORGIOU, C., CELECHOVSKY, C., and TAKAI, S. (2002). Fate of donor bone marrow cells in medial collateral ligament after simulated autologous transplantation. Microsc Res Tech **58**, 39-44.

WEST, R.V., and HARNER, C.D. (2005). Graft selection in anterior cruciate ligament reconstruction. J Am Acad Orthop Surg **13**, 197-207.

WEYTS, F.A., BOSMANS, B., NIESING, R., VAN LEEUWEN, J.P., and WEINANS, H. (2003). Mechanical control of human osteoblast apoptosis and proliferation in relation to differentiation. Calcif Tissue Int **72**, 505-512.

WINKLER, T., VON ROTH, P., SCHUMANN, M.R., SIELAND, K., STOLTENBURG-DIDINGER, G., TAUPITZ, M., PERKA, C., DUDA, G.N., and MATZIOLIS, G. (2008). In Vivo Visualization of Locally Transplanted Mesenchymal Stem Cells in the Severely Injured Muscle in Rats. Tissue Eng Part A.

WOLFMAN, N.M., HATTERSLEY, G., COX, K., CELESTE, A.J., NELSON, R., YAMAJI, N., DUBE, J.L., DIBLASIO-SMITH, E., NOVE, J., SONG, J.J., WOZNEY, J.M., and ROSEN, V. (1997). Ectopic induction of tendon and ligament in rats by growth and differentiation factors 5, 6, and 7, members of the TGF-beta gene family. J Clin Invest **100**, 321-330.

WOO, S.L., ABRAMOWITCH, S.D., KILGER, R., and LIANG, R. (2006a). Biomechanics of knee ligaments: injury, healing, and repair. J Biomech **39**, 1-20.

WOO, S.L., JIA, F., ZOU, L., and GABRIEL, M.T. (2004). Functional tissue engineering for ligament healing: potential of antisense gene therapy. Ann Biomed Eng **32**, 342-351.

WOO, S.L., WU, C., DEDE, O., VERCILLO, F., and NOORANI, S. (2006b). Biomechanics and anterior cruciate ligament reconstruction. J Orthop Surg **1**, 2.

YOUNG, R.G., BUTLER, D.L., WEBER, W., CAPLAN, A.I., GORDON, S.L., and FINK, D.J. (1998). Use of mesenchymal stem cells in a collagen matrix for Achilles tendon repair. J Orthop Res **16**, 406-413.

8.2 Abbreviations

ACL	Anterior cruciate ligament
ACT	Autologous chondrocyte transplantation
AnnV-Cy3	Annexin V-Cy3
bFGF	Basic fibroblast growth factor
BGN	Biglycan
BMP	Bone morphogenetic protein
Bp	Base pair
℃	Degree Centigrade
cDNA	Complementary desoxyribonucleid acid
CFDA	Carboxyflurescein diacetate
CO_2	Carbon dioxide
COL	Collagen
3D	Three-dimensional
2D	Two-dimensional
Da	Dalton
DCN	Decorin
DMEM	Dulbecco´s modified Eagle´s medium
DNA	Desoxyribonucleid acid
ECM	Extracellular matrix
EF-1α	Elongation factor 1α
EGF	Epidermal growth factor
ELA	Elastin
E-modulus	Elastic modulus = Young's modulus
ETOH	Collagen fibers sterilized with 70% ETOH
FCS	Fetal calf serum
FN	Fibronectin
FOV	Field-of-view
GAM	Collagen fibers sterilized with γ-irradiation
GAMOH	Collagen fibers sterilized with 70% ETOH and γ-irradiation
GDF	Growth and differentiation factor
GFP	Green fluorescent protein
h	Hours
H&E	Haematoxylin & Eosin
IGF	Insulin-like growth factor

ip	Infectious particles
Luc	Luciferase
MCL	Medial collateral ligament
mm^2	Square millimeter
mm^3	Cubic millimeter
MPa	Megapascal (1 MPa = 1 N/mm^2)
µCi	Microcurie
µg	Microgram(s)
µL	Microliter
µm	Micrometer(s)
min	Minute
mM	Millimolar = millimol per liter
mmol	Millimol
MRI	Magnetic resonance imaging
MSCs	Mesenchymal stem cells
MSZ	Mesenchymale Stammzellen
N	Newton
NAT	Native collagen fibers
nm	Nanometer
PCL	Posterior cruciate ligament
PGA	Polyglycolic acid (PGA),
PLA	Poly lactic acids
PLGA	Polylactic-co-glycolic acid
PLLA	Poly-L-lactic acid
PDGF	Platelet-derived growth factor
SCL	Scleraxis
SD	Standard deviation
SEM	Scanning electron microscopy
SIS	Small intestinal submucosa
SSP	Musculus supraspinatus
T	Tesla
TE	Echo time
TEM	Transmission electron microscopy
TN-C	Tenascin-C
TNMD	Tenomodulin
TR	Repetition time
TGF-β	Transforming growth factor beta

U	Units
VIM	Vimentin
vp	Virus particles
VSOP	Very small superparamagnetic iron oxide particles

8.3 Curriculum Vitae

Personal information

Surname and first name	Haddad-Weber, Meike (geb. Weber)
Date of birth	13.02.1975
Place of birth	Wimbern/Wickede
Address	Methfesselstr. 11, 97074 Würzburg, Germany
Familiy status	married, 1 child
Nationality	German

Education and training

1981 – 1985	Elementary school, Menden
1985 – 1986	Grammar school “Heilig-Geist Gymnasium”, Menden
1986 – 1995	Grammar school “Armin-Knab-Gymnasium”, Kitzingen
June 1995	General qualification or university entrance (“Abitur”)
1995 – 2000	Studies of biology at the Julius-Maximilians-University Würzburg; Main subjects: biotechnology, microbiology, and behavioral physiology and socio-biology Diploma thesis at the Chair of Biotechnology: “Immobilisierung von autologen Zellen in eine Alginatmatrix: Am Modellsystem von embryonalen Mausfibroblasten”
December 2000	Diploma certificate as biologist
2000 – 2005	Scientific assistant, Chair of biotechnology Würzburg
2005 – 2009	PhD thesis at the Julius-Maximilians-University Würzburg, Orthopedic Clinic, Orthopedic Center for Musculoskeletal Research, Division of Tissue Engineering; supervised by PD. Dr. Ulrich Nöth
2009 –	Project leader EXIST-Forschungstransfer at the Julius-Maximilians-University Würzburg, Orthopedic Clinic,

Orthopaedic Center for Musculoskeletal Research, Division of Tissue Engineering

Award

2004 Publication award of the “Deutsche Akademie der Osteologischen und Rheumatologischen Wissenschaften”, for Steinert A, Weber M, Dimmler A, Julius C, Schütze N, Nöth U, Cramer H, Eulert J, Zimmermann U, Hendrich C. Chondrogenic differentiation of mesenchymal progenitor cells encapsulated in ultrahigh-viscosity alginate. J Orthop Res. 21(6):1090-7, 2003

2010 Winner of the business plan award of the business plan contest of the netzwerk|nordbayern

2010 Winner of the “Hochschul-Gründer-Preis” of the netzwerk|nordbayern

Invention disclodure

2008 Invention disclosure for Weber M and Nöth U (“Kollagenfaser-Konstrukte für den Kreuzbandersatz”, SP-103.100-1/8). Claim of the invention disclosure of the Julius-Maximilians University Würzburg

2009 Intervention disclosure at the German Patent Office (102009059901.0)

Research grant

2009 EXIST-Forschungstransfer of the „Bundesministerium für Wirtschaft und Technologie“ for Weber M, Haddad D, Knauer M, and Nöth U. “Entwicklung Kollagenfaser-basierter Kreuzbandimplantate für den Kreuzbandersatz“.

8.4 Publications

Publications in peer reviewed journals

Haddad-Weber M, Stehle J, Seefried L, Hurscheler C, Krohne G, Steinert AF, Nöth U. Collagen fiber-based ACL constructs (The publication of this manuscript has to be postponed until a envisioned second patent application has been filed).

Haddad-Weber M, Haddad D, Wilms A, Rackwitz L, Steinert AF, Lotz C, Hiller KH, Gohlke F, Rolf O, Nöth U. Intratendinous injection of mesenchymal stem cells after rotator cuff repair - an experimental study in rabbits (submitted).

Kampf T, Basse-Lüsebrink TC, **Haddad-Weber M**, Heymer A, Ebert R, Stötzel C, Gbureck U, Nöth U, Bauer WR, Jakob PM, Haddad D. Double-labeling of cells using VSOPs and PFPE nanoparticles for application in $^{1}H/^{19}F$ MRI (submitted).

Haddad D, Hildenbrand M, Hiller KH, **Haddad-Weber M**, Jakob P. Positive Identification of Iron Oxide labeled Stem Cells using Magnetic Field Hyperthermia and Magnetic Resonance Thermometry (submitted).

Haddad-Weber M, Prager P, Kunz M, Seefried L, Jakob F, Murray MM, Evans CH, Nöth U, Steinert AF. BMP12 and BMP13 gene transfer induce ligamentogenic differentiation in mesenchymal progenitor and anterior cruciate ligament cells. Cytotherapy 12:505-13; 2010.

Steinert AF, **Weber M**, Kunz M, Palmer GD, Nöth U, Evans CH, Murray MM. In situ IGF-1 gene delivery to cells emerging from the injured anterior cruciate ligament. Biomaterials 29:904-916, 2008.

Heymer A, Haddad D, **Weber M**, Gbureck U, Jakob P, Nöth U. Iron Oxide Labelling of Human Mesenchymal Stem Cells in Collagen Type I Hydrogels for Cellular MR Imaging. Biomaterials 29:1473-1483; 2008.

Nöth U, Rackwitz L, Heymer A, **Weber M**, Baumann B, Steinert A, Schütze N, Jakob F, Eulert J. Chondrogenic differentiation of human mesenchymal stem cells in a collagen type I hydrogel for articular cartilage repair. J Biomed Mat Res-A 83(3):626-35, 2007.

Wolf R, Zimmermann D, **Weber M**, Feilen P, Ehrhart F, Salinas Jungjohann M, Katsen A, Behringer M, Gessner P, Pliess L, Steinbach A, Spitz J, Vásquez JA, Schneider S, Bamberg E, Weber MM, Zimmermann U, Zimmermann H. Real-time 3-D dark-field microscopy for the validation of the cross-linking process of alginate microcapsules. Biomaterials 26(32):6386-93; 2005.

Steinert A*, **Weber M***, Dimmler A, Julius C, Schütze N, Nöth U, Cramer H, Eulert J, Zimmermann U, Hendrich C. Chondrogenic differentiation of mesenchymal progenitor cells encapsulated in ultrahigh-viscosity alginate. J Orthop Res. 21(6):1090-7, 2003. *Both autors have equally contributed to the experimental work.

Zimmermann H, Hillgartner M, Manz B, Feilen P, Brunnenmeier F, Leinfelder U, **Weber M**, Cramer H, Schneider S, Hendrich C, Volke F, Zimmermann U. Fabrication of homogeneously cross-linked,

functional alginate microcapsules validated by NMR-, CLSM- and AFM-imaging. Biomaterials 24(12):2083-96, 2003.

Weber M, Steinert A, Jork A, Dimmler A, Thurmer F, Schütze N, Hendrich C, Zimmerman U. Formation of cartilage matrix proteins by BMP-transfected murine mesenchymal stem cells encapsulated in a novel class of alginates. Biomaterials 23(9):2003-13; 2002

Review articles

Ebert R, Schütze N, Schilling T, Seefried L, **Weber M**, Nöth U, Eulert J, Jakob F. The influence of hormones on osteogenic differentiation processes of mesenchymal stem cells. Expert Rev Endocrinol Metab 1:79-90, 2007.

Stehle J, **Weber M**, Heymer A, Schütze N, Jakob F, Eulert J, Nöth U. Effect of cyclic stretching on anterior cruciate ligament-constructs fabricated from human MSCs and collagen type I hydrogels. In: Liepsch D. (Herausgeber) 5th World Congress of Biomechanics. Medimond International Proceedings, Bologna, pp 95-100, 2006.

Zimmermann H, Zimmermann D, Reuss R, Feilen PJ, Manz B, Katsen A, **Weber M**, Ihmig FR, Ehrhart F, Gessner P, Behringer M, Steinbach A, Wegner LH, Sukhorukov VL, Vasquez JA, Schneider S, Weber MM, Volke F, Wolf R, Zimmermann U. Towards a medically approved technology for alginate-based microcapsules allowing long-term immunoisolated transplantation. J Mater Sci Mater Med. 16(6):491-501, 2005.

Hendrich C, **Weber M**, Battmann A, Schütze N, Julius C, Steinert AF, Faltin M, Balling S, Zimmermann H, Nöth U, Zimmermann U. Differentiation of human and murine chondrogenic cells encapsulated in ultra-high viscosity alginate. In: Hendrich C, Nöth U, Eulert J. (Herausgeber) Cartilage surgery and future perspectives. Springer Verlag, Heidelberg, pp 171-181, 2003.

Zimmermann U, Leinfelder U, Hillgärtner M, Manz B, Zimmermann H, Brunnenmeier F, **Weber M**, Vásquez JA, Volke F, Hendrich C. Homogeneously cross-linked scaffolds based on clinical-grade alginate for transplantation and tissue engineering. In: Hendrich C, Nöth U, Eulert J. (Herausgeber) Cartilage surgery and future perspectives. Springer Verlag, Heidelberg, pp 77-86, 2003.

Zimmermann U, Thurmer F, Jork A, **Weber M**, Mimietz S, Hillgartner M, Brunnenmeier F, Zimmermann H, Westphal I, Fuhr G, Nöth U, Haase A, Steinert A, Hendrich C. A novel class of amitogenic alginate microcapsules for long-term immunoisolated transplantation. Ann N Y Acad Sci 944:199-215; 2001.

Published abstracts of national and international symposia

Weber M, Haddad D, Rolf O, Nöth U. Stem cell-based therapy for the fatty infiltration of the rotator cuff. Chirurgische Forschertage 2009.

Weber M, Prager P, Stehle J, Seefried L, Nöth U, Steinert A. BMP-12 and BMP-13 transfizierte MSZ und Firoblasten im Kollagenhydrogel für die Ligamentrekonstruktion. DGOOC 2009.

Weber M, Haddad D, Wilms A, Steinert A, Nöth U, Rolf O. Nachweis von SPIO-markierten MSZ für die zellbasierte Therapie der fettig infiltrierten Rotatorenmanschette. DGOOC 2009.

Rolf O, Stehe J, **Weber M**, Haddad D, Nöth U, Gohlke F. Stem cell-based therapy of fatty degenerated rotator cuff. SECEC 2009.

Basse-Lüsebrink TC, Kampf T, Melkus G, Ladewig G, **Weber M**, Stoll U, Jakob PM, Bauer WR, Haddad D. A fast approach to distinguish between cells labeled with different PFCs in a single MR measurement. ESMRMB 2008.

Haddad D, Lorenscheit J, Hildenbrand M, **Weber M**, Ebert R, Jakob P. In vitro MR thermometry on magnetically heated iron oxide labeled stem cells. ISMRM 2008.

Weber M, Haddad D, Wilms A, Hiller K-H, Rolf O, Nöth U. Monitoring of SPIO-labelled MSCs for cell-based therapy of fatty degenerated rotator cuff: a preliminary study. SMI 2008.

Weber M, Stehle J, Heymer A, Seefried L, Eulert J, Nöth U, Steinert A. BMP-12 and BMP-13 transduced MSCs in collagen type I hydrogel for ACL constructs. Tissue Eng 14:691-943, 2008.

Weber M, Kunz M, Stehle J, Nöth U, Steinert A. BMP-12 and BMP-13 transduced MSCs in collagen hydrogel for ACL reconstruction. Trans Orthop Res Soc 33:778 ,2008.

Steinert AF, **Weber M**, Kunz M, Palmer GD, Nöth U, Evans CH, Murray MM. In situ IGF-1 gene delivery to cells emerging from the injured anterior cruciate ligament. Trans Orthop Res Soc 33:782,2008.

Weber M, Stehle J, Heymer A, Seefried L, Eulert J, Nöth U, Steinert A. BMP-12 and BMP-13 transfizierte MSZ im Kollagenhydrogel für die Ligamentrekonstruktion. Z Orthop, 2007.

Weber M, Stehle J, Heymer A, Seefried L, Eulert J, Nöth U, Steinert A. BMP-12 and BMP-13 transduced MSCs in collagen type I hydrogel for ACL constructs. Tissue Engineering 2008.

Heymer A, Haddad D, **Weber M**, Jakob P, Noth, U. MR imaging of VSOP labeled human mesenchymal stem cells in a collagen type I hydrogel for cartilage repair. Trans Orthop Res Soc 32:637, 2007.

Weber M, Stehle J, Heymer A, Nöth U. Collagen fiber based ACL graft. ISL&T 2007.

Ebert R, Arnholt J, Weber M, Heymer A, Mertsching H, Nöth U, Jakob F. Mikroarray und FACS Analysen differenzieren Stammzell-Populationen aus Knochenmarksstroma und Knochentrabekeln. Osteologie S1:VIO5.1, 2007.

Rolf O, **Weber M**, Heymer A, Wilms A, Haddad D, Steinert A, Gohlke F, Nöth U. Zellbasierte Therapie der fettig-degenerierten Rotatorenmanschette. DVSE 2007.

Weber M, Seefried L, Kirsch L, Stehle J, Heymer A, Hurschler C, Krohne G, Nöth U. Collagen fiber-based anterior cruciate ligament grafts. Tissue Engineering 13(7):1658, 2007.

Haddad D, Basse-Lüsebrink TC, Kampf T, **Weber M**, Heymer A, Nöth A, Bauer WR, Jakob P. 1H / 19F MR Imaging of SPIO and PFC double-labeled Mesenchymal Stem Cells. SMI 2007. (Molecular Imaging 2007).

Heymer A, Haddad D, **Weber M**, Jakob P, Nöth U. Iron oxide labeling of human mesenchymal stem cells in collagen type I hydrogels for cellular MR imaging. GSZ 2007.

Basse-Lüsebrink TC, Kampf T, **Weber M**, Heymer A, Ebert R, Nöth U, Bauer WR, Jakob P, Haddad D. Double-labeled Mesenchymal Stem Cells for 1H / 19F MR Imaging. GSZ 2007.

Wilms A, **Weber M**, Haddad D, Heymer A, Basse-Lüsebrink T, Steinert A, Jakob P, Nöth U, Gohlke F, Rolf O. Cell-based therapy of fatty degeneration after rotator cuff tears. GSZ 2007.

Weber M, Kunz M, Stehle J, Nöth U, Steinert A. BMP-12 transduced MSCs in collagen hydrogel for ligament reconstruction. GSZ 2007.

Weber M, Stehle J, Heymer A, Seefried L, Eulert J, Nöth U. Entwicklung von Kollagenfaser-Konstrukten für den vorderen Kreuzbandersatz. Z Orthop, 2007.

Weber M, Heymer A, Stehle J, Schütze N, Jakob F, Nöth U. Anterior cruciate ligament constructs produced from human mesenchymal stem cells in a three-dimensional matrix. Cytotherapy 2006; 8(Suppl 2):64.

Heymer A, Bradica G, **Weber M**, Eulert J, Nöth U. Chondrogenic Differentiation of Human Mesenchymal Stem Cells on Different PLA-Collagen Composites for Articular Cartilage Repair. Cytotherapy 2006; 8(Suppl 2):57.

Heymer A, Haddad D, **Weber M**, Jakob P, Nöth U. In vitro MR Imaging of Iron Oxide-labeled Human Mesenchymal Stem Cells in Collagen Type I Hydrogels. Cytotherapy 2006; 8(Suppl 2):42

Haddad D, Hiller KH, Purea A, Heymer A, **Weber M**, Hock R, Noeth U, Jakob P. Magnetic Resonance Imaging on a cellular level. Cytotherapy 2006; 8(Suppl 2):42.

Reichert J, Heymer A, **Weber M**, Nöth U. Construction of an osteogenic PCL-MSC-Hydrogel-Interponate for Regeneration of segmental Bone Defects. Cytotherapy 2006; 8(Suppl 2):62.

Fensky F, Heymer A, **Weber M**, Eulert J, Nöth U. Chondrogenic predifferentiation of human mesenchymal stem cells (hMSCs) in collagen type I hydrogels under the influence of TGF-β1. Cytotherapy 2006; 8(Suppl 2):58.

Merklein F, Laun K, Wagemanns R, Heymer A, Bradica G, **Weber M**, Schütze N, Duda G, Sebald W, Jakob F, Nöth U. Testing of a new PLA/β-TCP Matrix as a carrier for BMP-2 in the rat model. Cytotherapy 2006; 8(Suppl 2):63

Heymer A, Haddad D, **Weber M**, Jakob P, Nöth U. Iron Oxide-labeling of Human Mesenchymal Stem Cells for cellular MR imaging. Tissue Engineering

Nöth U, Ebert R, Arnholt J, **Weber M**, Mertsching H, Eulert J, Jakob F. Mesenchymal Stem Cells derived from Bone Marrow and Trabecular Bone – Microarray- and FACS-Analysis for the Description of Differences. Tissue Engineering

Haddad D, Heymer A, **Weber M**, Nöth U, Jakob P. MR imaging of VSOP labeled Human Mesenchymal Stem Cells. SMI 2006

Heymer A, Haddad D, **Weber M**, Jakob P, Nöth U. Detektion humaner mesenchymaler Stammzellen in der Hochfeld MR-Tomographie nach Beladung mit superparamagnetischen Nanopartikeln. Z Orthop, 2006

Fensky F, Heymer A, **Weber M**, Nöth U. Prädifferenzierung von humanen mesenchymalen Stammzellen in Kollagen-Typ-I-Hydrogelen unter dem Einfluss von TGF-β1. Z Orthop, 2006

Reichert J, Heymer A, **Weber M**, Nöth U. Herstellung eines osteogenen Polycaprolacton-Stammzell-Hydrogel Konstruktes für die Rekonstruktion segmentaler Knochendefekte. Z Orthop, 2006

Merklein F, **Weber M**, Faltin M, Zimmermann U, Hendrich C. Chondrogenic differentiation of encapsulated chondrocytes and mesenchymal stem cells *in vivo*. Cytotherapy 2004; 6(3):270.

Weber M, Merklein F, Faltin M, Nöth U, Steinert A, Hendrich C, Zimmermann U. Hypertrophic chondrogenesis of TGF-β induced MSCs in UHV-alginate. Cytotherapy 2004; 6(3):301.

Hendrich C, **Weber M**, Mattmann A, Steinert A, Faltin M, Zimmermann H, Balling S, Schütze N, Nöth U, Zimmermann U. Chondrogene Differenzierung von humanen Chondrozyten und mesenchymalen Stamzellen in einem in-vivo Modell. Z Orthop, 141 (Suppl 1):S113; 2003.

8.5 Acknowledgement

I would like to thank my supervisor PD Dr. Ulrich Nöth for giving me the opportunity to work on this very interesting scientific topic at the Orthopedic Centre for Musculoskeletal Research and for the fruitful discussions.

I am thankful to Prof. Dr. Georg Krohne of the Faculty of Biology (University of Würzburg) for accepting the position of an assessor and for performing TEM and SEM measurements for my thesis.

I am very thankful to Prof. Dr. Franz Jakob for the confidence in regard to the organization of the 2nd Congress of the German Society for Stem Cell Research and many helpful advices, scientific discussions, and the sponsorship.

I am very thankful to Prof. Dr. Norbert Schütze for his support in the last years.

I am very grateful to Prof. Dr. Jochen Eulert, the former head of the Orthopedic Clinic, who appreciates and supports basic research at his clinic, thus providing an excellent interdisciplinary academic environment.

I like to thank Christa Amrehn, Martina Regensburger, Viola Monz, Manuela Kunz, and Doris Hetzer for excellent technical support and many helpful ideas and discussions.

Furthermore, I like to thank Dr. Tatjana Schilling, Dr. Andrea Heymer, Dr. Rita Wagemanns, Dr. Lothar Seefried, and all who shared the office with me for encouraging scientific and non-scientific discussions and the good working atmosphere.

I am grateful to Dr. Lars Rackwitz, Dr. Andre Steinert, Dr. Olaf Rolf, Dr. Alexander Rucker, and Dr. Jens Stehle for their support and interesting discussions.

I am thankful to all trainees and medical students, especially to Simon Bischofberger, Andreas Gerken, Antje Wilms, and Franziska Stöckhert for their contribution to my projects and their interest in research.

I like to thank Karl-Heinz „Charly“ Hiller for „having an open ear for me“ and for Daniel.

Particularly, I like to thank my husband Daniel very much for his support, understanding, and encouragement during all stages of this thesis, especially in the last months.

Finally, I am particularly grateful to my parents and my brother Lars for their unquestioning support during the whole course of my studies.